Orchestrating Pore Structure of Hybrid Silica Membranes for Molecular Separations

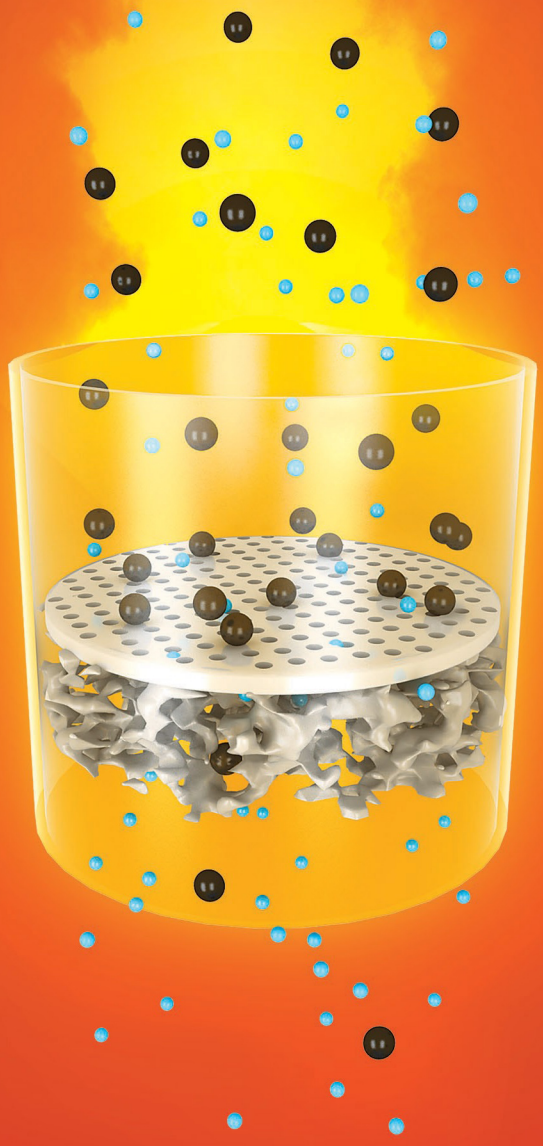

Hammad Fayyaz Qureshi

ORCHESTRATING PORE STRUCTURE OF HYBRID SILICA MEMBRANES FOR MOLECULAR SEPARATIONS

HAMMAD FAYYAZ QURESHI

Promotion committee members:

Chairman and Secretary:

Prof. dr. H.B.J. Karperien	University of Twente

Promoters:

Prof. dr. ir. A. Nijmeijer	University of Twente
Prof. dr. A.J.A. Winnubst	USTC Hefei, China / University of Twente

Members:

Prof. dr. ir. R.G.H. Lammertink	University of Twente, The Netherlands
Prof. dr. ir. L. Lefferts	University of Twente, The Netherlands
Prof. dr. ir. J.E. ten Elshof	University of Twente, The Netherlands
Prof. dr. J. Caro	Leibniz University Hannover, Germany
Dr. V. Boffa	Aalborg University, Denmark.

The work described in this thesis was performed at the Inorganic Membranes group, MESA+ Institute for Nanotechnology, at the University of Twente. This research is financially supported by the Dutch Technology Foundation STW under the framework of project number 10454 entitled “Hydrothermally stable organosilica-based hybrid membranes for molecular separations”.

Cover Concept: Hammad F. Qureshi (facilitated by www.tingle.nl)

ISBN: 978-90-365-3688-2
Printed by: Gildeprint drukkerijen, Enschede, The Netherlands.

ORCHESTRATING PORE STRUCTURE OF HYBRID SILICA MEMBRANES FOR MOLECULAR SEPARATIONS

DISSERTATION

to obtain
the degree of doctor at the University of Twente,
on the authority of the rector magnificus,
Prof. dr. H. Brinksma,
on account of the decision of the graduation committee,
to be publicly defended
on Thursday, the 26th of June 2014 at 16:45

by

Hammad Fayyaz Qureshi

Born on the 12th November 1982
in Multan, Pakistan.

This dissertation has been approved by the promotors:

Prof. dr. ir. A. Nijmeijer

Prof. dr. A.J.A. Winnubst

Humans are also membranes; only selective people permeate through our compatibility barriers and get access to our minds and hearts

Table of Contents

Chapter 7

Chapter 1

Introduction

1.1 General Introduction

A membrane is a permselective barrier between two phases. It facilitates a faster transport of a specific component compared to others present in the feed, which results in a purified or a separated stream. Membrane-based separations are considered a preferred separation method due to their uncomplicated operation in process development schemes aiming at decreasing the production costs, energy utilization and waste generation [1].

In general, membranes are classified as either organic (polymeric) or inorganic membranes, according to the materials they are made of. For molecular separation, the polymeric membranes commonly in use for gas separation are made of cellulose acetate, polysulfone, polyamide, polyimide, etc. They commonly show relatively good permeability, but their performance is majorly hindered by poor thermal and chemical stability [2]. By comparison with conventional polymeric membranes, inorganic membranes offer an improvement in thermal and chemical stability, which is a substantial advantage. Inorganic membranes have been developed by using various materials such as silica, alumina, titania, or zirconia that resulted in membranes with a porous microstructure [2-4].

According to IUPAC definitions, porous membranes can be categorized into macroporous (pore diameter > 50 nm), mesoporous (50 > pore diameter > 2 nm) and microporous (pore diameter < 2nm) membranes [5]. Based on the pore size, separation processes ranging from microfiltration to gas separation can be exploited by using porous inorganic membranes.

Porous inorganic membranes can either be symmetric or asymmetric in their structure. Symmetric membranes have a single layer of a porous inorganic material possessing a considerable thickness for mechanical stability [4]. However to obtain large fluxes the separation layer thickness must be as small as possible. Thin separation layers can be achieved by using an asymmetric configuration where a selective top layer is mounted on a porous support thus forming a graded structure. The support is generally made from a metal oxide on top of which layers are applied with gradually decreasing pore size.

This thesis focuses on asymmetric microporous membranes for gas separation. The stacked system of interest in this work is an α-alumina (macroporous) / γ-alumina or hybrid silica (mesoporous) / hybrid silica (microporous) membrane. The macroporous support has a thickness of about 2 mm (pore size: d_p 50-70 nm) that provides essential mechanical strength to the stack. On top of this support, an intermediate mesoporous layer is coated, having a thickness of 3 μm (pore size: d_p 4-5 nm). The main purpose of such an intermediate layer is to provide sufficient smoothness and sufficient small pore size for the deposition of a very thin gas selective layer. This microporous top layer has a thickness of few tens to few hundred nanometers and is responsible for the gas separation properties of the membrane. Amongst porous inorganic membranes, silica membranes are a prime candidate for gas separation due to their small pore size (d_p < 0.5 nm), the relative easy way of fabrication, low production costs and scalability [4, 6].

1.2 Sol-gel derived microporous silica membranes: Synthesis and structural properties

Sol–gel processing is a wet chemical technique that offers a wide variety in reaction tunability and choice of precursors for the fabrication of microporous ceramic membranes. The fabrication of microporous silica membranes by means of the sol-gel technique has been a focus in research for the past few decades [7-9].

Sol-gel processing offers two routes to develop an inorganic membrane *i.e.* either via a colloidal or a polymeric sol. In the colloidal route, the synthesis takes place in an aqueous medium while in polymeric route it occurs in an alcoholic medium. In the colloidal route the colloids remain isolated due to electrostatic repulsion, whereas in the polymeric route the sol particles remain separated in solution because of their small size. In both cases the condensation reactions occur at the sol stage with the formation of colloids or clusters which later on interact to form a gel. Both routes yield nano-sized particles from which porous materials can be developed. The polymeric route yields particles useful for making microporous materials and membranes [10].

Inorganic membrane fabrication by sol-gel processing is usually done by dip-coating with subsequent thermal treatment (sintering/calcining) in the temperature range

between 400 and 800 °C. Figure 1.1 summarizes the fabrication procedure of inorganic membranes by sol-gel processing.

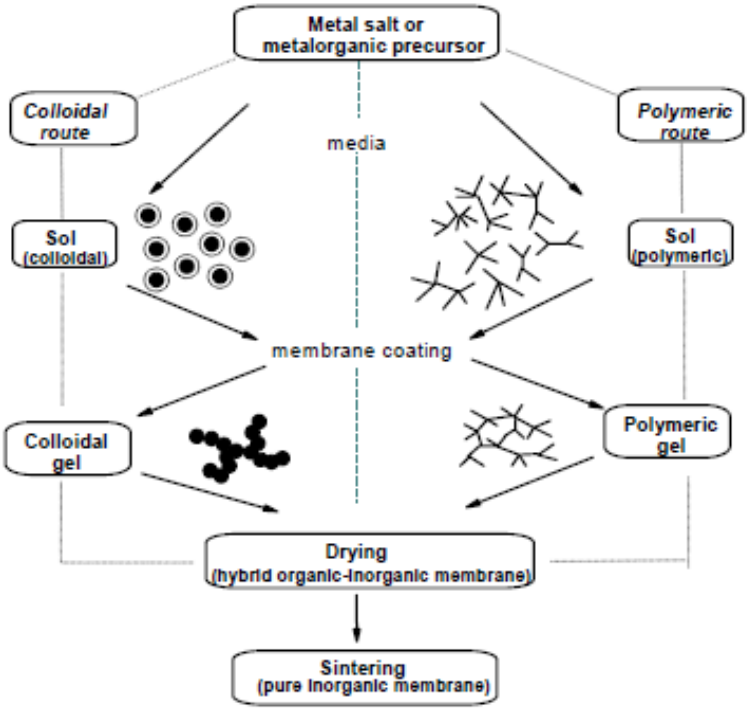

Figure 1.1: Sol-gel routes commonly used to make inorganic membranes [10].

Microporous silica membranes are made by sol-gel processing following the polymeric route. Silica sols, typically synthesized in acid environments, are deposited on porous substrates in a dust-free environment. The resulting supported layer undergoes a thermal treatment of at least 400 °C which results in a microporous membrane having a pore size of approximately 0.4 nm and a thickness of a few tens of nanometers [9, 11, 12]. They show good separation properties for various gas mixtures, such as H_2/CO_2, H_2/N_2, H_2/CH_4, and in some cases these membranes were found nitrogen and methane impermeable [13, 14]. However, these membranes were found unstable in water vapor, particularly at high temperatures; that is, the gas permeance decreases with time under hydrothermal conditions, resulting in a decreased overall gas permselectivity. This membrane

instability is due to the continuous condensation of the silanol groups in the amorphous silica structure, which is accelerated at high temperatures under humid conditions. This results in the densification of the silica matrix starting with closing of the small pores leading to the formation of larger pores and eventually ends up in a complete delamination of the selective top layer [3, 15, 16].

This limitation with silica membranes could be overcome by using an organic–inorganic hybrid silica, which contains at least one organic group that cannot be hydrolyzed, such as methyltriethoxysilane (MTES), to control the pore size under hydrothermal conditions [17-20]. In these references, hybrid organic–inorganic polymeric sols and membranes were prepared by the copolymerization of TEOS and MTES. However, these modifications did not sufficiently increase the hydrothermal stability of membranes and the membrane structure deteriorated within 100 days under pervaporation conditions (shown in figure 1.2) [21]. Another attempt to improve the hydrothermal stability of silica membranes is to incorporate metal ions such as Zr, Al, Ni, Nb and Co to the silica matrix [22-26]. For Co [27, 28] and Nb [29, 30] doping a considerable improvement in the performance of silica membranes under hydrothermal conditions was found. However, for Zr, Al, Mg, and Ni-doped silica, no improvement in hydrothermal stability was found [24, 31, 32].

1.3 Hybrid silica Membranes for Molecular Separation

Castricum et al. [21, 33-36] developed organosilica membranes starting from bridged *bis*(silyl) precursors: *bis*(triethoxysilyl)ethane (BTESE) and bis(triethoxysilyl) methane (BTESM), with methytriethoxysilane (MTES) showing superior hydrothermal stability if compared with silica-derived membranes. These type of membranes will now be termed as hybrid silica membranes in this chapter. The BTESE/MTES membranes showed high solvolytical and long-term acid stability for almost 2 years during the dehydration of *n*-butanol at 150 °C, as shown in figure 1.2. The authors proposed that the enhanced durability of these hybrid silica membranes, if compared with pure silica membranes, was due to the incorporation of organic linking groups [21]. As the organic groups are nonpolar, they “shield” the siloxane bonds from water, which leads to less concomitant hydrolysis [37] that is pivotal in maintaining the consistency in performance of BTESE membranes for an extended period of time.

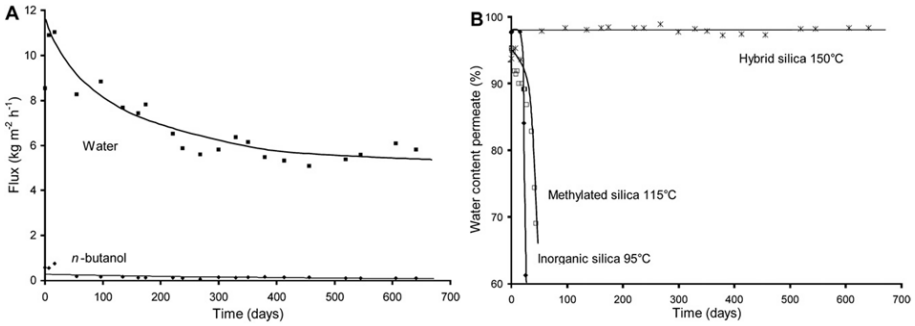

Figure 1.2: Long-term separation performance of BTESE/MTES hybrid silica membranes for dehydration of *n*-butanol (5 wt. % water) by pervaporation at 150 °C. **(A)** A 4% change in H_2O-flux was observed in 700 days. **(B)** Very high water selectivity was observed by these membranes at 150 °C in comparison with inorganic and methylated silica membranes [21].

The viability of BTESE membranes in gas separation was first exploited by Tsuru et. al [38, 39]. They developed a BTESE membrane that showed a H_2-permeance in the range of 10^{-5} mol/[m^2.s.Pa] at 200 °C with a H_2/N_2 permselectivity of less than 10. The reported synthesis was a very complicated multi-step sol synthesis. The formation of the hybrid sols in this case was discontinuous as the reaction was stopped and water was added at various times during the synthesis. This procedure resulted in an irregular pore microstructure and formed less selective membranes. Therefore, a systematic engineering of pores on structural level must be pursued to exploit the application window of this material with tailor-made pore sizes for targeting small molecular separations.

1.4 Aim of the thesis

The main focus of this thesis is the development of molecular sieving hybrid silica (BTESE) membranes by sol-gel processing, with substantial improvement and precision in their pore size and pore-size distribution to render them suitable for gas separation applications. This stresses an in-depth understanding of the sol-gel process parameters and their implications in forming a defect-free selective film that would result in molecular separation performance equal (or close) to conventional silica membranes.

A systematic investigation, targeting hybrid silica (BTESE) sols and gels, will be carried out to examine the influence of sol-gel process conditions and doping of metal ions into the hybrid silica materials on the pore size and performance of BTESE membranes. Sol process parameters such as reaction time and temperature, acid catalyst, hydrolysis ration and dip-sol rheology will be studied in detail and their implication in making a defect-free microporous layer will be examined. The realization of incorporating a metal ion in a hybrid silica network is not a straightforward route due to the mismatch in reactivities between the precursors. The fabrication recipe must be tuned and optimized with the aid of varying either process conditions or the reactivity of precursors. In addition to that, the prospects of fabricating a mesoporous hybrid-silica intermediate layer as a substitute of gamma-alumina will be studied.

References

[1] M. Mulder, Basic Principles of Membrane Technology, 2nd edition., Kluwer Academic Publishers, Dordrecht, 2000.

[2] R.W. Baker, Membrane technology and Applications, John Wiley & Sons, Ltd. West Sussex, England., 2004.

[3] N.W. Ockwig, T.M. Nenoff, Membranes for Hydrogen Separation, Chemical Reviews, 107 (2007) 4078-4110.

[4] A.J. Burggraaf, L. Cot, Fundamentals of Inorganic Membrane Science and Technology (Series 4), Elsevier, 1996.

[5] W.J. Koros, Y. H. Ma, T. Shimidzu, Terminology for membranes and membrane processes ((IUPAC Recommendations 1996), Pure & Appl. Chem., 68 (1996) 11.

[6] C. Casadocoterillo, A. Mariaurtiagamendia, I. Ortizuribe, Pervaporation and Gas Separation Using Microporous Membranes, 13 (2008) 217-253.

[7] R.J. Uhlhorn, Ceramic Membranes for Gas Separation: Synthesis and transport properties. PhD thesis, University of Twente, 1990.

[8] R.S.A. de Lange, J.H.A. Hekkink, K. Keizer, A.J. Burggraaf, Formation and characterization of supported microporous ceramic membranes prepared by sol-gel modification techniques, Journal of Membrane Science, 99 (1995) 57-75.

[9] R.d. Vos, High-Selectivity, High-Flux Silica Membranes for Gas Separation: Synthesis, Transport and Stability. PhD Thesis University of Twente, 1998.

[10] C. Guizard, Sol-gel chemistry and its applications to porous membrane processing (Chap. 7), in: A.J. Burggraaf, L. Cot (Eds.) Fundamentals of Inorganic Membrane Science and Technology, Elsevier Science, Amsterdam, 1996.

[11] G.W.S. C. Jeffrey Brinker, Sol-Gel Science: The Physics and Chemistry of Sol-Gel Processing, (1990).

[12] B.C. Bonekamp, A. van Horssen, L.A. Correia, J.F. Vente, W.G. Haije, Macroporous support coatings for molecular separation membranes having a minimum defect density, Journal of Membrane Science, 278 (2006) 349-356.

[13] N.K. Raman, C.J. Brinker, Organic “template” approach to molecular sieving silica membranes, Journal of Membrane Science, 105 (1995) 273-279.

[14] R.M. de Vos, H. Verweij, High-Selectivity, High-Flux Silica Membranes for Gas Separation, Science, 279 (1998) 1710-1711.

[15] R.d. Vos, High-Selectivity, High-Flux Silica Membranes for Gas Separation, PhD Thesis, University of Twente, 1998.

[16] G.Q. Lu, J.C. Diniz da Costa, M. Duke, S. Giessler, R. Socolow, R.H. Williams, T. Kreutz, Inorganic membranes for hydrogen production and purification: A critical review and perspective, Journal of Colloid and Interface Science, 314 (2007) 589-603.

[17] J. Campaniello, C.W.R. Engelen, W.G. Haije, P.P.A.C. Pex, J.F. Vente, Long-term pervaporation performance of microporous methylated silica membranesElectronic Supplementary Information (ESI) available: details of the sol synthesis; GPC and NMR measurements; and additional SEM micrographs. See http://www.rsc.org/suppdata/cc/b4/b401496k, Chemical Communications, (2004) 834.

[18] R.M. de Vos, W.F. Maier, H. Verweij, Hydrophobic silica membranes for gas separation, Journal of Membrane Science, 158 (1999) 277-288.

[19] H.L. Castricum, A. Sah, M.C. Mittelmeijer-Hazeleger, C. Huiskes, J.E.t. Elshof, Microporous structure and enhanced hydrophobicity in methylated SiO_2 for molecular separation, Journal of Materials Chemistry, 17 (2007) 1509.

[20] G. Cao, Y. Lu, L. Delattre, C.J. Brinker, G.P. López, Amorphous silica molecular sieving membranes by sol-gel processing, Advanced Materials, 8 (1996) 588-591.

[21] H.L. Castricum, A. Sah, R. Kreiter, D.H.A. Blank, J.F. Vente, J.E. ten Elshof, Hydrothermally stable molecular separation membranes from organically linked silica, Journal of Materials Chemistry, 18 (2008) 2150.

[22] Y.H. Kazuhiro Yoshida, Hironori Fujii, Toshinori Tsuru, Masashi Asaeda, hydrothermal stability and performance of silica-zirconia membranes for hydrogen separation in hydrothermal conditions, Journal of Chemicla Engineering of Japan, 34 (2001) 523-530.

[23] T. Tsuru, Nano/subnano-tuning of porous ceramic membranes for molecular separation, Journal of Sol-Gel Science and Technology, 46 (2008) 349-361.

[24] M. Asaeda, Ni-Silica mems for H_2 permeation and hydrothermal stability, Journal of Membrane Science, 271 (2006) 8.

[25] V. Boffa, Niobia-silica and silica membranes for gas separation, Ipskamp PrintPartners, The Netherlands.

[26] S. Battersby, T. Tasaki, S. Smart, B. Ladewig, S. Liu, M.C. Duke, V. Rudolph, J.C. Diniz da Costa, Performance of cobalt silica membranes in gas mixture separation, Journal of Membrane Science, 329 (2009) 91-98.

[27] S. Battersby, S. Smart, B. Ladewig, S. Liu, M.C. Duke, V. Rudolph, J.C.D.d. Costa, Hydrothermal stability of cobalt silica membranes in a water gas shift membrane reactor, Separation and Purification Technology, 66 (2009) 299-305.

[28] J. Wang, T. Tsuru, Cobalt-doped silica membranes for pervaporation dehydration of ethanol/water solutions, Journal of Membrane Science, 369 (2011) 13-19.

[29] V. Boffa, D. Blank, J. Tenelshof, Hydrothermal stability of microporous silica and niobia–silica membranes, Journal of Membrane Science, 319 (2008) 256-263.

[30] V. Boffa, J.E. ten Elshof, R. Garcia, D.H.A. Blank, Microporous niobia–silica membranes: Influence of sol composition and structure on gas transport properties, Microporous and Mesoporous Materials, 118 (2009) 202-209.

[31] M. Asaeda, Y. Sakou, J. Yang, K. Shimasaki, Stability and performance of porous silica–zirconia composite membranes for pervaporation of aqueous organic solutions, Journal of Membrane Science, 209 (2002) 163-175.

[32] G. P. Fotou, Y.S. Lin, S.E. Pratsinis, Hydrothermal stability of pure and modified microporous silica membranes, Journal of Materials Science, 30 (1995) 2803-2808.

[33] H.L. Castricum, A. Sah, R. Kreiter, D.H.A. Blank, J.F. Vente, J.E. ten Elshof, Hybrid ceramic nanosieves: stabilizing nanopores with organic links, Chemical Communications, (2008) 1103.

[34] H.L. Castricum, R. Kreiter, H.M. van Veen, D.H.A. Blank, J.F. Vente, J.E. ten Elshof, High-performance hybrid pervaporation membranes with superior hydrothermal and acid stability, Journal of Membrane Science, 324 (2008) 111-118.

[35] R. Kreiter, M.D.A. Rietkerk, H.L. Castricum, H.M. Veen, J.E. ten Elshof, J.F. Vente, Evaluation of hybrid silica sols for stable microporous membranes using high-throughput screening, Journal of Sol-Gel Science and Technology, 57 (2010) 245-252.

[36] Robert Kreiter, M.D.A. Rietkerk, H.L. Castricum, Henk M van Veen, J.E.t. Elshof, J.F. Vente, Stable Hybrid Silica Nanosieve Membranes for the Dehydration of Lower Alcohols, ChemSusChem, 2 (2009) 158-160.

[37] R. Kreiter, H.L. Castricum, J.F. Vente, J.E.T. Elshof, M.D. Anna, H.M. Veen, Hybrid silica membrane for water removal from lower alcohols and hydrogen separation (WO 2010008283 A1), in, 2011.

[38] M. Kanezashi, K. Yada, T. Yoshioka, T. Tsuru, Design of Silica Networks for Development of Highly Permeable Hydrogen Separation Membranes with Hydrothermal Stability, Journal of the American Chemical Society, 131 (2009) 414-415.

[39] M. Kanezashi, K. Yada, T. Yoshioka, T. Tsuru, Organic–inorganic hybrid silica membranes with controlled silica network size: Preparation and gas permeation characteristics, Journal of Membrane Science, 348 (2010) 310-318.

Chapter 2

Influence of sol-gel process parameters on the micro-structure and performance of hybrid silica membranes

This chapter is published as:
Hammad F. Qureshi, Arian Nijmeijer, Louis Winnubst "Influence of sol-gel process parameters on the micro-structure and performance of hybrid silica membranes" Journal of Membrane Science 446 (2013) 19-25

Abstract

A facile, versatile and reproducible sol-gel process to make microporous organosilica membranes by using 1,2-*bis* (triethoxysilyl) ethane (BTESE) as a precursor is reported. The influence of process parameters on sol particle size and rheology of BETSE-derived sols was investigated to produce defect-free composite membranes by a single dipping procedure and subsequent calcination. The microporous structure of a BTESE layer on mesoporous alumina supports enabled selective molecular sieving of gas molecules. Single gas permeation (SGP) experiments, performed at 200°C, showed that a H_2/CH_4 permselectivity of 24 was reproducibly achieved. No SF_6 gas permeance through these membranes proof the presence of a defect-free microstructure. SEM cross-section analysis showed a hybrid selective layer with a thickness dependent on the sol precursor concentration.

2.1 Introduction

Membrane applications can result in a significant energy reduction for industrial applications like in the areas of biofuels [1] and organic solvents recovery [2, 3]. However, for several separation applications, the membranes must overcome the desired selectivity and permeability trade-off as well as to achieve high stability and reliability under reactive operating conditions. Membranes that possess a microporous-structure (pore size < 2nm) can separate molecules either by molecular sieving or by affinity of specific molecules with the membrane material. When the pore size distribution of the porous structure is almost similar to the size of smallest molecule, this molecule can be separated from larger ones by simple molecular sieving. Generally, the term molecular sieving in membranes is used when the membrane pore size is < 1nm.

Acid catalyzed sol-gel derived silica membranes (pore size approximately 0.3 nm) are favorable candidates for gas separation due to their high thermal stability, high porosity and unprecedented performance. Sol-gel processing brings a strong possibility of controlling the pore structure of silica membranes and allows an ultra-thin coating of few tens of nanometers with high hydrogen permeance and performance [4]. These membranes are preferred over membranes developed by other techniques like chemical vapor deposition (CVD) due to ease of fabrication and higher H_2 permeance ($2X10^{-6}$ mol/m^2.s.Pa [4]) than for CVD derived membranes (H_2 permeance in the order of 10^{-8} mol/m^2.s.Pa [5]). However in wet conditions, the silica structure collapses due to hydrolysis of Si-O-Si groups, resulting in a reduced performance of the membrane.

The use of organic-inorganic silica alkoxides, such as *bis* (triethoxysilyl) ethane (BTESE), which contains organic groups between two silicon atoms, as a precursor, has demonstrated several times to be applicable for pervaporation and gas permeation [6-10]. The presence of a hydrocarbon group in this precursor brings the essential stability for these membranes under harsh industrial conditions but lacks the thermal stability at elevated temperatures (i.e. at 600 °C) in comparison to silica membranes due to the presence of organic groups inside the membrane matrix [6]. Castricum et. al [6] have shown that these type of hybrid silica membranes can be exceptionally stable in alcohol dewatering applications at

elevated temperatures. In gas separation, the commercial viability of these membranes is yet to occur due to poor H_2/CO_2 and H_2/CH_4 permselectivity. Another approach to modify the porous membrane microstructure for specific gas separation is the use of dopants like niobia in the BTESE matrix [11]. It is shown that niobia doping has improved H_2/CO_2 permselectivity to above 700. The author claims that niobia contents create acid sites in the membrane matrix that resulted in a very low CO_2 permeance through the membrane.

Although high hydrogen permeance values through BTESE membranes have been reported by Tsuru et. al [7], these membranes also show excessive permeance of SF_6, raising serious concerns about the uniformity in the pore size distribution and/or the presence of (micro-) defects in the membrane separation layer. A careful control and a critical check on sol process parameters (i.e. hydrolysis ratio, acid ratio, precursor concentration, reaction time) can give us more insight in sol morphology development during sol synthesis and in this way a better control in membrane formation can be achieved.

The BTESE sol synthesis strategy involves in most cases a multi-step addition of reagents with long sol processing (condensation) times (around 6-8 hours) [7, 8]. It is assumed that addition of any reagent during sol processing results in discontinuities during the reaction, which might complicate reaction kinetics, and may produce inhomogeneous sols and consequently inhomogeneous membrane characteristics (morphology, pore-size distribution etc.). Besides, with long sol condensation times, it is very likely that the sol particles might aggregate. Besides, in the sol-gel membrane fabrication process, dip coating is one of the most critical steps for the formation of the selective layer formation, followed by drying and calcination. Multi-step dip-coating, which is often used in literature, results in a multi-layered structure with thicker selective layers that can be more selective but will show lower permeances [12].

In this paper a simple and relatively fast approach for developing BTESE hybrid sols is described. All reactants could be added in one single step giving a monodispersed polymeric sol with particles of suitable size, which, after deposition on a multi-layered structure via a single dipping procedure, produces membranes with effective gas permselectivity results. The sol rheology was fine tuned to make the sols adaptable for a defect-free (no SF_6 permeance) selective layer. The effect of sol

reaction time on membrane microstructure has been studied, and implications of sol rheology in producing membranes with sufficient H_2/CH_4 permselectivity are presented in this contribution.

2.2 Experimental

As precursor 1,2-*bis*(triethoxysilyl)ethane (BTESE) (purity 97%, ABCR Germany) was used. Water was deionized at 18.2 MΩ/cm using a Millipore purification system. A polymeric sol was prepared by drop-wise adding BTESE to a nitric acid (65%, Aldrich) water-ethanol mixture. Addition was done in an ice-bath under vigorous stirring to control pre-mature (partial) hydrolysis. This mixture was refluxed at 60°C for either 1.5 or 3 hours under continuous stirring to produce hybrid sols. The effect of several process parameters i.e. precursor concentration [Si], hydrolysis ratio (HR), defined as hydrolysable ethoxy groups i.e. $[H_2O]$:$[OC_2H_5]$, and acid-precursor ratios (AR) $[H^+]$:[Si], was studied to produce defect-free membranes.

Disc-shaped α-alumina supported γ-alumina membranes (pore size 3-5 nm) were prepared by a dip-coating procedure of a boehmite sol on α-alumina supports (support thickness of 2.08±0.01 mm and pore diameter of 100nm; Pervatech B.V. The Netherlands), followed by subsequent drying and calcination, as described in detail in [4]. The boehmite-PVA dip-sol was twice coated on α-alumina supports to develop a smooth mesoporous intermediate layer. A pore size for the γ-alumina intermediate layer of 3-5nm was determined by permporometry, using the method as described in [13].

Dip-coating of a BTESE sol (with dipping speed of 1.4 cm/sec) on γ-alumina membranes was done in a cleanroom class 1000 to minimize defect formation due to dust particles. The dipping procedure was performed only once to deposit the selective hybrid layer on the mesoporous support. After coating of the hybrid sol, the membranes were calcined at 300°C for 3 hours under nitrogen flow (99.99% pure), applying heating and cooling rates of 0.5 °C/min.

The sol and membrane fabrication experiments were performed several times to confirm the reproducibility of these results.
Particle sizes of freshly prepared hybrid sols were determined by dynamic light scattering (DLS) using a Malvern Zetasizer Nano ZS at 25°C. The viscosity of the sols

with several [Si] was determined by a rolling ball viscometer (Anton Paar, Belgium) at 25°C. The thickness of the calcined hybrid silica layers was determined by analyzing cross-sectional views of the membranes using a high-resolution scanning electron microscope HR-SEM (ZEISS 1550) at an accelerating voltage of 2.0kV.

Membrane characterization was performed on an in-house designed single gas permeation (SGP) set-up in a dead-end mode without backpressure. The membranes were sealed in a stainless steel module using Viton® 51414 O-rings with the separation layer exposed to the feed side. The gas permeance was measured at 200°C in a sequence, starting with the gas of smallest kinetic diameter, from He (0.255 nm), H_2 (0.289 nm), N_2 (0.364 nm), CO_2 (0.33 nm), CH_4 (0.389 nm) to SF_6 (0.55 nm) and H_2 (again) at 200°C with a trans-membrane pressure of 2 bar. The H_2 permeance measurements were performed again at the end of all measurements to ensure stable membrane microstructure. Only a 1 - 3 % variation in H_2 permeance was observed between the two measurements. The gas permeation results of each Si concentration were reproduced four times.

Membrane performance via SGP was determined by:

$$F_i = \frac{N_i}{\Delta P} \quad (1)$$

Where F is the permeance of gas *i*, determined by calculating the molar flux (N) of the gas through the membrane at a pressure difference (ΔP) between feed and permeate side.

2.3 Results and Discussion

2.3.1 Hybrid Silica Membrane Fabrication

A first indication whether a sol is suitable for membrane fabrication is that it must not gelate during the sol synthesis. Thus, a careful control of sol process parameters (Si concentration, AR, HR) was critical in obtaining a non-gelated BTESE sol. In membrane fabrication, control of sol particle size determines the quality of coated layer. The particle size of developed sols must be in a range that, when deposited on mesoporous intermediate layer, the sol should form a homogenous and smooth selective layer. Deposition of sols with particle sizes smaller than the mean pore size

of the porous support will result in sol infiltration and coating with a too large polymeric sol leads to a thick layer that is prone to crack formation [6, 14].

In this work, BTESE sols were produced starting with Si concentrations of 0.9 M and 1.8 M. A sol, prepared with a Si concentration of 0.9 M, produced systems with an average particle size of 4 nm. The particle size of these sols was of the same order of magnitude as the pore size of the γ-alumina intermediate layer. A test of the membrane after coating/calcining with a rhodamine solution showed a bare γ-alumina surface, indicating that no dense hybrid layer was formed on the top of the γ-alumina. Therefore the Si concentration was increased to 1.8 M to obtain larger sol particles in order to avoid sol infiltration in the membrane support, resulting in a homogeneous layer after coating. It is possible that a Si concentration between 0.9 M and 1.8 M can also produce BTESE sols with the desired particle size and morphology, but in the current work the Si concentration of 1.8 M was further investigated for finding optimal experimental conditions for reproducible fabrication of BTESE hybrid membranes.

Table 2.1 represents BTESE sol fabrication recipes at a Si concentration of 1.8 M, a reaction time of 1.5 hours and a reaction temperature of 60 ^{o}C. Different hydrolysis and acid ratios were used to produce sols. Acid ratios of 0.3 and 0.5 resulted in gelated sols at all hydrolysis ratios. It is observed [15] that higher acid contents accelerated cluster formation inside the sol, which forced sol aggregation and ended up in sol gelation. A higher acid ratio also leads to liquid-liquid immiscibility that disrupted reaction kinetics, also causing sol gelation. In the present work no liquid-liquid immiscibility was observed during the sol fabrication process, while only an acid ratio of 0.1 produced non-gelated sols at hydrolysis ratios of 1, 2 and 3 (table 2.1).

Table 2.1: T = 60 ^{o}C, t = 1.5 h, Si = 1.8 M (BTESE = [Si / 2)

Acid Ratio [H^+:Si]	**Hydrolysis Ratio [H_2O:OC_2H_5]**	**Sol particle size and distribution after Sol processing**
0.1	1	Monodisperse; Z^*_{mean} = 8 nm
	2	Very high polydispersity; Z_{mean} > 40 nm
	3	Very high polydispersity; Z_{mean} > 100 nm
	4	Sol gelation
0.3	1	Sol gelation
	2	Sol gelation
	3	Sol gelation
	4	Sol gelation
0.5	1	Sol gelation
	2	Sol gelation
	3	Sol gelation
	4	Sol gelation

Z* = sol particle size

BTESE sols, produced at a Si concentration of 1.8 M, AR = 0.1 and HR = 1, were chosen for membrane coating because the average particle size of these sols was about 7-8 nm and it was the only sol with a uniform particle-size. This mother sol was called sol 1. To study the effect of reaction time on sol properties, another mother sol (sol 2) was synthesized under identical reaction conditions as sol 1, though with an increased reaction time of 3 hours. The increased reaction time produced a sol with a bimodal particle size distribution with relatively larger sol particles than sol 1 (as shown in figure 2.1).

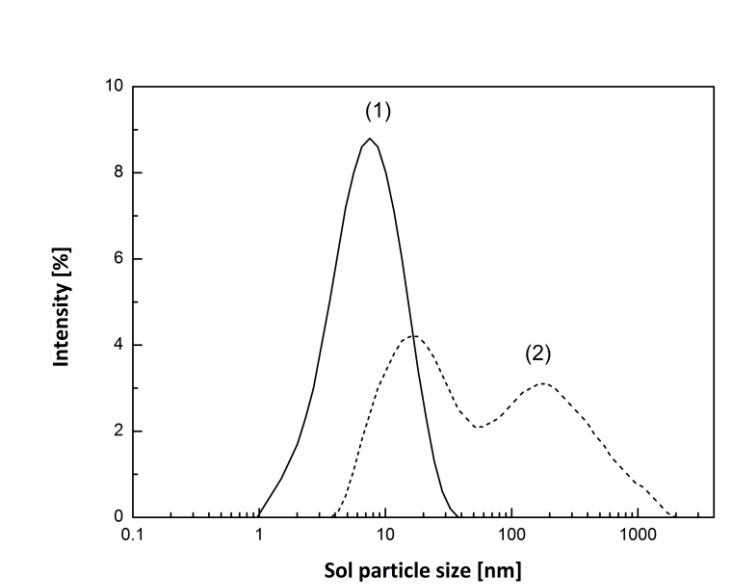

Figure 2.1: Particle size and particle-size distribution of sol 1 (1.5 hours) and sol 2 (3 hours), as determined by dynamic light scattering at 25°C.

Figure 2.2 shows the viscosity at 25°C of fresh mother sols 1 and 2 as a function of [Si], as achieved by diluting the respective sols with appropriate amounts of ethanol. It is clear from this figure that sol 2 shows a stronger increase in viscosity with increasing Si concentration if compared with sol 1. This can be explained by the fact that with an increase in reaction time, the extent of cross-linking between the sol particles (i.e. sol entanglement) increases resulting in an increase in sol viscosity [16]. The broad sol particle size distribution as observed for sol 2 can also be explained by this "sol-entanglement" effect. The particle size distribution in sol 1 is more uniform and its viscosity only slightly increases with increasing sol concentration. Since high viscous sols tends to gelate faster than the moderate ones [16] and the fact that this gelation plays a pivotal role in dip-coating and consequently in the development of a defect-free membrane, it is a pre-requisite that the sol must not have a too high viscosity. In general, viscous sols exhibit more slip effects than lower viscous sols at the same concentration and tend to form a non-uniform and thicker deposited layer [12]. Therefore the membranes developed by high viscous sols will be more prone to get cracked than those developed by

lower viscous sols. Besides, during drying and calcination of viscous dipped sols, the capillary forces of the gel (in the selective layer) can exceed the adhesion limit between support and gel, ending up in delaminating the selective layer completely from the substrate.

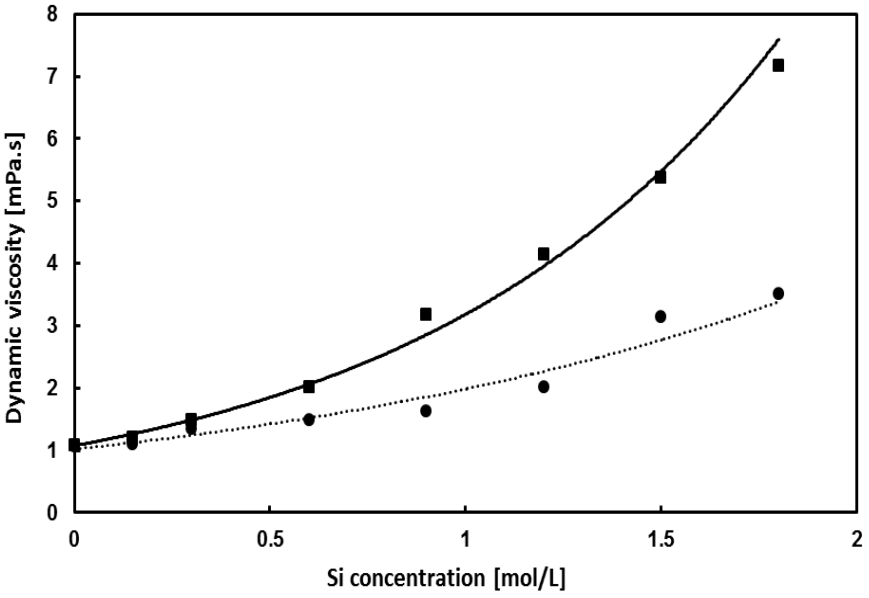

Figure 2.2: Sol viscosity at 25°C as a function of precursor concentration and varying sol processing time. ● (1.5 hours) and ■ (3 hours).

Figure 2.3 shows a 0.6 M crack-free membrane from sol 1 (right) and a 1.8 M cracked membrane from sol 2 (left) after calcination. The 1.8 M membrane of sol 2 was selected as illustration because of more visible surface cracks than other membranes. Crack-free BTESE membranes from sol 1 were produced at Si concentrations of 0.09 M, 0.15 M, 0.3 M, and 0.6 M respectively. If, by applying this sol 1, a concentration of more than 0.6 M was used, not all membranes remained crack free. Membranes produced from sol 2 only results in crack-free membranes at concentrations of 0.15 M and 0.3 M. Although there was a very small difference in sol viscosity between sol 1 and sol 2 at a sol concentration of 0.6 M (see figure 2.2), sol 1 gave crack-free membranes while sol 2 gave cracked membranes. This is due to the difference in sol particle size and morphology between sol 1 and sol 2 that

developed into a completely different pore-microstructure after dipping and calcination.

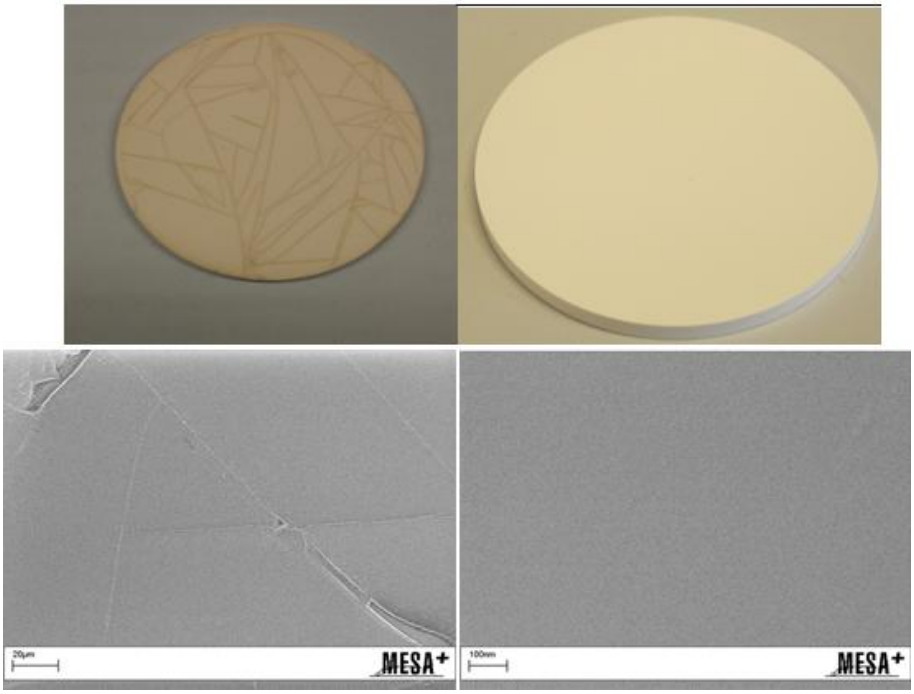

Figure 2.3: Surface of a disc-shaped cracked BTESE membranes **(left)** and crack-free membrane **(right)** after calcination at 300°C under nitrogen. **Left:** BTESE membrane from sol 2 with a Si concentration of 1.8 M; **Right:** BTESE membrane from sol 1 with a Si concentration of 0.6 M.

During calcination at high Si concentration the entangled network of the more viscous sol 2 increased the capillary forces between deposited particles, and destroyed the pore microstructure resulting in cracks on the membrane surface and eventually the top layer gets detached from the surface resulting in a complete breakdown in microstructure. Castricum et. al. [6] showed that membrane coating starting from polymeric sols with large particle sizes and high fractal dimensions lead to thicker membranes, which are prone to crack formation. Defects can be minimized by controlling the sol viscosity, withdrawing speed during dip-coating [17], and post dipping treatment procedure (calcination conditions like heating /cooling program, atmosphere etc.).

High resolution scanning electron microscopy was carried out to study the thickness of membranes made by both sols using various dipping concentrations. All membranes discussed in this part are defect free; i.e. no cracks were found by HR-SEM and no detectable permeance of SF_6 was observed (see later). Micrographs of membranes from sol 1 gave a sequential array of membrane thickness as a function of Si concentration, as shown in figure 2.4. Membranes with a Si concentration of 0.6 M have a membrane thickness of 550 nm while the membrane with a Si concentration of 0.09 M possessed a thickness of 90 nm. The membrane from sol 2 with a Si concentration of 0.15 M developed into a layer thickness of 170 nm (figure 2.5), which is almost twice as thick as a membrane from sol 1 with a similar Si concentration (90 nm: see figure 2.4). In conclusion, by controlling the sol viscosity and the particle size of the dip sols, an ultra-thin and homogenous selective layer can be produced.

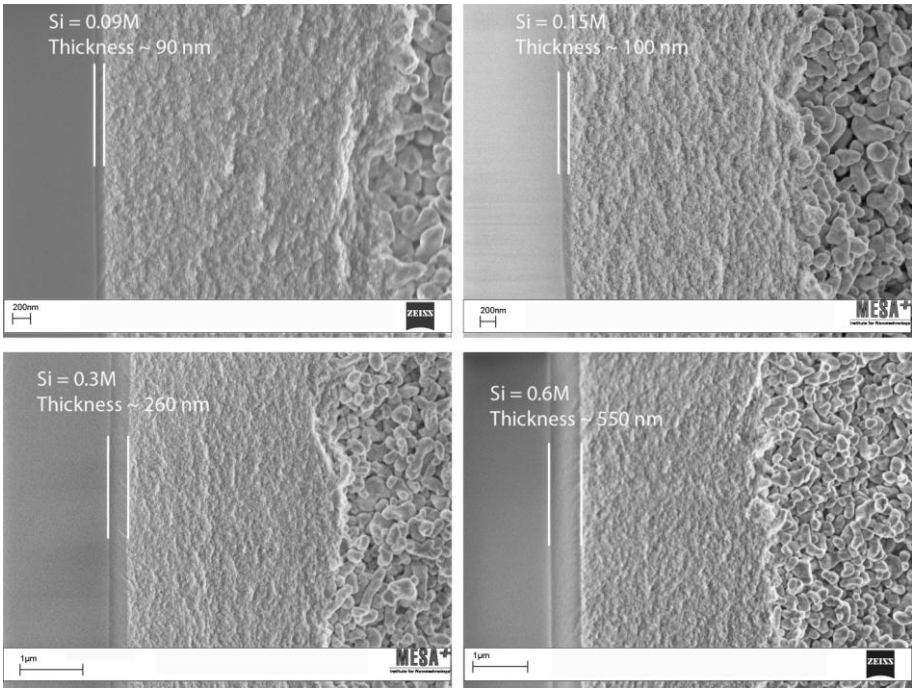

Figure 2.4: Cross-sectional SEM micrographs of defect-free BTESE membranes developed from sol 1 with varying sol concentrations (degree of dilution).

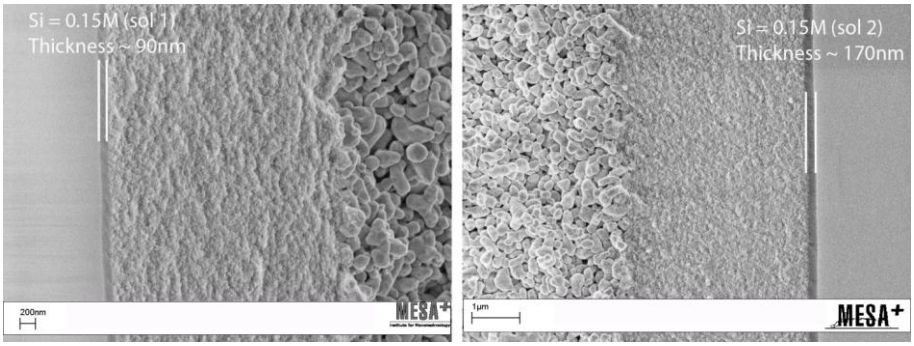

Figure 2.5: Cross-sectional SEM micrographs of BTESE membranes made of sol 1 (left) and sol 2 (right) with an identical Si concentration of 0.15 M.

2.3.2 Hybrid Silica Membrane Performance

Single gas permeation (SGP) results of calcined BTESE membranes from sol 1 and 2 are shown in table 2.2 and 2.3 respectively. All membranes showed no SF_6 permeance (detection limit of the equipment is 5 x 10^{-10} mol/m^2.s.Pa), indicating a defect-free structure. It can therefore be concluded that the pore size of all the fabricated membranes (from both sol 1 and sol 2) was less than 0.55 nm (= kinetic diameter of SF_6).

Table 2.2: Single Gas Permeation and selectivity results at 200°C of hybrid membranes produced from sol 1 at dip-sol concentrations: 0.09, 0.15, 0.3 and 0.6 M.

Gas Kinetic Diameter [nm]	Gas Permeance (10^{-7} mol/m^2.s.Pa)	Selectivity H_2/X	Gas Permeance (10^{-7} mol/m^2.s.Pa)	Selectivity H_2/X	Gas Permeance (10^{-7} mol/m^2.s.Pa)	Selectivity H_2/X	Gas Permeance (10^{-7} mol/m^2.s.Pa)	Selectivity H_2/X
	(0.09 M)		**(0.15 M)**		**(0.3 M)**		**(0.6 M)**	
He = 0.26	3.32	1.39	3.52	1.22	2.52	1.23	2.05	1.31
H_2 = 0.289	4.62	1	4.32	1	3.12	1	2.7	1
CO_2 = 0.33	1.24	3.7	1.19	3.6	0.8	3.9	0.46	5.8
N_2 = 0.364	0.44	10.5	0.34	12.2	0.23	13.5	0.13	20.8
CH_4 = 0.369	0.4	11.5	0.23	18.8	0.16	19.5	0.11	23.7
SF_6 = 0.55	*	∞	*	∞	*	∞	*	∞

* Below detection limit of equipment i.e. below 5 X 10^{-10} mol/m^2.s.Pa.

Table 2.3: Single Gas Permeation and selectivity results at 200°C of hybrid membranes produced from sol 2 at dip-sol concentrations: 0.15 and 0.3 M.

Gas Kinetic Diameter [nm]	Gas Permeance (10^{-7} mol/m^2.s.Pa)	Selectivity H_2/X	Gas Permeance (10^{-7} mol/m^2.s.Pa)	Selectivity H_2/X
	(0.15 M)		**(0.3 M)**	
He = 0.26	2.6	1.4	1.6	1.6
H_2 = 0.289	3.17	1	2.07	1
CO_2 = 0.33	0.89	3.7	0.56	3.5
N_2 = 0.364	0.33	10.2	0.2	9.6
CH_4 = 0.369	0.39	14.7	0.14	8.1
SF_6 = 0.55	*	∞	*	∞

* Below detection limit of equipment i.e. below 5 X 10^{-10} mol/m^2.s.Pa.

Membranes developed from both sols showed for all gases a decrease in permeance with increasing dip-sol concentration (table 2.2 and 2.3). It elucidates that membranes prepared from a more diluted sol offered less gas flow resistance, but at the cost of H_2/X selectivity. A H_2/CH_4 selectivity of 24 was achieved (almost 10 times more than the Knudsen diffusion value of 2.8) with membranes made from sol 1 with a Si concentration of 0.6 M, while it was dropped to almost to 12 with membranes made from sol 1 with a Si concentration of 0.09 M. Similarly, a H_2/N_2 permselectivity of 21 was achieved with a Si concentration of 0.6 M which is almost 6 times more than the Knudsen selectivity of 3.7, indicating the molecular sieving effect of these membranes. All these results show that membrane performances were dependent on precursor concentration. Membranes developed by sol 2 at Si concentrations of 0.15 M and 0.3 M, show in most cases permeances as well as permselectivities lower than those made from sol 1, but still with H_2/N_2 and H_2/CH_4 permselectivities higher than selectivities calculated from Knudsen indicating that also here the transport mechanism is dominated by molecular sieving. To conclude, all membranes studies in this work showed better H_2/N_2 and H_2/CH_4 permselectivities than obtained with only Knudsen diffusion.

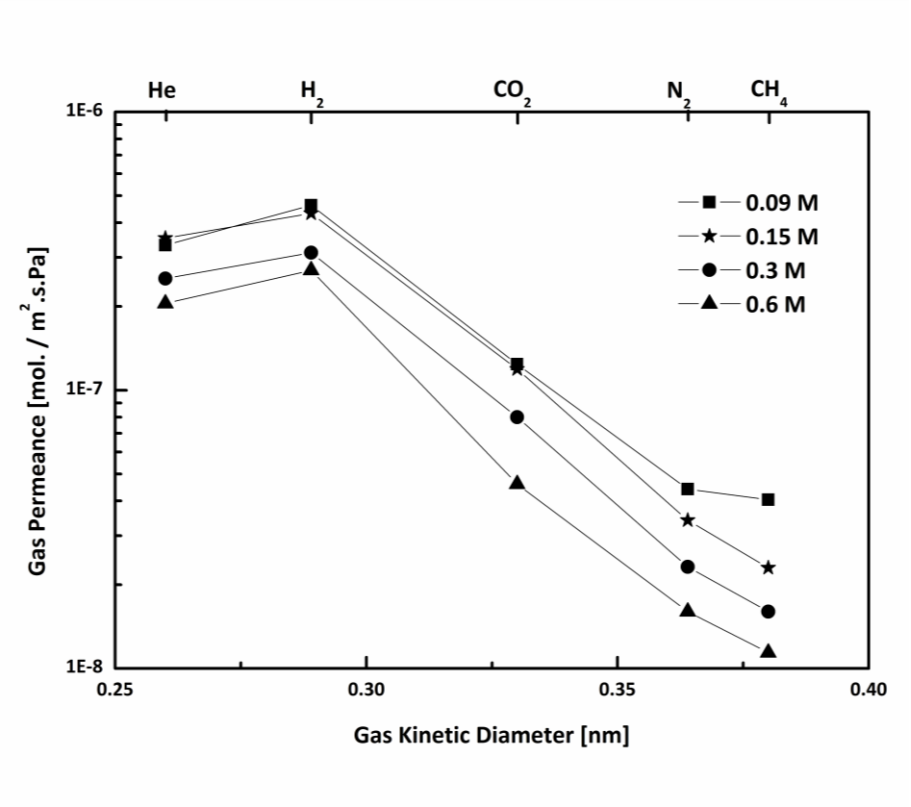

Figure 2.6: Single gas permeance results as a function of gas kinetic diameter of BTESE membranes made by sol 1.

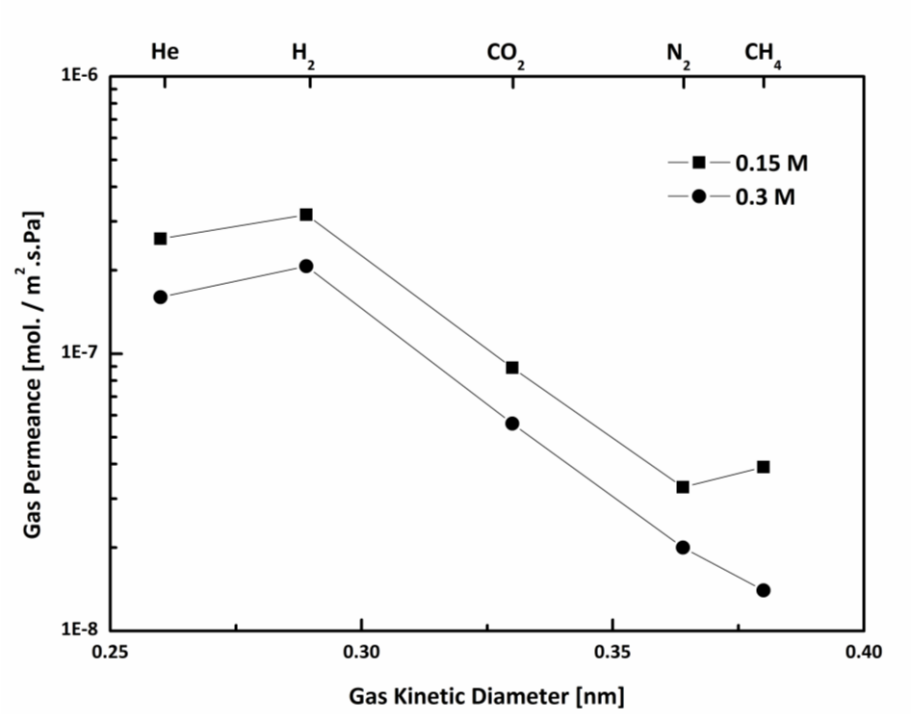

Figure 2.7: Single gas permeance results as a function of gas kinetic diameter of BTESE membranes made by sol 2.

For inorganic silica (SiO_2) membranes the He permeance is higher than H_2 permeance because for these membranes the transport mechanism is based on molecular sieving resulting in a He/H_2 permselectivity larger than 1 [4]. Lower permeances for He than for H_2 are expected if the pores in the membrane are larger than 0.3 nm, because in that case Knudsen diffusion is dominating for these small molecules (He having lower mass), resulting in a He/H_2 permselectivity of less than 1. For all BTESE hybrid membranes, produced from sols 1 and 2, the He/H_2 permselectivity was less than 1 (between 0.7 and 0.75) indicating that the average pore size was bigger than 0.3 nm i.e. the BTESE membrane pore size is larger than the pure silica membrane pore size. For pure silica a pore size of less than 0.36 nm was determined [4]. Combined with the non-detectable SF_6 permeance (d_k = 0.55 nm) through these BTESE hybrid membranes made us conclude that the membranes studied in this work, have a pore size ranging from 0.3 nm to 0.54 nm.

To the best of our knowledge, these are by far the best pure and undoped hybrid silica membranes developed with a H_2/CH_4 permselectivity of 24 and an infinite H_2/SF_6 permselectivity at 200°C. Results, as given in literature, dealing with gas permeation of BTESE-derived hybrid membranes observed some SF_6 [7, 10] permeance indicating a relatively more open pore microstructure.

For porous membranes, the H_2/CO_2 Knudsen permselectivity is 4.7. A deposited selective layer must show a H_2/CO_2 permselectivity of more than 4.7 to inscribe its significance as a CO_2-selective membrane. The BTESE membranes developed in this work however showed H_2/CO_2 permselectivities below Knudsen diffusion except only one with 0.6M Si concentration showing a H_2/CO_2 permselectivity of about 6, which is also not sufficient for industrial application. Castricum et. al. [9] has demonstrated that hybrid silica membranes exhibits affinity towards CO_2 that can be tuned by tailoring the bridged hydrocarbons chains in the silicon moieties. From our work we can conclude that the CO_2 transport across BTESE derived membranes is dominated by surface diffusion and not by molecular sieving.

Table 2.4: Gas separation performances of BTESE membrane are compared with the silica and other state-of-the-art BTESE membranes.

Membrane (Calc. T / °C)	**H_2 permeation [mol/m^2.s.Pa]**	**Selectivity H_2/N_2**	**Selectivity H_2/CH_4**	**Selectivity H_2/SF_6**	**Reference**
Silica 400	2×10^{-6}	70	> 500	Infinity	[4]
Silica 600	5×10^{-7}	infinity	infinity	Infinity	[4]
BTESE 300	2×10^{-5}	10	-	-	[7]
BTESE 250	1.3×10^{-6}	16	-	-	[9]
BTESE 300*	5.6×10^{-6}	22	-	25,500	[10]
BTESE 300	4.3×10^{-7}	21	24	Infinity	This work

* Membrane that showed the best permselectivity results amongst the ones reported in the contribution.

2.4 Conclusions

Hybrid silica membranes with interesting gas permselectivity properties have been reproducibly prepared from a single-step sol-gel synthesis route, using an ethoxy-bridged silane (BTESE) as precursor. The resulting membrane obtained by a single dipping/calcining step, consists of organically bridged silica moieties and has a more open micropore structure than pure silica membranes. The fabrication protocol is optimized and has undergone substantial simplification which enables us to develop sols with a mono-disperse particle size distribution. Sol rheology and its variation with Si concentration was investigated and defect-free hybrid membranes with varying layer thicknesses, dependent on sol concentration, could be produced. A H_2/CH_4 permselectivity of 24 was achieved with membranes having a precursor concentration of 0.6 M.

Acknowledgements

This research is supported by Netherlands Technology Foundation (STW). We are grateful to Antonio Moreno Mora (Erasmus student from University of Barcelona, Spain) for assistance in the viscosity measurements, and Mark Smithers (Laboratory for Materials Characterization at the MESA+ institute for Nanotechnology) for capturing high resolution SEM images.

References

[1] L.M. Vane, A review of pervaporation for product recovery from biomass fermentation processes, Journal of Chemical Technology & Biotechnology, 80 (2005) 603-629.

[2] A.M. Urtiaga, E.D. Gorri, P. Gómez, C. Casado, R. Ibáñez, I. Ortiz, Pervaporation Technology for the Dehydration of Solvents and Raw Materials in the Process Industry, Drying Technology, 25 (2007) 1819-1828.

[3] S. Sommer, T. Melin, Performance evaluation of microporous inorganic membranes in the dehydration of industrial solvents, Chemical Engineering and Processing: Process Intensification, 44 (2005) 1138-1156.

[4] R.M. de Vos, H. Verweij, High-Selectivity, High-Flux Silica Membranes for Gas Separation, Science, 279 (1998) 1710-1711.

[5] G.R. Gavalas, C.E. Megiris, S.W. Nam, Deposition of H2-permselective SiO_2 films, Chemical Engineering Science, 44 (1989) 1829-1835.

[6] H.L. Castricum, R. Kreiter, H.M. van Veen, D.H.A. Blank, J.F. Vente, J.E. ten Elshof, High-performance hybrid pervaporation membranes with superior hydrothermal and acid stability, J Membrane Sci, 324 (2008) 111-118.

[7] M. Kanezashi, K. Yada, T. Yoshioka, T. Tsuru, Design of Silica Networks for Development of Highly Permeable Hydrogen Separation Membranes with Hydrothermal Stability, J Am Chem Soc, 131 (2009) 414-415.

[8] H.L. Castricum, A. Sah, R. Kreiter, D.H.A. Blank, J.F. Vente, J.E. ten Elshof, Hydrothermally stable molecular separation membranes from organically linked silica, Journal of Materials Chemistry, 18 (2008) 2150.

[9] H.L. Castricum, G.G. Paradis, M.C. Mittelmeijer-Hazeleger, R. Kreiter, J.F. Vente, J.E. ten Elshof, Tailoring the Separation Behavior of Hybrid Organosilica

Membranes by Adjusting the Structure of the Organic Bridging Group, Advanced Functional Materials, 21 (2011) 2319-2329.

[10] M. Kanezashi, K. Yada, T. Yoshioka, T. Tsuru, Organic–inorganic hybrid silica membranes with controlled silica network size: Preparation and gas permeation characteristics, J Membrane Sci, 348 (2010) 310-318.

[11] H. Qi, H. Chen, L. Li, G. Zhu, N. Xu, Effect of Nb content on hydrothermal stability of a novel ethylene-bridged silsesquioxane molecular sieving membrane for H_2/CO_2 separation, J Membrane Sci, 421–422 (2012) 190-200.

[12] A.J. Burggraaf, Fundamentals of Inorganic Membrane Science and Technology, in: B.C. Bonekamp (Ed.) Preparation of asymmetric ceramic membrane supports by dip-coating, Elsevier Science, 1996.

[13] A.J. Burggraaf, Permporometry study on the size distribution of active pores in porous ceramic membranes, J Membrane Sci, 83 (1993) 14.

[14] C.J. Brinker, R. Sehgal, S.L. Hietala, R. Deshpande, D.M. Smith, D. Loy, C.S. Ashley, Sol-gel strategies for controlled porosity inorganic materials, J Membrane Sci, 94 (1994) 85-102.

[15] A.C. Pierre, Introduction to Sol-Gel Processing, Kluwer Academic Publishers (1998).

[16] G.W.S. C. Jeffrey Brinker, Sol-Gel Science: The Physics and Chemistry of Sol-Gel Processing, (1990).

[17] A.F.M. Leenaars, Burggraaf, A. J., The Preparation and Characterization of alumina membranes with Ultrafine Pores 2. The Formation of Supported Membranes, Journal of Colloid and Interface Science, 105 (1985) 14.

Chapter 3

Hybrid silica membranes with enhanced gas separation properties

This chapter is in preparation to be published as:
Hammad F. Qureshi, Hessel L. Castricum, Arian Nijmeijer, Louis Winnubst, "Hybrid silica membranes with enhanced gas separation properties".

Abstract

A reliable and reproducible sol-gel process is reported for the fabrication of highly size-selective microporous hybrid silica membranes by using 1,2-*bis* (triethoxysilyl)ethane (BTESE) as a precursor. The acid concentration and the condensation time were tuned to synthesize membranes with a constricted pore structure by using a single dipping procedure. Single gas permeation experiments, performed at 200 °C, showed that the developed membranes could be impermeable towards nitrogen and methane, while all membranes showed a H_2/N_2 permselectivity of at least 50. The size selectivity is far better than of all other hybrid silica membranes developed to date. SEM cross-section analysis showed a thin hybrid layer of about 440 nm, an isotropic surface and a flawless microstructure.

3.1 Introduction

The separation and purification of molecular mixtures in the chemical industry consume substantial amounts of energy. To reduce fossil fuel consumption, efficient separation processes are needed to obtain high-grade products in food and pharmaceutical industries [1, 2], high quality pure water [3], and to remove or recover toxic or valuable components from industrial effluents [4]. Today, membranes are used on a large scale for the production of potable water, for cleaning industrial effluents, to recover valuable constituents in biomass fermentation[5, 6], as well as for bio gas upgrading [7, 8] and gas and vapor separation [9, 10]. Besides, membranes are also a key component in energy conservation and - storage systems [11], artificial organs [12] and drug delivery devices [13].

Amorphous silica is an attractive material for application in microporous inorganic membranes, because of its thermal stability and high gas separation selectivity [14]. Through acid catalyzed sol-gel processing of e.g. tetraethylorthosilicate (TEOS), it is relatively easy to develop a thin separation layer with a narrow pore size that is applied onto a support that provides mechanical strength [15]. After calcination of the dip coated sol-gel derived silica network a homogeneous membrane is formed [16] that allows the selective permeation of small molecules such as helium (kinetic diameter = 0.26 nm) and hydrogen (0.29 nm), while showing little or no permeation of the bigger molecules like nitrogen (0.36 nm) or methane (0.39 nm) [17]. However, the modest stability of the silica structure to water severely limits its application in many industrial processes that involve hydrothermal conditions [18]. Modification of the silica network with metal ions [19-22] or the use of hydrophobic silanes [23, 24] has been reported to improve the hydrothermal stability.

An even more effective way to improve the hydrothermal stability of silica-based membranes is by using organic-inorganic silicon alkoxides (silsesquioxanes) that contain an organic bridging groups between two silicon atoms [25-27], such as 1,2-*bis*(triethoxysilyl) ethane (BTESE). This hybrid silica material has shown stability in water up to several years in pervaporation studies [18, 25]. It was suggested from computer simulations that the size of the bridging groups limits the size-based gas permselectivity, as the structural units may allow some permeance of molecules of

the size of N_2 [28, 29]. By using only BTESE as a silicon precursor, not only highly permeable hydrogen separation membranes can be successfully prepared [26], but also a homogenous and uniform pore-microstructure is possible by a single-dipping procedure resulting in a thin isotropic selective layer down to 90 nm thickness, showing a flawless pore microstructure [30]. However, no H_2/N_2 and H_2/CH_4 permselective ratios higher than 25 have yet been reported for these BTESE-derived membranes.

In a previous contribution we studied BTESE membranes prepared from acid-catalyzed sols using an acid ratio (AR, $[H^+:Si]$) of 0.1, a hydrolysis ratio (HR, $[H_2O:OC_2H_5]$, where $–OC_2H_5$ are the hydrolysable alkoxy-groups in the Si-precursor) of 1 and a precursor concentration [Si] of 1.8 M [30]. It is well-known that acid-catalyzed synthesis results in sols with linear polymer chains [17] which give microporous materials after drying and calcination. Reduction of the acid concentration results in lower hydrolysis and condensation rates [31]. In this work, BTESE sols are synthesized at a reduced acid ratio of 0.01. It was anticipated that this would lead to more constricted pores, and improve the size selectivity to gases.

3.2 Experimental

As a hybrid silica precursor 1,2-*bis*(triethoxysilyl) ethane (BTESE) (purity 97%, ABCR Germany) was used. Water was deionized at 18.2 MΩ/cm using a Millipore purification system. A polymeric sol was prepared by drop-wise addition of BTESE to a nitric acid (65 wt.%, Aldrich)–water–ethanol mixture. Addition was done in an ice bath under vigorous stirring to control pre-mature (partial) hydrolysis. This mixture was subsequently refluxed at 60 °C for 30 minutes under continuous stirring to produce hybrid silica sols at an acid ratio AR = 0.01, hydrolysis ratio HR = 1, and [Si] = 2.7 M. The molar ratio of added reagents was BTESE/EtOH/HNO_3/ H_2O of 1/4.6/6.8/0.02 respectively.

The acid catalyzed BTESE sol synthesis is expected to follow the same S_N2-reaction mechanism as is observed for the synthesis of tetraethoxysilane (TEOS)-based sols [31-33]. The hydrolysis reaction of the hybrid siloxane (BTESE) under the formation of a silanol, with the liberation of alcohol as a by-product, is shown in the following scheme (equation 1).

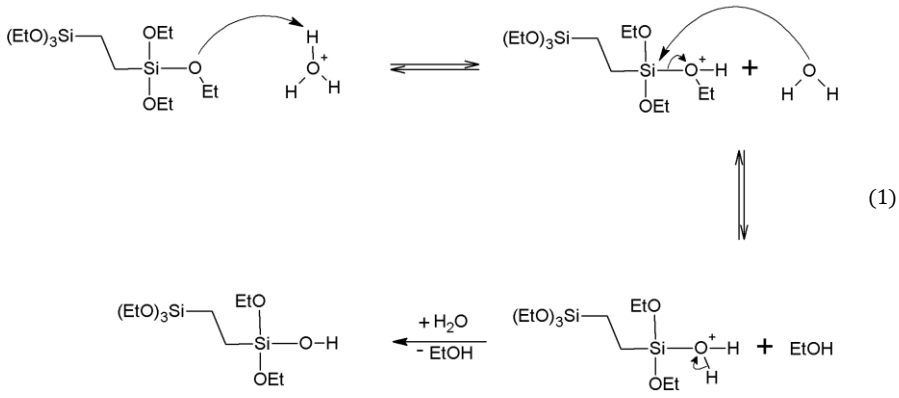

During the hydrolysis reaction, the alkoxide group is rapidly protonated, resulting in the withdrawal of electrons from the silicon atom and consequently making the Si atom more electrophilic and more likely to be attacked by water. This is followed by the detachment of alcohol from the substrate, making it a 'leaving group'. As a result of this S_N2 mechanism, the hydrolysis reaction is fast and it decreases after the removal of one ethoxy-group, because less electron providing substitutes become available to stabilize the positive charge on silicon atom.

The condensation reaction already starts before completion of the hydrolysis reaction [32]. During condensation the protonation of the hydroxyl groups in the silanols results in oxo-bridged siloxane (Si-O-Si) groups. Condensation is initiated by protonation of either an ethoxy or hydroxy group, which makes the neighboring silicon atom more electrophilic. Then this silicon atom is attacked by another silanol group, which resulted in the formation of an oxo-bridge. Depending on whether an ethoxy or a hydroxyl group was protonated, either ethanol or water will be the leaving group of the primer silicon atom respectively. Therefore, the BTESE condensation reaction follows two possible routes: water and alcohol condensation which are given in equation 2 and 3 respectively. The initial condensation is fast and decreases, as less electron providing substituents are left to stabilize the positive charge of protonated group.

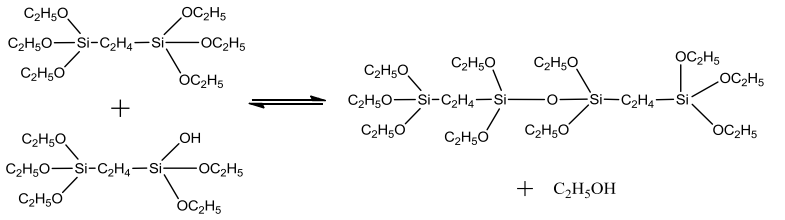

(2)

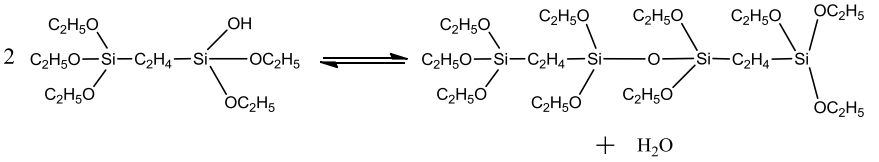

(3)

From these sols membranes were synthesized by means of coating these sols on porous γ-alumina ceramics. Disc-shaped α-alumina supported γ-alumina was prepared by a dip coating procedure of a boehmite sol on α-alumina supports (support thickness of 2.08±0.01 mm and pore diameter of about 100 nm; Pervatech B.V. The Netherlands), followed by subsequent drying and calcination, as described in detail in [17]. The boehmite-PVA dip-sol was twice coated on α-alumina supports in order to create a smooth mesoporous intermediate layer. A pore size for the -alumina intermediate layer of 3-5 nm was determined by permporometry, using the method as described elsewhere [34].

For membrane fabrication, the BTESE sol was diluted to a final dip-sol with [Si] = 0.6 M. This BTESE separation layer was applied onto the alumina support by a single dipping procedure as described elsewhere [30], followed by a thermal treatment at 300 °C for 3 h under nitrogen (99.99% pure) with a heating / cooling rate of 0.5 °C/min. The sol and membrane fabrication experiments were performed several times to confirm the reproducibility of the results. The hybrid sol was synthesized three times and at least two membranes were produced from each sol and were characterized to validate the proof of concept.

Particle sizes of freshly prepared hybrid sols (with 75% dilution in ethanol) were determined by dynamic light scattering (DLS) using a Malvern Zetasizer Nano ZS at 25°C. The hydrodynamic diameter of the sol particles was determined from the

Brownian motion of the particles as defined by the translational diffusion coefficient *D* in the ethanol solvent. The hydrodynamic diameter *d* was obtained by the Stokes-Einstein equation:

$$d = kT / 3\pi\eta D \quad (4)$$

Where *k* = Boltzmann's constant; *T* = the temperature; η = solvent viscosity; *D* = diffusion coefficient in the solvent.

The thickness of the calcined hybrid silica layers was determined by analyzing cross-sectional micrographs of the membranes acquired with a high-resolution scanning electron microscope HR-SEM (ZEIS 1550) at an accelerating voltage of 1.0 kV.

Membrane performance was characterized on an in-house designed single gas permeation (SGP) set-up in a dead-end mode without back pressure. The membranes were sealed in a stainless steel module using Viton® 51414 O-rings with the separation layer exposed to the feed side. The gas permeance was measured at 200 °C in a sequence, starting with the gas of smallest kinetic diameter, from He (0.255 nm), H_2 (0.289 nm), CO_2 (0.33 nm), N_2 (0.364 nm), CH_4 (0.389 nm) to SF_6 (0.55 nm) at 200°C with a pressure difference of 2 bar. After the measurement of the different gases, the hydrogen flux was determined again to ensure that no changes had occurred in the membrane (micro) structure during the measurements.

The membrane performance via SGP was determined by equation 5:

$$F_i = \frac{N_i}{\Delta P} \quad (5)$$

Where *F* is the permeance of the gas *i*, determined by calculating the molar permeance (*N*) of the gas through the membrane with pressure difference (ΔP) between feed and permeate side.

3.3 Results and Discussion

3.3.1 Sol-gel chemistry and fabrication of a hybrid silica membrane

Sol synthesis is one of the most critical parts in the fabrication of meso and microporous ceramics for membrane applications. Therefore, the sol process parameters i.e. acid ratio [H^+:Si], hydrolysis ratio [H_2O:OC_2H_5] and precursor concentration [Si] must be carefully controlled to obtain sols with appropriate particle size, morphology and homogeneity. The degree of homogeneity of the sols is crucial for obtaining a defect-free membrane pore-structure because coating with too large sol particles leads to thick layers that are prone to crack formation [30, 35].

In this work, sols from the BTESE precursor were prepared at a reduced nitric acid concentration compared with previous work [30] where a ten times higher amount of acid had been used to produce BTESE sols, *i.e.* at an acid ratio (AR) of 0.1. When sols with AR=0.01 were synthesized under the same experimental conditions, *i.e.* at 60 °C for 1.5 hours, the sol particle size was about 2 nm with a wide variation in size distribution. For microporous membrane fabrication, the sol particles must be larger than the pores of the (α-alumina-supported) mesoporous γ-alumina supports, *i.e.* above 4 nm [35]. To synthesize larger sol particles, a higher precursor concentration was applied, *i.e.* at [Si]=2.7. This recipe was named “R-1”. After 30 minutes at 60 °C, the sols acquired a mean particle size of about 7 nm with neat and uniform homogeneity as shown in figure 3.1. This size distribution is considered suitable for membrane preparation. At longer times, the sols were less suitable: the mean sol particle size after 1 hour and 1.5 hours were 12.5 nm and 13.7 nm respectively with high polydispersity. In figure 3.1, the sol particle size as obtained by sol recipe R-1, using a reaction time of 30 minutes, is compared with the sol particle size of BTESE as reported in [30], from which defect-free membranes had been prepared. While the lower AR of 0.01 resulted in decreased hydrolysis and condensation rates, this was compensated by a higher overall reactant concentration, keeping the reaction time within reasonable limits. Although the effect of the acid concentration could be further investigated, care should be taken that the conditions are still acid-catalyzed, *i.e.* below the isoelectric point, which is around pH=2 in an aqueous medium, as base-catalyzed systems (at pH > 2) may rather lead to a mesoporous structure.

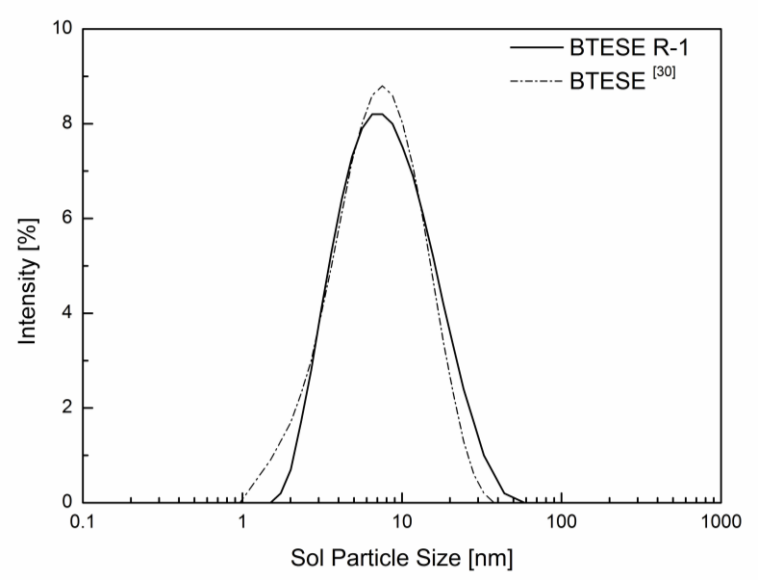

Figure 3.1: Sol particle size distribution of BTESE R-1 sols . The sol particle size distribution is compared with results from [30].

A cross-sectional high resolution scanning electron micrograph (HR-SEM) of a membrane is shown in figure 3.2-(Right), indicating an isotropic thickness of about 440 nm of the BTESE separation layer on the α-alumina support with a γ-alumina intermediate layer. This separation layer is about 100 nm thinner than a BTESE membrane developed from a sol prepared with an acid ratio (AR) of 0.1 and using an identical dip-sol concentration of 0.6 M [30] (figure 3.2-Left).

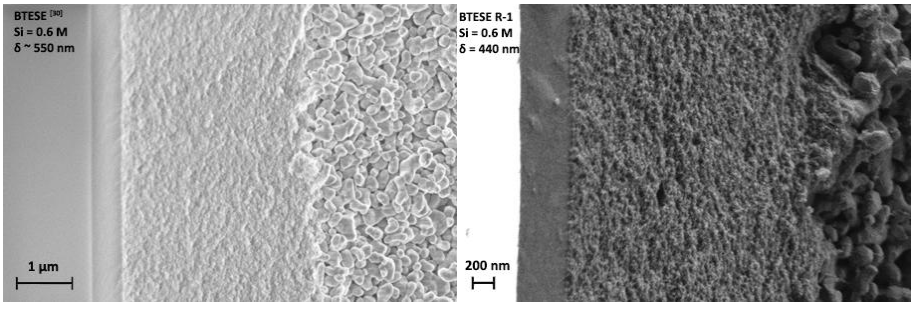

Figure 3.2: Cross sectional SEM-micrograph comparison of BTESE membranes developed with identical dip-sol concentration of 0.6 M. **Left**: BTESE membrane with AR 0.1 [30] with a

selective layer thickness of about 550 nm. **Right**: BTESE derived hybrid silica membrane developed from modified sol recipe R-1 (AR 0.01) with a selective layer of 440 nm.

3.3.2 Membrane Performance

Single gas permeation (SGP) results of calcined hybrid silica (BTESE) membranes, reported in [30] at AR = 0.1 and membranes made by the modified R-1 method (with AR = 0.01) described in this work, are given in table 3.1 and in figure 3.3. At 200 °C none of the membranes showed SF_6 permeance (detection limit of the equipment is 5 X 10^{-10} mol/m^2.s.Pa) indicating a flawless microstructure. Two of the four synthesized R-1 membranes were found nitrogen and methane impermeable, while for the third membrane, there was no detectable methane permeance and a N_2 permeance of 3 X 10^{-9} mol/m^2.s.Pa, giving a H_2/N_2 permselectivity of 80. A fourth membrane showed H_2/N_2 and H_2/CH_4 permselectivities of respectively 50 and 88. All these results are far superior in performance when compared with membranes starting from sols, prepared with an acid ratio (AR) of 0.1 (see table 1 and Fig 2). It should also be noted that the isotropic selective hybrid layer of the R-1 derived sol is 440 nm thick (Fig. 3), while the other BTESE derived selective layer has a thickness of 550 nm [30]. The permeance values for the smaller gases He, H_2 and CO_2 were found slightly lower, while permeances of bigger gases (N_2, CH_4) were reduced considerably for R-1 derived membranes. In general, by reducing the selective layer thickness gas permeances increase, which is in contrast with the results as discussed in this work. Furthermore, gas permeance of helium and nitrogen are comparable which strongly indicates that the pore microstructure by the R-1 method (AR 0.01) is more dense and homogenous, making it more difficult for bigger gas molecules to permeate through these membranes if compared with membranes made from sols, fabricated at higher AR [30].

Table 3.1: Single gas permeation results of BTESE membranes synthesized from sol recipe R-1 at an acid ratio AR=0.01, compared to those synthesized at AR=0.1 (*) [30].

Gas Permeances [mol/m^2.s.Pa]					Permselectivity [-]				
He	H_2	CO_2	N_2	CH_4	H_2/He	H_2/CO_2	H_2/N_2	H_2/CH_4	CO_2/CH_4
1.79E-07	2.10E-07	4.37E-08	-	-	1.2	5	∞	∞	∞
1.79E-07	2.21E-07	5.03E-08	-	-	1.2	4	∞	∞	∞
2.10E-07	2.38E-07	5.61E-08	2.99E-09	-	1.1	4	80	∞	∞
1.33E-07	1.88E-07	3.27E-08	3.79E-09	2.14E-09	1.4	6	50	88	15
2.05E-07*	2.70E-07*	4.60E-08*	1.30E-08*	1.10E-08*	1.3*	6*	21*	24*	4*

- Below detection limit of equipment *i.e.* below 5 X 10^{-10} mol/m^2.s.Pa.

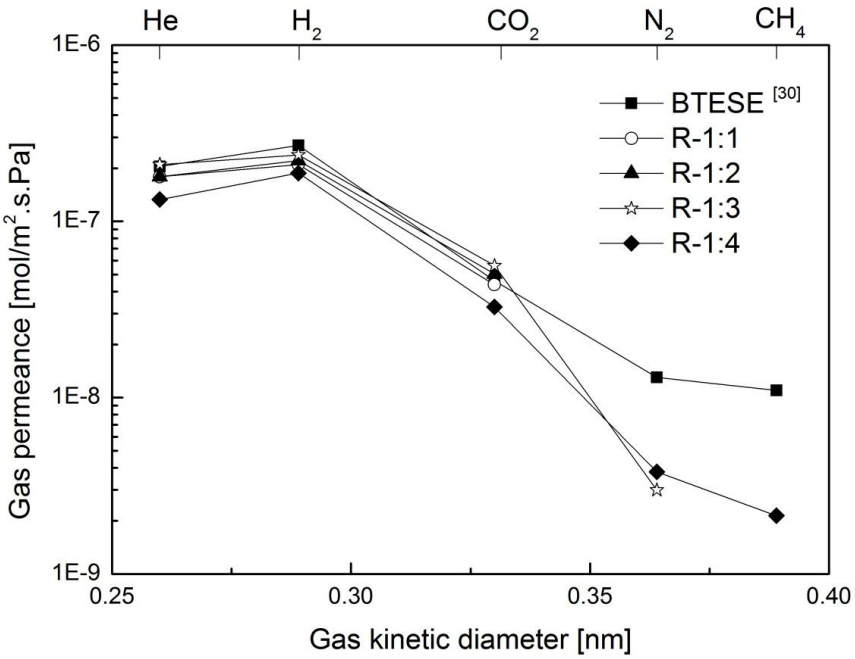

Figure 3.3: Single gas permeation of all BTESE-based membranes developed from recipe R-1 (AR=0.01) and those of a BTESE membrane reported in [30] with AR=0.1.

A lower hydrogen permeance, a thinner selective layer, and better permselectivities with BTESE R-1 membranes, when compared with our previous findings [30], made us convince that there is a significant effect of reducing the acid concentration during sol fabrication on the final membrane microstructure. The pore structure has become more constricted and in some cases the membranes were found nitrogen impermeable. The least performing membrane, made by this method showed a H_2/N_2 permselectivity of 50, which is still far better than observed with BTESE derived membranes made from a sol, using an acid ratio of 0.1 (i.e. H_2/N_2 of 21) [30]. The findings can be of relevance for industrial application, not only for the separation of H_2, but also for CO_2/CH_4 separation in natural gas exploitation. Also in view of their excellent hydrothermal stability, BTESE-based membranes may find increased application in bio-and natural-gas separation and purification.

3.4 Conclusions

An efficient procedure to polymerize hybrid silica sols is reported that developed into high-performance membranes. Reducing the concentration of acid catalyst from 0.3 to 0.02 moles during the sol synthesis resulted in a notable influence on the membrane microstructure. The effectiveness of low acid concentration during the sol processing step was delicately utilized in developing high performance gas separation membranes. The condensation reaction is faster but by reducing its time we have developed monodispersed sol particles that formed a constricted pore microstructure. It has not only reduced the sol processing time to one-third (*i.e.* 30 minutes) from hybrid silica, but also the developed membranes showed an improved hydrogen permselectivity performance for bigger gases (*i.e.* H_2/N_2 and H_2/CH_4) with a selective isotropic layer thickness of 440 nm. Further investigation of the structural development during sol synthesis and coating could enhance understanding of the processes that results in pore structures with very small pores. More insight in these sol-gel processes may lead to further improvement of the size selectivity of BTESE-based hybrid silica membranes for gas separation.

References

[1] F. Lipnizki, Cross-Flow Membrane Applications in the Food Industry, in: S.P.N. Klaus-Viktor Peinemann, and Lidietta Giorno (Ed.) Membrane Technology,Volume 3: Membranes for Food Applications, WILEY-VCH Verlag GmbH & Co. KGaA, Weinheim, 2010.

[2] T.C. David Avnir, Ovadia Lev, Jacques Livage, Recent bio-applications of sol-gel materials, Journal of Materials Chemistry, 16 (2006) 1013-1030.

[3] O. Lefebvre, R. Moletta, Treatment of organic pollution in industrial saline wastewater: A literature review, Water Research, 40 (2006) 3671-3682.

[4] L.S. White, Development of large-scale applications in organic solvent nanofiltration and pervaporation for chemical and refining processes, Journal of Membrane Science, 286 (2006) 26-35.

[5] S. Sommer, T. Melin, Performance evaluation of microporous inorganic membranes in the dehydration of industrial solvents, Chemical Engineering and Processing: Process Intensification, 44 (2005) 1138-1156.

[6] A.M. Urtiaga, E.D. Gorri, P. Gómez, C. Casado, R. Ibáñez, I. Ortiz, Pervaporation Technology for the Dehydration of Solvents and Raw Materials in the Process Industry, Drying Technology, 25 (2007) 1819-1828.

[7] L.M. Vane, A review of pervaporation for product recovery from biomass fermentation processes, Journal of Chemical Technology & Biotechnology, 80 (2005) 603-629.

[8] L. Deng, M.-B. Hägg, Techno-economic evaluation of biogas upgrading process using CO_2 facilitated transport membrane, International Journal of Greenhouse Gas Control, 4 (2010) 638-646.

[9] P. Vandezande, L.E.M. Gevers, I.F.J. Vankelecom, Solvent resistant nanofiltration: separating on a molecular level, Chemical Society Reviews, 37 (2008) 365-405.

[10] L. Lin, Y. Zhang, Y. Kong, Recent advances in sulfur removal from gasoline by pervaporation, Fuel, 88 (2009) 1799-1809.

[11] H.B.P. Naiying Du, Gilles P. Robertson, Mauro M. Dal-Cin, Tymen Visser, Ludmila Scoles, Michael D. Guiver, Polymer nanosieve membranes for CO2-capture applications, Nature Materials, 10 (2011) 372-375.

[12] D.F. Stamatialis, B.J. Papenburg, M. Gironés, S. Saiful, S.N.M. Bettahalli, S. Schmitmeier, M. Wessling, Medical applications of membranes: Drug delivery, artificial organs and tissue engineering, J Membrane Sci, 308 (2008) 1-34.

[13] S.Y. Gumhye Jeon, Jin Kon Kim, Functional nanoporous membranes for drug delivery, Journal of Materials Chemistry, 22 (2012) 14814-14834.

[14] R.W. Baker, Membrane technology and Applications, John Wiley & Sons, Ltd. West Sussex, England., 2004.

[15] R.J.R. Uhlhorn, M.H.B.J.H.t. Veld, K. Keizer, A.J. Burggraaf, Synthesis of ceramic membranes, Journal of Materials Science, 27 (1992) 527-537.

[16] C.J. Brinker, Structure Property Relationships in Thin Films and Membranes.pdf, J Sol-Gel Sci Techn, 4 (1995) 117-133.

[17] R.M. de Vos, H. Verweij, High-Selectivity, High-Flux Silica Membranes for Gas Separation, Science, 279 (1998) 1710-1711.

[18] H.L. Castricum, A. Sah, R. Kreiter, D.H.A. Blank, J.F. Vente, J.E. ten Elshof, Hybrid ceramic nanosieves: stabilizing nanopores with organic links, Chem Commun, (2008) 1103.

[19] V. Boffa, D. Blank, J. Tenelshof, Hydrothermal stability of microporous silica and niobia–silica membranes, J Mem
brane Sci, 319 (2008) 256-263.
[20] Y.H. Kazuhiro Yoshida, Hironori Fujii, Toshinori Tsuru, Masashi Asaeda, hydrothermal stability and performance of silica-zirconia membranes for hydrogen separation in hydrothermal conditions, Journal of Chemicla Engineering of Japan, 34 (2001) 523-530.
[21] T.Y. Ryosuke Igi, Yumi H. Ikuhara, Yuji Iwamoto, Toshinori Tsuru., Characterization of Co-Doped Silica for Improved Hydrothermal Stability and Application to Hydrogen Separation Membranes at High Temperatures, J. Am. Ceram. Soc, 91 (2008) 7.
[22] J. Wang, T. Tsuru, Cobalt-doped silica membranes for pervaporation dehydration of ethanol/water solutions, J Membrane Sci, 369 (2011) 13-19.
[23] H.L. Castricum, A. Sah, M.C. Mittelmeijer-Hazeleger, C. Huiskes, J.E. ten Elshof, Microporous structure and enhanced hydrophobicity in methylated SiO_2 for molecular separation, Journal of Materials Chemistry, 17 (2007) 1509.
[24] W.F.M. Renate M. de Vos, Henk Verweij, Hydrophobic silica membranes for gas separation, Journal of Membrane Science, 158 (1999) 277-288.
[25] H.L. Castricum, R. Kreiter, H.M. van Veen, D.H.A. Blank, J.F. Vente, J.E. ten Elshof, High-performance hybrid pervaporation membranes with superior hydrothermal and acid stability, J Membrane Sci, 324 (2008) 111-118.
[26] M. Kanezashi, K. Yada, T. Yoshioka, T. Tsuru, Design of Silica Networks for Development of Highly Permeable Hydrogen Separation Membranes with Hydrothermal Stability, J Am Chem Soc, 131 (2009) 414-415.
[27] H.L. Castricum, G.G. Paradis, M.C. Mittelmeijer-Hazeleger, R. Kreiter, J.F. Vente, J.E. ten Elshof, Tailoring the Separation Behavior of Hybrid Organosilica Membranes by Adjusting the Structure of the Organic Bridging Group, Advanced Functional Materials, 21 (2011) 2319-2329.
[28] K.S. Chang, T. Yoshioka, M. Kanezashi, T. Tsuru, K.L. Tung, Molecular simulation of micro-structures and gas diffusion behavior of organic-inorganic hybrid amorphous silica membranes, J Membrane Sci, 381 (2011) 90-101.
[29] K.S. Chang, T. Yoshioka, M. Kanezashi, T. Tsuru, K.L. Tung, A molecular dynamics simulation of a homogeneous organic-inorganic hybrid silica membrane, Chem Commun, 46 (2010) 9140-9142.

[30] Hammad F. Qureshi, Arian Nijmeijer, L. Winnubst, Influence of sol-gel process parameters on the micro-structure and performance of hybrid silica membranes., J Membrane Sci, 446 (2013) 19-25.

[31] A.C. Pierre, Introduction to Sol-Gel Processing, Kluwer Academic Publishers (1998).

[32] G.W.S. C. Jeffrey Brinker, Sol-Gel Science: The Physics and Chemistry of Sol-Gel Processing, (1990).

[33] R.K. Iler, The Chemistry of Silica, John Wiley and Sons, New York, 1979.

[34] G.Z. Cao, Meijerink, J., Brinkman H. W., Burggraaf, A. J., Permporometry study on the size distribution of active pores in porous ceramic membranes, J Membrane Sci, 83 (1993) 14.

[35] R.S.A. de Lange, J.H.A. Hekkink, K. Keizer, A.J. Burggraaf, Formation and characterization of supported microporous ceramic membranes prepared by sol-gel modification techniques, J Membrane Sci, 99 (1995) 57-75.

Chapter 4

Doped microporous hybrid silica membranes

Abstract

Hybrid silica (*i.e. bis*-triethoxysilylethane: BTESE) membranes doped with B, Ta or Nb, were made through a sol-gel process. Triethyl borate (TEB), tantalum (V) ethoxide (TPE), and niobium (V) ethoxide (NPE) were selected as doping precursors. The doping concentration was optimized to produce sols suitable for membrane fabrication. Thermal stability, structural analysis, cross-sectional micrographs and single gas permeation experiments were performed for doped-BTESE membranes and results are compared with an undoped BTESE membrane. It was observed that the synthesized doped-BTESE materials and membranes resulted into a more open (and, in one occurrence, SF_6 permeable) pore microstructure showing high permeances of larger gas molecules, while having a cross-sectional thickness comparable to un-doped BTESE membranes.

4.1 Introduction

Inorganic membranes have attracted considerable attention for their applicability in gas separation processes in conditions where polymeric membranes cannot be used. Inorganic membranes remain stable at high temperature (*i.e.* > 400 °C), do not swell in solvents, and are resistant to abrasion [1, 2]. Porous inorganic membranes with either size and/or affinity based selectivity offer potential advantages in separating gaseous mixtures at elevated temperatures [3], in catalytic membrane reactors [4] and in hydrogen separation [5]. The application of microporous silica membranes for hydrogen purification has been subject of study for a long time [4]. These membranes are either prepared by a chemical vapor deposition (CVD) technique [6, 7] or by using sol-gel methods [8-10]. Although silica membranes, fabricated by sol-gel methods, show great promise in gas separation, the technical challenges such as hydrothermal stability are still a point of concern [11]. Hybrid organosilica (e.g. *bis*-triethoxysilylethane: BTESE) membranes are very suitable to overcome such problems, since they show an improved hydrothermal stability [12, 13]. The exposure of silica to moisture (or steam) at around 70 °C leads to the hydrolysis of Si-O-Si bonds [1]. The introduction of organic bridges in the silica microstructure makes it less susceptible for hydrolysis which extends the industrial application of silica membranes [14]. It has been reported that the shape, flexibility and length of organic bridges in the hybrid silica network have an influence on the membrane pore size, structure and affinity [15].

For a gas permselective membrane the pore size and pore size distribution should be small and sufficiently uniform to ensure that the membrane acts as an efficient sieve to block larger gas molecules for permeating through the membrane. The presence of hydrocarbon chains in the silica backbone improves the hydrothermal stability of such a hybrid silica matrix however at the cost of reduced gas selectivity [11]. A possible approach to improve the gas permselectivity of these hybrid silica membranes is the incorporation of metal-ions in the hybrid silica matrix. This approach was successfully implemented by doping the silica network with metal ions, such as aluminum and magnesium [16], zirconium [17, 18], niobium [19, 20], nickel [21] and cobalt [22, 23]. For hybrid silica (*i.e.* BTESE) only the incorporation of niobia was reported to date [24, 25], where it is claimed that the introduction of niobia created surface active sites resulting in a reduced CO_2 permeance. These

authors observed that the H_2/CO_2 permselectivity at 450°C was higher (*i.e.* H_2/CO_2 = 220) compared to hydrogen selectivity over larger molecule such as nitrogen (H_2/N_2 = 125) and thus claiming that CO_2 permeance through these Nb-BTESE membranes was not only determined by size exclusion. However, in the same work, this enhanced H_2/CO_2 permselectivity was not observed at 300 °C and 350 °C [$(H_2/CO_2)_{300°C}$ = 11.4, $(H_2/CO_2)_{350°C}$ = 11, $(H_2/CO_2)_{400°C}$ = 50; $(H_2/N_2)_{300°C}$ = 50, $(H_2/N_2)_{350°C}$ = 45, $(H_2/N_2)_{400°C}$ = 65] which raises questions regarding niobia incorporation, its influence on reduced CO_2 permeance and the reproducibility in fabrication of Nb-BTESE membranes. Because of this inconsistency in results a new study on Nb-doped BTESE was performed as described in this chapter.

Furthermore, we report the incorporation of boron and tantalum in the hybrid silica (BTESE) matrix with the aim to fabricate a defect-free, gas selective membrane film. Boron has extensively been used as a glass forming agent due to their low thermal expansion coefficient. In membrane fabrications, Boron was doped in a silica matrix using boric acid powder as boron source to reduce the defect density and enhance the membrane performance [26]. The Si-C-C-Si bond strength of hybrid silica is unknown but in silica, Si-O has a bond strength of 368 KJ/mol [27] and the bond B-O strengths are respectively 560 KJ/mol and 790 KJ/mol for BO^-_4 and BO_3 species respectively [27]. The incorporation of boron in the hybrid silica matrix was expected to bring more rigidity and tightness to hybrid silica matrix. In this research triethylborate (TEB) is used as a boron source for doping the hybrid silica matrix.

Tantalum is known for its high chemical and hydrothermal stability and belongs to the refractory metal group [28]. Thin films of tantalum oxide are already in use in transistors [29], sensors [30], and capacitors [31]. It has been reported that sol-gel derived ultra-thin tantalum membranes resulted in a dense structure with very low hydrogen permeance [32]. On the other hand, hybrid silica membranes possess a relatively loose pore microstructure [33]. In the current work, tantalum is used as a dopant in hybrid silica, to form a relatively denser microstructure than that of undoped BTESE [33] for improved H_2/X gas permselectivities.

4.2 Experimental

As hybrid silica precursor 1,2-*bis*(triethoxysilyl) ethane (BTESE) (97%, ABCR Germany) was used. Triethyl borate [TEB] ($B(OC_2H_5)_3$), 99%, Aldrich), niobia (V) ethoxide [NPE] ($Nb(OC_2H_5)_5$, 99.99%, ABCR Chemicals) and tantalum (V) ethoxide [TPE] ($Ta(OC_2H_5)_5$, (99%, ABCR Chemicals) were respectively used as boron, niobium and tantalum source.

For the synthesis of boron doped hybrid silica (B-BTESE) sols the following procedure was used. Triethyl borate (2.51 ml) was added to a BTESE-ethanol mixture (11.10 ml BTESE in 6.38 ml ethanol) in a round bottom flask. Into that flask, a mixture of nitric acid (0.5 ml, 65 wt.% Aldrich), water (3.65 ml, deionized) and ethanol (15.85 ml, Absolute, Aldrich) was added under vigorous stirring in an ice-bath. The solution was kept at 60 °C for 1.5 hr. The sol contained 20 at% B (= [B]/[B + Si]).
The hydrolysis step for the synthesis of tantalum-doped hybrid silica (Ta-BTESE) sols was performed in a glove box under nitrogen atmosphere. A solution of 0.495 ml nitric acid (pH 2.56) in 12.25 ml ethanol was added to a BTESE-ethanol mixture (3.26 ml BTESE in 9.44 ml ethanol) and stirred for 2 hrs at 20 °C. TPE (1.11 ml in 40.77 ml ethanol) was added to the aforementioned solution and the reaction was further allowed to run for 1 hr at 20 °C under constant vigorous stirring. Finally 0.43 ml nitric acid (pH 2.5) dissolved in 12.25 ml ethanol, was added to the doped-hybrid silica mixture and the reaction was allowed to run at 60 °C for another 1 hr. The Ta-BTESE hybrid sol contained 20% Ta (=[Ta]/[Ta + Si]).

Niobium-doped hybrid silica (Nb-BTESE) sols were made by using the following reaction scheme. A solution of 0.46 ml nitric acid (pH 2.5) in 12.25 ml of ethanol was added to a BTESE-ethanol mixture (3.26 ml BTESE in 9.44 ml ethanol) in a glove-box under nitrogen atmosphere. The solution was stirred at 20 °C for 2 hrs. After that 1.05 ml NPE in 40.83 ml ethanol was added to the solution and the reaction was allowed to run for 1 hr at 20 °C under constant vigorous stirring. Finally 0.43 ml nitric acid, dissolved in 12.25 ml ethanol, was added to the solution and the reaction was allowed to run at 60 °C for 1 hr under reflux. The Nb-BTESE hybrid sol contained 20% Nb (=[Nb]/[Nb + Si]).

Figure 4.1 presents a schematic description of the Ta-BTESE and Nb-BTESE sol synthesis procedure. If not applied immediately after synthesis, all doped-BTESE sols were stored at -28 °C. For membrane dip-coating the sols were diluted 6 times with ethanol resulting in a final concentration of 0.3 M ([Si] + [M]).

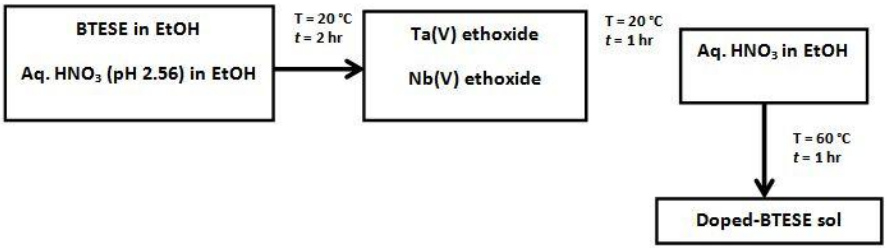

Figure 4.1: Sol Fabrication scheme of niobia and tantalum doped BTESE sols.

Particle sizes of freshly prepared hybrid sols (with an extra 75% dilution in ethanol) were determined by dynamic light scattering (DLS) using a Malvern Zetasizer Nano ZS at 25°C. Measurements were performed using 1.0-1.5 ml of the sol in a disposable size cuvette (Type DTS0012, Malvern Instruments).

Disc-shaped α-alumina supported γ-alumina was prepared by a dip coating procedure of a boehmite sol on α-alumina supports (support thickness of 2.08±0.01 mm and pore diameter of about 100 nm, Pervatech B.V. The Netherlands), followed by subsequent drying and calcination, as described in detail in [34]. The boehmite-PVA dip-sol was coated twice on the α-alumina disc supports to create a smooth mesoporous intermediate layer. A pore size for the γ-alumina intermediate layer of 3-5 nm was determined by permporometry, using the method as described elsewhere [35].

For membrane fabrication, the separation layer was applied onto the α-alumina supported γ-alumina by a single dipping procedure as described elsewhere [33], followed by a thermal treatment at 300 °C for 3 hr under nitrogen (99.99% pure) with a heating / cooling rate of 0.5 °C/min. The sol and membrane fabrication experiments were performed several times to confirm the reproducibility of the results.

The thickness of the calcined hybrid silica layers was determined by analyzing cross-sectional micrographs of the membranes, acquired from a high-resolution scanning electron microscope HR-SEM (Zeiss 1550) at an accelerating voltage of 1.0 kV.

Dried powders of doped-hybrid silica sols were obtained by drying the corresponding sols in a petri dish overnight at room temperature. These powders were analyzed using thermogravimetry (TGA). Measurements were carried out on a STA 449 F3 Jupiter® (Netzsch) instrument under nitrogen atmosphere. About 20 mg of sample was used and each measurement run from room temperature until at least 800 °C at a heating rate of 10 °C min^{-1}.

FTIR spectra of calcined un-doped and doped-hybrid silica powders were obtained with a TGA-IR Tensor 27 system spectrometer (Bruker Optick GmbH) in the range 400-4000 cm^{-1}, using a resolution of 4 cm^{-1} and 16 scans.

Membrane performance was characterized on an in-house designed single gas permeation (SGP) set-up in a dead-end mode. The membranes were sealed in a stainless steel module using Viton® 51414 O-rings with the separation layer exposed to the feed side. The gas permeance was measured at 200 °C in a sequence, starting with the gas with the smallest kinetic diameter, from He (0.255 nm), H_2 (0.289 nm), CO_2 (0.33 nm), N_2 (0.364 nm), CH_4 (0.389 nm) to SF_6 (0.55 nm) at 200°C with a trans membrane pressure of 2 bar.

4.3 Results and Discussions

4.3.1 Doped-BTESE sol characterization

The sol fabrication of B-BTESE was a relatively straight forward synthesis scheme. However, only 20% boron doping was possible for producing stable sols with appropriate particle sizes, necessary for membrane fabrication. Lower boron concentrations (*i.e.* 5%, 10%, and 15%) resulted in sol particles with an average size smaller than 4 nm with high polydispersity. 20% doping of TEB in BTESE showed to be sufficient to synthesize uniform bigger sol particles (of about 8 nm) which were applicable for membrane coating. It might be possible that more than 20% of TEB doping in the BTESE precursor during the sol synthesis would also lead to doped-

hybrid silica sols, suitable for membrane fabrication, but in this work a maximum of only 20% doping was employed.

During the synthesis of hybrid silica sols, containing the ethoxides of niobium or tantalum, by adding these ethoxides at the same time to the reaction mixture as the BTESE precursor, the system gelated within minutes, while a well-defined sol with a small and homogeneous particle size distribution was obtained for pure BTESE under identical synthesis conditions (*i.e.* temperature of 60 °C) [33]. As the reactivity of the tantalum and niobium precursors is very high, an alternative route was developed to control hydrolysis/condensation during sol-synthesis. This procedure not only resulted in the incorporation of these metal ion in the hybrid silica structure but also resulted in a homogenous sol particle size distribution with sizes slightly larger than (or equal to) the γ-alumina pore size of about 5 nm. Preliminary experiments confirmed that the metal precursors hydrolyze very fast, hence hydrolysis must be done under water lean conditions to enhance the possibility of their integration in the hybrid silica matrix. To investigate this, in-situ FTIR analysis was performed during the synthesis of a (undoped) BTESE sol at 20 °C. The evolution of different reactive groups and hydrolysis products as function of reaction time was examined by monitoring the changes in intensities of its specific IR vibration lines, as shown in figure 4.2. From this figure it can be observed that the intensities of the Si-O-Si remained relatively constant for an extended period of time. During the first 120 minutes of reaction the IR lines, corresponding to the BTESE ethoxy groups (SiOEt) as well as the one representative for (free) water decreased in intensity, while the intensity of the Si-OH vibration (corresponding to the hydrolysis product) increased simultaneously. After around two hours of reaction the free water line intensity increased slightly, which can be ascribed as a water condensation reaction where water is released as a by-product [9]. This FTIR analysis might not provide accurate information, but it gives an indication that hydrolysis of BTESE at 20 °C proceeds in 2 hrs. The combination of the lower amount of water in the reaction mixture and of already (partly) hydrolysis of BTESE after 2 hrs of reaction might sufficiently prevent the Nb- or Ta-alkoxide precursors from fast hydrolysis, and enhance the reaction of the metal ion with the BTESE hybrid silica precursor.

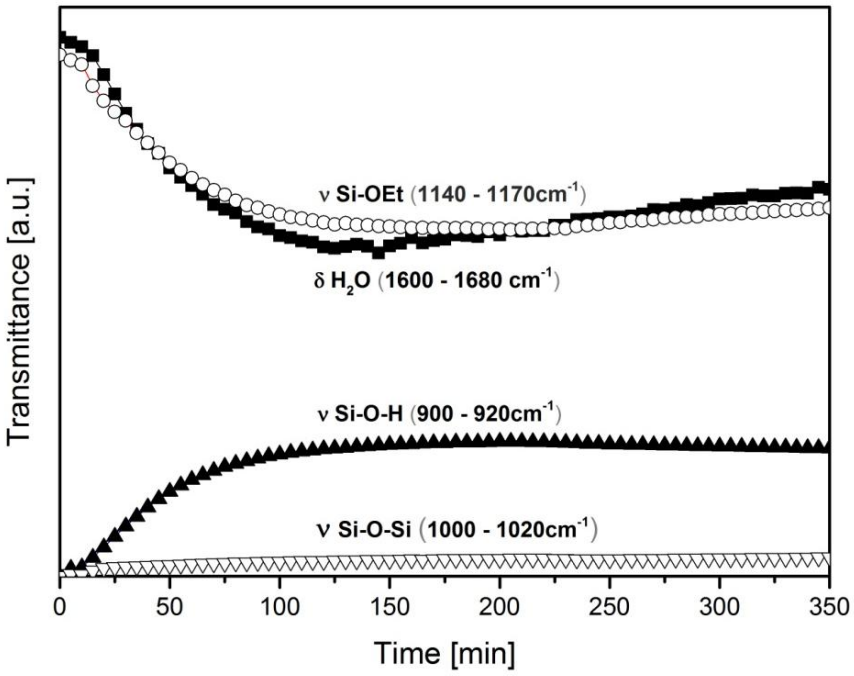

Figure 4.2: Variation in the transmittance intensity of IR-vibrations related with the hydrolysis of BTESE precursor at 20 °C.

The synthesis recipe was modified accordingly, in a way as shown in figure 4.1, to obtain a sol with uniform particle size and particle size distribution, applicable for membrane coating. BTESE and aqueous HNO_3 were allowed to react inside a glove-box for 2 hrs at 20 °C as a pre-hydrolysis step before the addition of either Ta- or Nb-alkoxide. In this way the dopants are allowed to react with the hybrid silica matrix under water lean conditions, which is also suitable for a homogenous dispersion of the dopant in the hybrid silica matrix [36]. Finally, after 1 hr. the remaining nitric acid was added and the temperature was increased to 60 °C to ensure complete hydrolysis of all ethoxy groups and to facilitate the condensation process. This resulted in hybrid sols with high monodispersity and average particle size of about 6 nm for Ta-BTESE and about 7 nm for Nb-BTESE derived sols (figure 4.3).

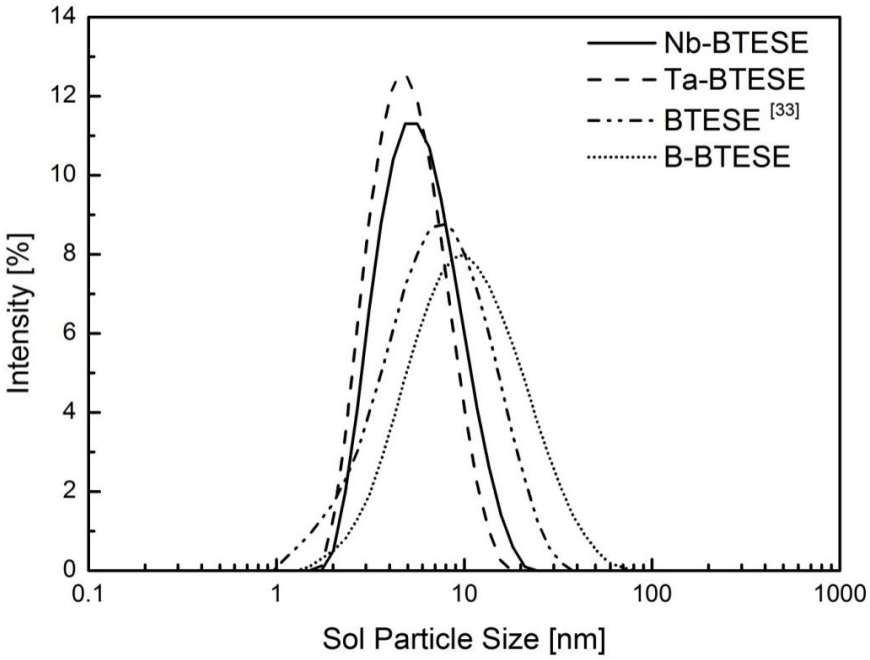

Figure 4.3: Average sol particle size and size distribution of freshly synthesized doped-BTESE sols. The sol particle size is compared with undoped BTESE sol [33].

Figure 4.4 shows the TGA data of dried pure and doped-BTESE hybrid gels in nitrogen atmosphere. The color of the pure and all doped-hybrid silica gels changed from initially white into black or dark-brown after the TGA measurement, indicating pyrolysis of the samples during heating up to 800 °C. The continuous weight loss up to 200 °C for pure BTESE, Nb-BTESE and Ta-BTESE gels and up to about 150 °C for B-BTESE can be assigned to the evaporation of residual water and ethanol. After this evaporation step a slight weight loss is observed until 550 °C, which is assigned to a continuous decomposition (partial pyrolysis), followed by a stronger weight loss after 550 °C, which can be ascribed to the degradation of the ethylene bridge [37]. This weight loss observed at high temperature is more pronounced for the undoped and B-doped BTESE than for the Ta- or Nb-BTESE systems.

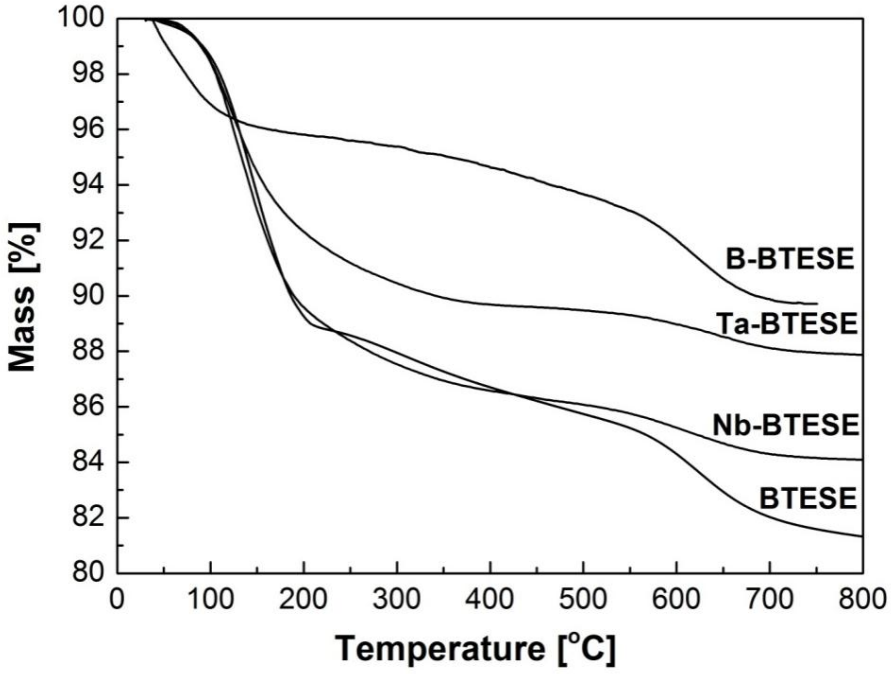

Figure 4.4: Thermo-gravimetric analysis (TGA) data of un-doped BTESE and doped (TEB, Ta and Nb) – BTESE dried gels recorded under nitrogen atmosphere.

No clear explanation is available in the literature about the onset of the degradation of $–C_2H_4–$ in the hybrid silica precursor. In [37], it is claimed that the decomposition of the ethylene bridge in BTESE occurs between 480 °C and 800 °C in inert atmosphere. This is in good agreement with the results as depicted in figure 4.4. We can claim that a temperature of around 500 °C can be marked as a start of the degradation process of all doped- BTESE materials and that the hybrid system remains intact until 500 °C in an inert nitrogen atmosphere.

Figure 4.5 shows the FT-IR spectra of doped and undoped BTESE powders calcined at 300 °C under nitrogen atmosphere. For all samples CH_2 vibrations at 1270 cm^{-1} and 1413 cm^{-1} [1, 38] are visible, which can be regarded as an evidence of the presence of $Si–CH_2–CH_2–Si$ in these powders. The signals at 1000 cm^{-1} and 680 cm^{-1} are indicative for a Si–O–Si structure in the samples [38, 39]. The B-O stretching mode at 1467 cm^{-1} is reported in literature for boron-silica systems [40]. However

we were unable to find any proof of B-O in the hybrid silica matrix. For Nb-BTESE and Ta-BTESE, there was no indication either of any change in the hybrid structure by the inclusion of these elements, as also reported elsewhere [24]. From these results it can be concluded that all the dopants added to the BTESE did not disturb the hybrid silica network and that the central hinge of hybrid silica structure (*i.e.* ethylene bridge) is retained in all the doped-BTESE samples.

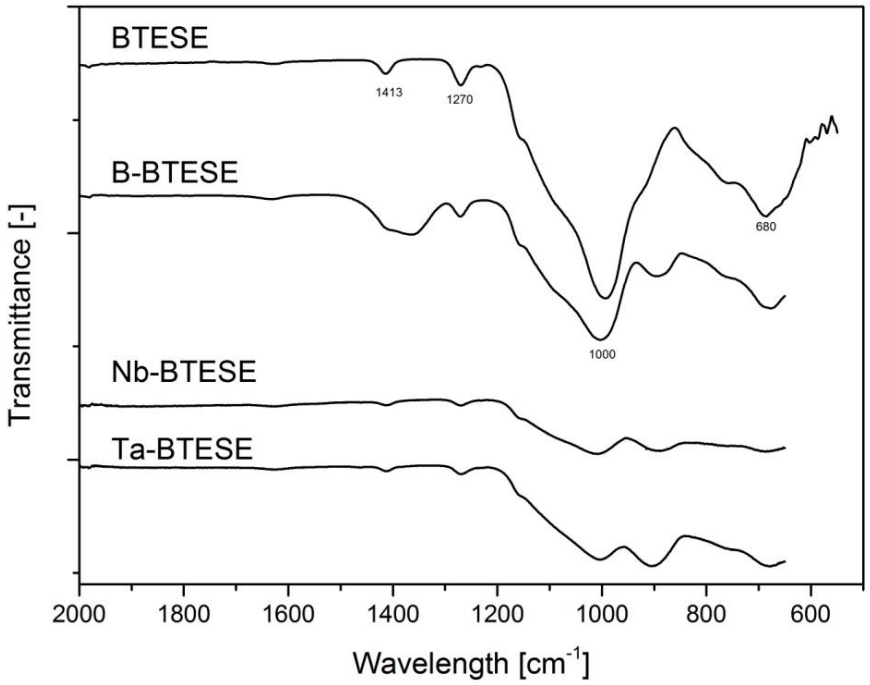

Figure 4.5: Fourier Transform IR spectra of un-doped and doped-BTESE powders after calcination at 300 °C.

Figure 4.6 shows cross-sectional HR-SEM micrographs of Nb-BTESE, Ta-BTESE and B-BTESE membranes. These membranes were fabricated using an identical dip-sol concentration of 0.3 M and an almost identical particle size distribution. Therefore any variation in thickness of the selective layer can be ascribed as an effect of doping to the hybrid silica matrix. The separation layers showed thicknesses of 360, 230 and 180 nm for respectively Nb-BTESE, Ta-BTESE and B-BTESE membranes. The undoped BTESE membrane formed a uniform selective layer of about 260 nm [33].

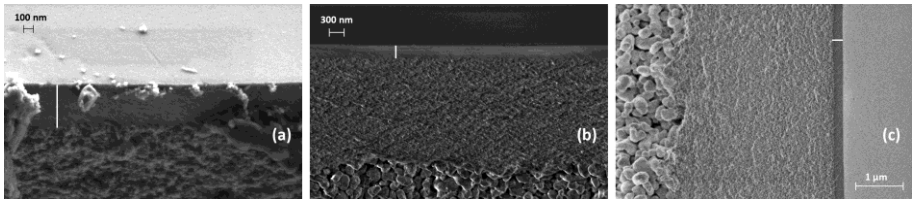

Figure 4.6: Cross-sectional HR-SEM micrographs of doped-BTESE derived membranes. **(a)** Nb-BTESE membrane with a selective layer thickness of about 360 nm, **(b)** Ta-BTESE derived with the selective layer thickness of about 230 nm, and **(c)** B-BTESE membrane with a selective layer thickness of about 180 nm.

4.3.2 Doped-BTESE membrane characterization

Single gas permeation experiments of Nb-BTESE, Ta-BTESE and B-BTESE membranes were performed at 200 °C. These results as well as those of undoped BTESE (taken from [33]) are given in table 4.1 and figure 4.7. In this way a judgment can be made over the pore size of these membranes.

The Nb-BTESE and Ta-BTESE membranes were impermeable to hexafluorosulfide (SF_6) gas molecules which ensured that the pore size of these membranes was smaller than 0.55 nm. B-BTESE membranes showed some SF_6 permeance which made us conclude that the B-BTESE membrane contains a few pores larger than 0.55 nm. The presence of pin-holes or defects in the selective layer was not visible by high resolution SEM and therefore it can be stated that the inclusion of boron, resulted in forming of relative larger pores when synthesized by sol-gel processing.

It was surprising to observe similar gas permeance values for all membranes because the B-BTESE membrane has a relatively thin selective layer if compared with the other doped and undoped BTESE membranes. The overall H_2/X gas permselectivity performance of all doped-BTESE membranes was less than for undoped BTESE membranes (see table 4.1). Nb-BTESE and Ta-BTESE membranes showed identical H_2/N_2 and H_2/CH_4 permselectivities. The incorporation of Nb and Ta in the hybrid silica matrix appears to form a similar pore microstructure but with a difference of almost 100 nm in the selective layer thickness. To enhance the selectivity of doped-BTESE membranes reported in this work, thermal treatment higher than 300 °C, or for much longer holding times than 3 hrs at 300 °C, could be

beneficial because the pore shrinkage due to thermal treatment might improve the gas permselective performance of these membranes. However, extreme care must be taken regarding the degradation of ethylene bridge. Although as it has been reported that the ethylene bridge might show a complete decomposition at 470 °C [37], it is not known yet at which temperature this degradation actually starts.

Table 4.1: Single Gas Permeation and permselectivity results at 200 °C of doped-BTESE developed with an identical dip-sol concentration. The results are compared with un-doped BTESE derived membranes [33].

Gas Kinetic Diameter [nm]	Gas Permeance (10^{-7} mol/m^2.s.Pa)	Selectivity H_2/X	Gas Permeance (10^{-7} mol/m^2.s.Pa)	Selectivity H_2/X	Gas Permeance (10^{-7} mol/m^2.s.Pa)	Selectivity H_2/X	Gas Permeance (10^{-7} mol/m^2.s.Pa)	Selectivity H_2/X
	BTESE [33]		**B-BTESE**		**Ta-BTESE**		**Nb-BTESE**	
	δ = 260 nm		**δ** = 180 nm		**δ** = 230 nm		**δ** = 360 nm	
He = 0.26	2.52	1.23	3.88	1.28	4.06	1.39	3.92	1.28
H_2 = 0.289	3.12	1	4.98	1	5.65	1	5.03	1
CO_2 = 0.33	0.8	3.9	1.24	4	1.56	3.6	1.43	3.5
N_2 = 0.364	0.23	13.5	0.43	11.5	0.81	7	0.77	6.5
CH_4 = 0.369	0.16	19.5	0.39	12.7	0.46	12.3	0.42	12
SF_6 = 0.55	*	∞	0.01	500	*	∞	*	∞

Gas detection limit of equipment: 5 X 10^{-10} mol/m^2.s.Pa.

δ: Thickness of the separation layer.

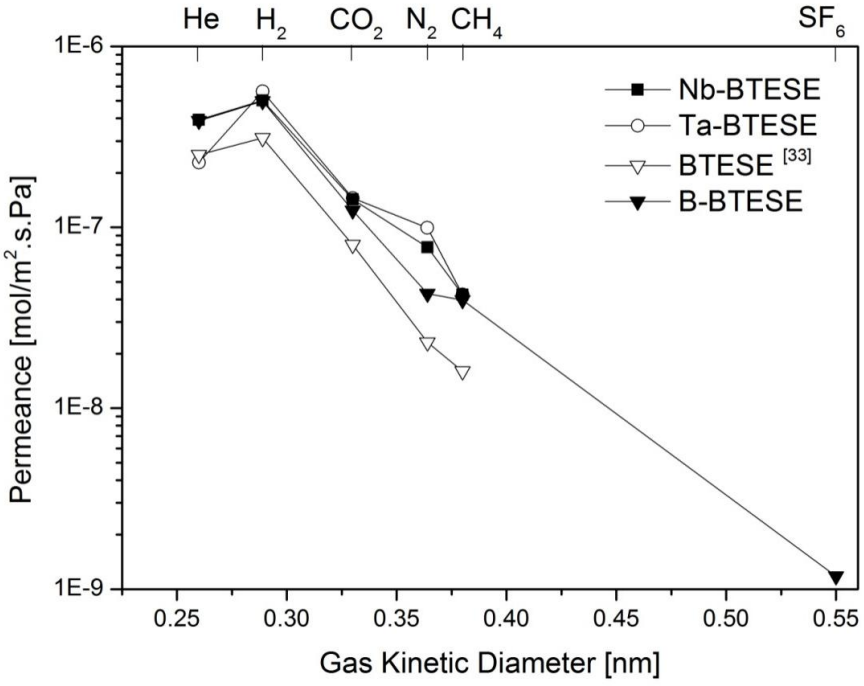

Figure 4.7: Single gas permeation analysis of Nb-BTESE, Ta-BTESE and B-BTESE derived membranes (calcined at 300 °C, with identical dip-sol concentration) as a function of gas kinetic diameter of permeating gas molecules measured at 200 °C. The results are compared with un-doped BTESE [33].

4.4 Conclusions

Three different membrane materials (B-BTESE, Ta-BTESE and Nb-BTESE) were fabricated by sol-gel processing and its applicability for gas separation was assessed by making microporous membranes, through a single dipping procedure. All the doped-BTESE sols formed a homogeneous selective layer of few hundreds of nanometers, as determined by high resolution SEM-micrographs. The structural evaluation by FT-IR spectroscopy of gels dried and calcined at 300 °C, indicated that the ethylene-bridge remains persistent in the silica backbone of BTESE for all systems. Single gas permeation analysis of Ta-BTESE and Nb-BTESE membranes indicated a defect-free pore microstructure with comparable H_2/N_2 and H_2/CH_4

permselectivities of 7 and 12 respectively. The boron doped BTESE membranes had a relatively open pore microstructure that limits their application for gas separation applications. No effect of niobia doping on a decrease in CO_2 permeance was found, *i.e.* lower CO_2 permeance when compared with nitrogen and methane permeances, as observed by Qi et. al. [41] for some cases. It might be that either the claimed low permeances of N_2 and CH_4 are realistic or there could be experimental errors in the results presented by the author. To conclude, it is still unclear that incorporation of niobia in hybrid silica matrix would impart any significant effect in lower CO_2 permeance.

References

[1] R.M.de Vos, Wilhelm F. Maier, H. Verweij, Hydrophobic silica membranes for gas separation, Journal of Membrane Science, 158 (1999) 277-288.

[2] Colin A. Scholes, S.E. Kentish, G.W. Stevens, Carbon Dioxide Separation through Polymeric Membrane Systems for Flue Gas Applications, Recent Patents on Chemical Engineering, 1 (2008).

[3] A.J. Burggraaf, L. Cot, Fundamentals of Inorganic Membrane Science and Technology (Series 4), Elsevier, 1996.

[4] J. Zaman, A. Chakma, Inorganic membrane reactors, Journal of Membrane Science, 92 (1994) 1-28.

[5] Ke Liu, Chunshan Song, V. Subramani, Hydrogen and Syngas Production and Purification Technologies, Wiley, AIChE.

[6] G. R. Gavalas, C.E. Megiris, S.W. Nam, Deposition of H_2-permselective SiO_2 films, Chemical Engineering Science, 44 (1989) 1829-1835.

[7] M. Tsapatsis, G. Gavalas, Structure and aging characteristics of H_2-permselective SiO_2-Vycor membranes, Journal of Membrane Science, 87 (1994) 281-296.

[8] R.J.R. Uhlhorn, M.H.B.J.H. Veld, K. Keizer, A.J. Burggraaf, Synthesis of ceramic membranes, J Mater Sci, 27 (1992) 527-537.

[9] C.J. Brinker, R. Sehgal, S.L. Hietala, R. Deshpande, D.M. Smith, D. Loy, C.S. Ashley, Sol-gel strategies for controlled porosity inorganic materials, Journal of Membrane Science, 94 (1994) 85-102.

[10] L.C. Klein, D. Gallagher, Pore structures of sol-gel silica membranes, Journal of Membrane Science, 39 (1988) 213-220.

[11] T. Tsuru, Nano/subnano-tuning of porous ceramic membranes for molecular separation, Journal of Sol-Gel Science and Technology, 46 (2008) 349-361.

[12] H.L. Castricum, A. Sah, M.C. Mittelmeijer-Hazeleger, C. Huiskes, J.E.ten Elshof, Microporous structure and enhanced hydrophobicity in methylated SiO_2 for molecular separation, Journal of Materials Chemistry, 17 (2007) 1509.

[13] H.L. Castricum, A. Sah, J.A.J. Geenevasen, R. Kreiter, D.H.A. Blank, J.F. Vente, J.E. Elshof, Structure of hybrid organic–inorganic sols for the preparation of hydrothermally stable membranes, Journal of Sol-Gel Science and Technology, 48 (2008) 11-17.

[14] H.L. Castricum, R. Kreiter, H.M. van Veen, D.H.A. Blank, J.F. Vente, J.E. ten Elshof, High-performance hybrid pervaporation membranes with superior hydrothermal and acid stability, Journal of Membrane Science, 324 (2008) 111-118.

[15] H.L. Castricum, G.G. Paradis, M.C. Mittelmeijer-Hazeleger, R. Kreiter, J.F. Vente, J.E. ten Elshof, Tailoring the Separation Behavior of Hybrid Organosilica Membranes by Adjusting the Structure of the Organic Bridging Group, Advanced Functional Materials, 21 (2011) 2319-2329.

[16] G.P. Fotou, Y.S. Lin, S.E. Pratsinis, Hydrothermal stability of pure and modified microporous silica membranes, J Mater Sci, 30 (1995) 2803-2808.

[17] Kazuhiro Yoshida, Yoshio Hirano, Hironori Fujii, Toshinori Tsuru, M. Asaeda, hydrothermal stability and performance of silica-zirconia membranes for hydrogen separation in hydrothermal conditions, Journal of Chemicla Engineering of Japan, 34 (2001) 523-530.

[18] M. Asaeda, Y. Sakou, J. Yang, K. Shimasaki, Stability and performance of porous silica–zirconia composite membranes for pervaporation of aqueous organic solutions, Journal of Membrane Science, 209 (2002) 163-175.

[19] V. Boffa, D. Blank, J. Tenelshof, Hydrothermal stability of microporous silica and niobia–silica membranes, Journal of Membrane Science, 319 (2008) 256-263.

[20] V. Boffa, J.E.t. Elshof, A.V. Petukhov, D.H.A. Blank, Microporous Niobia–Silica Membrane with Very Low CO_2 Permeability, ChemSusChem, 2008 (2008) 7.

[21] M. Kanezashi, M. Asaeda, Hydrogen permeation characteristics and stability of Ni-doped silica membranes in steam at high temperature, Journal of Membrane Science, 271 (2006) 86-93.

[22] Ryosuke Igi, Tomohisa Yoshioka, Yumi H. Ikuhara, Yuji Iwamoto, T. Tsuru., Characterization of Co-Doped Silica for Improved Hydrothermal Stability and

Application to Hydrogen Separation Membranes at High Temperatures, J. Am. Ceram. Soc, 91 (2008) 7.

[23] S. Battersby, M.C. Duke, S. Liu, V. Rudolph, J.C.D.d. Costa, Metal doped silica membrane reactor: Operational effects of reaction and permeation for the water gas shift reaction, Journal of Membrane Science, 316 (2008) 46-52.

[24] H. Qi, J. Han, N. Xu, H.J.M. Bouwmeester, Hybrid Organic-Inorganic Microporous Membranes with High Hydrothermal Stability for the Separation of Carbon Dioxide, ChemSusChem, 3 (2010) 1375-1378.

[25] H. Qi, J. Han, N. Xu, Effect of calcination temperature on carbon dioxide separation properties of a novel microporous hybrid silica membrane, Journal of Membrane Science, 382 (2011) 231-237.

[26] C. Barboiu, B. Sala, S. Bec, S. Pavan, E. Petit, P. Colomban, J. Sanchez, S.d. Perthuis, D. Hittner, Structural and mechanical characterizations of microporous silica–boron membranes for gas separation, Journal of Membrane Science, 326 (2009) 514-525.

[27] F. Albert Cotton, Geoffrey Wilkinson, Carlos A. Murillo, M. Bochmann, Advanced Inorganic Chemistry, 5th ed., John Wiley & Sons, 1998, p. 266.

[28] T. E. Tietz, J.W. Wilson, Behavior and Properties of Refractory Metals, Tokyo University International Edition ed., 1965.

[29] G.B. Alers, D.J. Werder, Y. Chabal, H.C. Lu, E.P. Gusev, E. Garfunkel, T. Gustafsson, R.S. Urdahl, Intermixing at the tantalum oxide/silicon interface in gate dielectric structures, Applied Physics Letters, 73 (1998) 1517-1519.

[30] K. Ueno, S. Abe, R. Onoki, K. Saiki, Anodization of electrolytically polished Ta surfaces for enhancement of carrier injection into organic field-effect transistors, Journal of Applied Physics, 98 (2005) -.

[31] R.A.B. Devine, C. Chaneliere, J.L. Autran, B. Balland, P. Paillet, J.L. Leray, Use of carbon-free Ta_2O_5 thin-films as a gate insulator, Microelectronic Engineering, 36 (1997) 61-64.

[32] M.J. Wolf, S. Roitsch, J. Mayer, A. Nijmeijer, H.J.M. Bouwmeester, Fabrication of ultrathin films of Ta_2O_5 by a sol–gel method, Thin Solid Films, 527 (2013) 4.

[33] Hammad F. Qureshi, Arian Nijmeijer, L. Winnubst, Influence of sol-gel process parameters on the micro-structure and performance of hybrid silica membranes., Journal of Membrane Science, 446 (2013) 19-25.

[34] R.M.de Vos, H. Verweij, High-Selectivity, High-Flux Silica Membranes for Gas Separation, Science, 279 (1998) 1710-1711.

[35] G.Z. Cao, J. Meijerink, H. W. Brinkman, A.J. Burggraaf, Permporometry study on the size distribution of active pores in porous ceramic membranes, Journal of Membrane Science, 83 (1993) 14.

[36] J.B. Miller, E.I. Ko, Control of mixed oxide textural and acidic properties by the sol-gel method, Catalysis Today, 35 (1997) 269-292.

[37] M. Kanezashi, K. Yada, T. Yoshioka, T. Tsuru, Organic-inorganic hybrid silica membranes with controlled silica network size: Preparation and gas permeation characteristics, Journal of Membrane Science, 348 (2010) 310-318.

[38] S.K. Medda, D. Kundu, G. De, Inorganic–organic hybrid coatings on polycarbonate: Spectroscopic studies on the simultaneous polymerizations of methacrylate and silica networks, Journal of Non-Crystalline Solids, 318 (2003) 149-156.

[39] B. Karmakar, G. De, D. Ganguli, Dense silica microspheres from organic and inorganic acid hydrolysis of TEOS, Journal of Non-Crystalline Solids, 272 (2000) 119-126.

[40] C. Barboiu, B. Sala, S. Bec, S. Pavan, E. Petit, P. Colomban, J. Sanchez, S. de Perthuis, D. Hittner, Structural and mechanical characterizations of microporous silica–boron membranes for gas separation, Journal of Membrane Science, 326 (2009) 514-525.

[41] H. Qi, H. Chen, L. Li, G. Zhu, N. Xu, Effect of Nb content on hydrothermal stability of a novel ethylene-bridged silsesquioxane molecular sieving membrane for H_2/CO_2 separation, Journal of Membrane Science, 421–422 (2012) 190-200.

Chapter 5

Metal-dispersed malonamide-bridged silsesquioxane precursors: Membrane fabrication and characterization

Abstract

To promote and facilitate dispersion of metal ions, such as Ce^{4+} and Ni^{2+}, within a hybrid silica matrix, a new hybrid silica precursor N,N,N',N'-tetrakis-(3-(triethoxysilyl)-propyl)-malonamide (TTPMA) has been successfully synthesized. The malonamide ligands coordinate the Ce^{4+} and Ni^{2+} metals and enhance their dispersion. Colloidal sols were successfully prepared from these metal-dispersed malonamide-bridged silsesquioxane precursors. After gelation and calcination the metal centers redistribute into small nanosized clusters of CeO_2 (< 5nm) and Ni_2O_3 (< 15nm). The sol-gel derived Ce-TTPMA and Ni-TTPMA membranes showed higher H_2/N_2 and H_2/CH_4 permselectivities than previously reported hybrid silica membranes. For Ce-TTPMA membranes, a 40% higher permselectivity for H_2/N_2 and a 30% higher permselectivity for H_2/CH_4 were observed. The Ni-TTPMA membranes were found nitrogen impermeable. The TTPMA-precursor can be a promising and versatile precursor for the incorporation of metal ions within hybrid silica matrices.

5.1 Introduction

The spectrum of membrane-based processes is extending and membranes can be employed for hydrogen separation in an industrial environment, oxygen enrichment for medical and industrial applications, natural gas purification, or in post-combustion carbon capture processes where CO_2 is separated from flue gases [1-5]. Currently, solvent-based absorption, using for example amines, is still the most commonly applied technique to capture CO_2, but their regeneration requires a lot of energy, that somehow limitize their use in industrial separation processes [6-9].

The difference in kinetic diameter between H_2 and gases such as CO_2, N_2 and CH_4 is very small (2.89 Å versus 3.30 Å, 3.64 Å and 3.89 Å respectively). However, these gases can be separated by size exclusion in silica membranes with a H_2/CO_2 permselectivity of 70, while nitrogen and methane were found impermeable [10]. Due to the poor stability of these silica membranes in steam atmosphere metal-ions (i.e. cobalt or nickel) were added, in order to render membranes that preserve a high H_2 gas selectivity under hydrothermal conditions [11, 12]. Although inorganic, size–exclusion based, membranes will never exceed the hydrogen selectivity of palladium membranes, they are less expensive, catalytically inactive and do not suffer from hydrogen enbrittlement and poisoning phenomena [13, 14].

Dispersion of metals on an atomic scale into a hybrid silica network is not a straightforward task: the metal oxide that is introduced, either in the form of a metal salt or a metal alkoxide, tends to phase separate while the silica matrix is formed. Metal salts, e.g. metal nitrates, have limited solubility in the alcohols in which the silica sol is formed and these salts tend to precipitate while the sol is drying [12]. Metal alkoxides dissolve well in apolar solvents, but they are much more reactive towards hydrolysis and condensation than silica precursors, generally resulting in the formation of metal oxide clusters within the silica sol [15-17]. The reactivity of these alkoxides can be tempered by chelating ligands such as acetylacetone and they clearly retard the gelation in the presence of water [18-20].

In the present work, a bridged silsesquioxane precursor is studied, having four triethoxysilyl-propyl groups attached to a single malonamide chelating group. As compared to pendant silsesquioxanes, glasses or coatings made from bridged

silsesquioxanes exhibit much higher mechanical strength and fracture resistance due to enhanced connectivity and the absence of dangling carbon substituents [21-23].

A bridged silsesquioxane that consists of a malonamide chelating group was formed through the formation of amide bonds between malonyl chloride and two *bis*-(3-(triethoxysilyl)-propyl)-amine (TTPMA) molecules. The synthesis was performed via a base-catalyzed (using a tertiary amine as base) N-acylation of malonyl chloride on N-substituted amines in dichloromethane at temperatures below T = 5 °C as reported before [24, 25] (see Figure 1). Malonamides are strong chelating units and through the formation of an enolic bidentate ligand they can easily form complex bonds with a large variety of metal cations, including lanthanides and actinides [26-33].

In this study, a hybrid silica precursor *N,N,N',N'*-tetrakis-(3-(triethoxysilyl)-propyl) malonamide (TTPMA) is developed consisting of a bridging malonamide group. This malonamide bridge can act as a chelating agent for the metal ions. Two metal ions i.e. Ce^{4+}, using cerium (IV) isopropoxide as a precursor and Ni^{2+}, using nickel nitrate precursor to investigate the metal-ions dispersion and membrane performance of metal-doped TTPMA. Ceria is reported as a catalyst in steam reforming of hydrocarbons and in water-gas shift reactions [34]. It is expected that a uniform dispersion of Ce inside the TTPMA matrix would result in a membrane with an enhanced affinity towards carbon dioxide leading to a higher CO_2/CH_4 permselectivity. Nickel is used for hydrogen storage in fuel cells [35]. Ni was chosen as a doping material in a hybrid silica (TTPMA) matrix for metal dispersion and enhanced hydrogen permeance that is expected to result in its higher permselectivity against bigger gas molecules like nitrogen and methane.

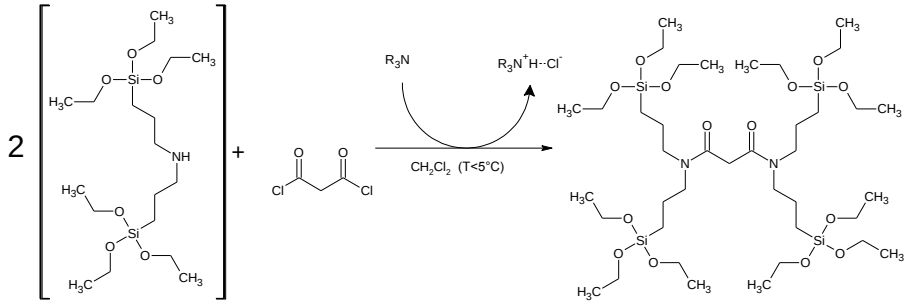

Figure 5.1: Synthesis of N,N,N',N'-tetrakis-(3-(triethoxysilyl)-propyl)-malonamide (TTPMA).

5.2 Experimental

5.2.1 Synthesis of *N,N,N′,N′*-tetrakis-(3-(triethoxysilyl)-propyl)malonamide (TTPMA)

Details on the synthesis of TTPMA are given in [36]. The solvents dichloromethane (BOOM, 99%), triethylamine (Sigma aldrich, 99%), and dimethylsulfoxide (Sigma Aldrich, 99%) were dried over anhydrous sodium sulphate (Sigma Aldrich, 99%). The synthesis was performed inside a glove box under nitrogen atmosphere. In a flask 30 mmol bis-(3-(triethoxysilyl)-propyl)-amine (ABCR chemicals, 97%) was dissolved in 183 ml dichloromethane. Subsequently, 30 mmol triethylamine was added to this solution. In a dropping funnel a 10 % excess (16.5 mmol) malonylchloride (Sigma Aldrich, 97%) was dissolved in 48.4 ml dichloromethane. This malonylchoride solution was drop-wise added in 30 min to the bis-(3-(triethoxysilyl)-propyl)-amine/triethylamine solution. After addition, the solution was stirred for 7 days at room temperature (*i.e.* at T = 20 °C). After that, the dichloromethane was distilled using a Vacuubrand vacuum pump that automatically adapts its pressure to the solvent pressure. After completion of the reaction 150 ml hexane was used to extract TTPMA from the remnant slurry.

5.2.2 Ce-TTPMA and Ni-TTPMA Sol preparation, Membrane fabrication and Characterization

A stock-solution was prepared of approximately 3 mmol (1.28 g) of a cerium(IV) isopropoxide isopropanol adduct ([$Ce(O^iPr)_4$.^{i}PrOH]: CeTiP; ABCR Chemicals, 31.5-

32.4% Ce by weight). A stoichiometric amount of TTPMA was added to this stock solution to yield a [Ce]/[Si+Ce] ratio of 1 : 10 (i.e. 10% Ce doping), which corresponded to [Ce]/[TTPMA] = 1/2.25. This mixture was diluted in 15 ml of isopropanol, yielding [TTPMA] = 0.29 mol/l and [Ce] = 0.13 mol/l. After stirring the solution for 24 h at room temperature (*i.e.* at *T* = 20 °C), 13.29 ml of this Ce-TTPMA stock solution was further diluted in 16.71 ml isopropanol yielding 30 ml alkoxide solution with [Ce-TTPMA] = 1.8 mole/l.

For the preparation of the Ce-TTPMA sol first a solution was prepared of 1.02 ml of 0.033 M HNO_3 diluted in 28.98 ml isopropanol yielding a solution with: [H_2O] = 1.8 mol/l and [HNO_3] = 0.06 mol/l. This solution was added drop-wise to 30 ml of the diluted Ce-TTPMA precursor solution (prepared earlier), which yielded: [OR] = 0.9 mol/l, where [OR] is the sum of ethoxy and iso-propoxy groups of TTPMA and CeTiP respectively. HR (hydrolysis ratio) = [H_2O]/[[OR] = 1, [HNO_3]/[OR] = 1/30, [TTPMA] = 65.4 mmol/l and [Ce] = 29.1 mmol/l. The sol particles were formed by heating this solution for 1 hour at 60 °C. For membrane preparation a 0.9 mol/l Ce-TTPMA sol was diluted 6 times by volume for membrane fabrication.

For the preparation of the Ni-TTPMA sol, first a Ni^{2+} solution was prepared by adding 10 g $Ni(NO_3)_2 \cdot 6H_2O$ to 46 ml ethanol resulting in a solution with [Ni] = 0.691 mol/l. This Ni solution and TTPMA were dissolved in ethanol to yield a diluted solution with [Ni]/[Si + Ni] ratio of 2:10 (*i.e.* 20% Ni doping) which corresponds to [Ni/TTPMA] = 1, [OR] = 2.4 mol/l; where [OR] is the sum of ethoxy groups of TTPMA and the nitrate groups from nickel nitrate *i.e.* [OR] = [NO_3^-] + [$-OC_2H_5$]. After stirring for 2 h at room temperature, nitric acid was added drop wise to yield a sol with an acid ratio (AR) [H^+]/[Si] = 0.23 and [OR] = 1.2 mol/l. The hydrolysis ratio [H_2O]/[OR] = 1 (including crystal water from the Ni solution) and complexing ratio [Ni]/[TTPMA] = 1 were held constant. The sols were heated for 1 h at *T* = 60 °C while stirring.

Particle sizes of freshly prepared Ce-TTPMA and Ni-TTPMA sols were determined by dynamic light scattering (DLS) technique using a Malvern Zetasizer Nano ZS at 25 °C. Prior to particle size analyses the sols were diluted 6 times with ethanol.

Fourier Transform Infra-Red (FTIR) measurements were performed by using a Brucker Tensor 27 equipped with a KBr beam splitter, a Pike GladiATR diamond

attenuated total reflectance (ATR) unit and a liquid nitrogen cooled MCT broadband detector. Samples of dried gels were applied on silicon wafers by spin coating and subsequently dried in air at 60 °C and calcined in nitrogen at 250 °C.

Disc-shaped α-alumina supported γ-alumina membranes were prepared by a dip-coating procedure of a boehmite sol on α-alumina supports (support thickness of 2.08 ± 0.01 mm and pore diameter of 100 nm; Pervatech B.V. The Netherlands), followed by subsequent drying and calcination, as described in detail elsewhere [37]. The boehmite-PVA dip-sol was twice coated on α-alumina supports to develop a smooth mesoporous intermediate layer. A pore size for the γ-alumina intermediate layer of 3-5nm was determined by permporometry, using the method as described in [38]. Dip coating of a Ce- and Ni-TTPMA sol (with dipping speed of 1.4 cm/sec) on γ-alumina membranes was done in a class 100 laminar flow cupboard, situated in a class 1000 clean room to minimize defect formation due to dust particles. The dip coating procedure was performed only once to apply the selective layer on the mesoporous support. After coating of the sol, the membranes were calcined at 250 °C for 3 hours under nitrogen flow (99.99% pure), applying heating and cooling rates of 0.5 °C/min.

The membrane performance was determined on an in-house designed single gas permeation (SGP) set-up in a dead-end mode without back pressure. The membranes were sealed in a stainless steel module using Viton® 51414 O-rings with the separation layer exposed to the feed side. The gas permeance was measured at 200 °C in a sequence, starting with the gas of smallest kinetic diameter, from He (0.255 nm), H_2 (0.289 nm), CO_2 (0.33 nm), N_2 (0.364 nm), CH_4 (0.389 nm) to SF_6 (0.55 nm) at 200°C at a trans membrane pressure of 2 bar. After the measurement of these gases, hydrogen flux was determined again to ensure that no change has occurred on the membrane (micro) structure due to permeation of several gases.

The membrane performance via SGP was determined by using the following equation;

$$F_i = \frac{N_i}{\Delta P}$$

Where F is the permeance of the gas *i*, determined by calculating the molar permeance (*N*) of the gas through the membrane with pressure difference (Δ*P*) between feed and permeate side.

For Transmission electron microscopy (TEM) analysis carbon-coated TEM copper grids (CF200-Cu, Electron Microscopy Sciences) were dip-coated in undiluted Ni-TTPMA or Ce-TTPMA sols. The as-prepared films were dried at 60°C for 24 h and calcined at 250 °C under identical conditions as the calcination procedure used for calcination of the membranes. The samples were analyzed with a Philips CM300STFEG TEM at an accelerating voltage of 300 kV. Samples were investigated at low magnification to find typical areas and features of interest were examined at high magnification (GATAN 2048 Ultrascan1000 CCD camera).

Scanning electron microscopy (SEM) was performed on the cross-section of Ni-TTPMA and Ce-TTPMA membranes with a Zeiss Merlin HR-SEM using 1.4 kV acceleration voltage.

5.3 Results and Discussion

5.3.1 Sol and gel characterization

The sol particle size distributions of cerium and nickel doped TTPMA sol are shown in figure 2, together with the sol particle size distribution of a pure BTESE sol as described in [39]. The BTESE sol has an average particle size of about 7 nm. A Ni-TTPMA sol showed a mono-model distribution curve with an average particle size of about 5 nm. The Ce-TTPMA sol showed a bi-modal size distribution with distinguishing average particle sizes of 2 nm and 40 nm respectively, while the Ni-TTPMA sol possessed a mono-modal size distribution with an average particle size of about 6 nm (as in figure 5.2).

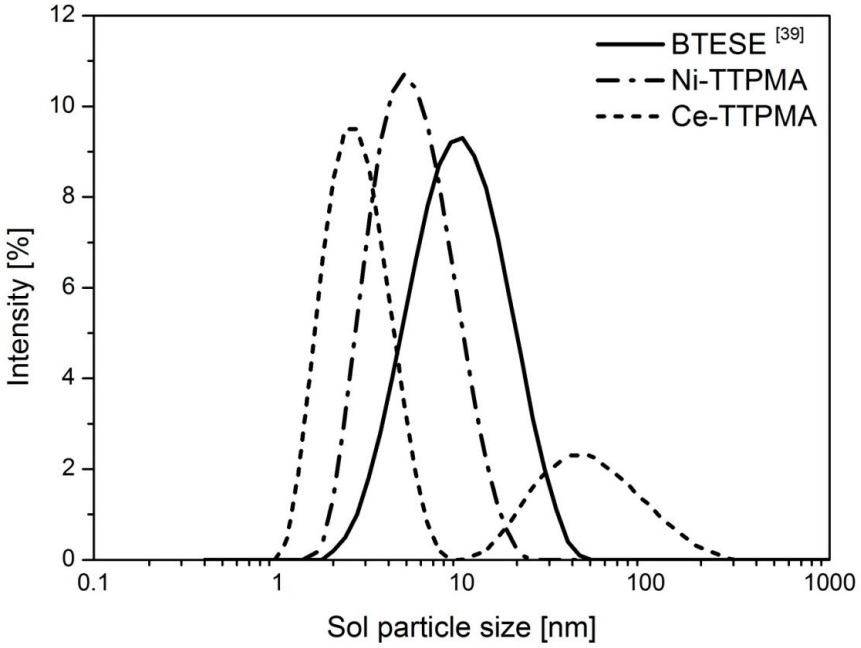

Figure 5.2: Sol particle size and distribution of Ce-TTPMA and Ni-TTPMA derived hybrid sols. The particle size and size distribution is compared with another hybrid precursor (BTESE).

High resolution cross-sectional SEM-micrographs of calcined Ce-TTPMA and Ni-TTPMA selective layers as deposited on γ-alumina are shown in Figure 5.3. The thickness of the Ni-TTPMA selective layer is about 210 nm (± 3 nm). This thickness is of the same order as a layer made from a BTESE sol, having the same dip-sol concentration (260 nm [39]). The Ce-TTPMA membrane shows a very thin and homogenous selective layer of only 35 nm (± 3 nm). The starting Ce-TTPMA sol has a bimodal particle size distribution (see Figure 5.2) with some particles smaller than pore size of the *γ*-alumina layer (5 nm). It can therefore be expected that some part of the Ce-TTPMA dip-sol penetrates inside the mesoporous *γ*-alumina layer, while another part (the bigger particles) form a smooth selective film.

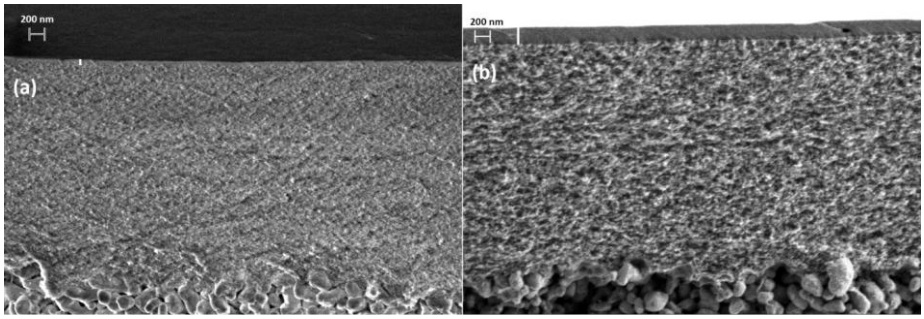

Figure 5.3: (a) HR-SEM images of a Ce-TTPMA membrane indicating an isotropic thin layer of about 35 nm. **(b)** HR-SEM images of a Ni-TTPMA membrane with an isotropic layer thickness of about 210 nm.

TEM images were made from Ce- and Ti- doped TTPMA samples to gain insight into the dispersion of ceria within the TTPMA silica matrix after calcination. In the case of Ce-TTPMA TEM data revealed the presence of small nanosized (2-5 nm) crystallites within an amorphous matrix (figure 5.4a). The crystallites, as indicated by the encircled particle (Figure 3), were found to have a lattice spacing of d ~ 3.1 Å. A Fourier transform image of such a crystallite is given in figure 5.4b. The observed lattice spacing value is consistent with CeO_2 (111) planes [40].

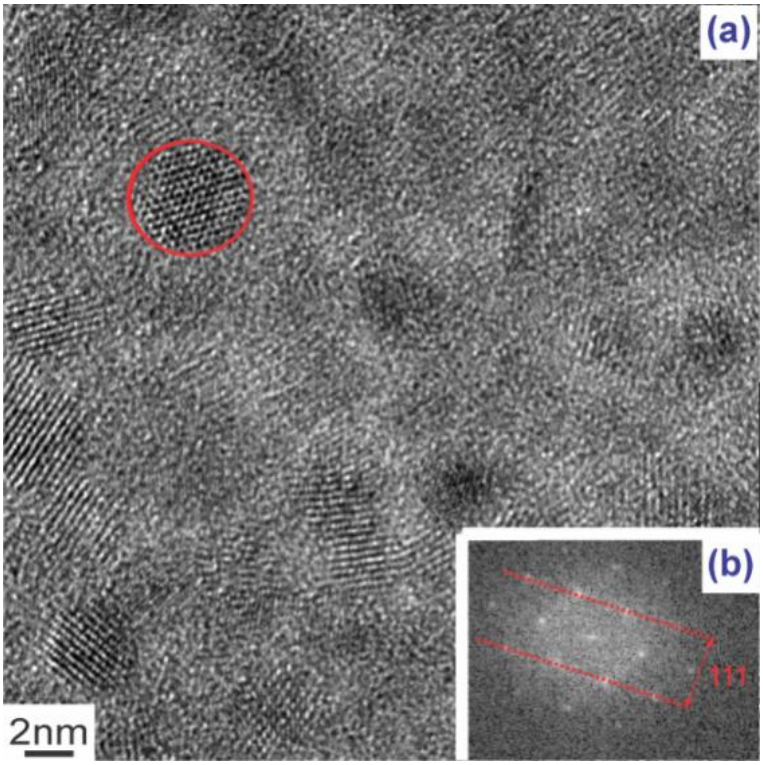

Figure 5.4: (a) HR-TEM images of a holey copper grid (with a carbon film) dip-coated with Ce-TTPMA sol and calcined at *T*=250 °C. **(b)** Fourier transform of the encircled region in section **(a)** of this figure.

TEM analysis on calcined Ni-doped TTPMA revealed a substantial amount of phase-separated electron rich particles. These particles with sizes ranging from 1 to 15 nm (figure 5.5) most likely consist of hydrated Ni_2O_3. As no lattice spacing could be determined for these particles, it might also be that these dark areas are clusters of "amorphous" Ni_2O_3 particles in a silica (TTPMA) matrix.

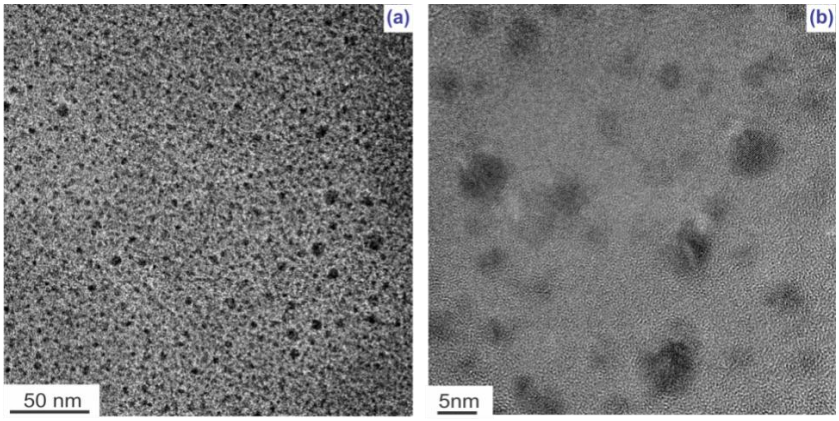

Figure 5.5: HR-TEM images of a copper grid dip-coated with Ni-TTPMA after calcination at *T* =2 50 °C at 2 different length scales. **(a)** overview image; **(b)** magnified image showing phase separated particles with sizes between 1 and 15 nm.

These TEM analyses give an indication on the metal distribution in the calcined gel. To investigate in what way the metal distribution evolves in the TTPMA matrix during calcination, FTIR analyses were performed. Figure 5.6 shows the FTIR absorbance spectra of a pure, calcined TTPMA, as well as dried and calcined gels of doped Ce-TTPMA and Ni-TTPMA.

When the Ce-TTPMA gel was dried at 60 °C, a *v* C=O was observed with a maximum at v = 1604 cm^{-1}. The shoulder at 1559 cm^{-1} was caused by a reduced force constant when the free C=O moeity was engaged by the metal cation [26, 41-43]. FTIR analyses reveal that the malonamide ligands are coordinated to Ce^{4+} in the dried gel, however, the exact structure could not be resolved solely by FTIR. After calcining the Ce-TTPMA sample at 250 °C for 3 hr, a new C=O vibration appeared at 1637 cm^{-1}, which is very close to the 1628 cm^{-1} C=O vibration of calcined TTPMA sample, which is indicative of free malonamide *v* C=O vibrations [26, 41, 44]. Furthermore, the signal near 1604 cm^{-1} decreased in intensity after calcination of the Ce-TTPMA sample, which corresponds to a reduction in the number of malonamide ligands that are coordinated to Ce^{4+}. In conclusion, cerium remains coordinated to the TTPMA ligand during sol-gel processing and drying, but during calcination at 250 °C, a substantial amount of the malonamide ligands became detached from cerium, which may subsequently have resulted in phase separation in the form of CeO_2, which also can be seen from the TEM image (figure 5.4).

When the Ni-TTPMA sol was dried at T=60 °C, a small shoulder at 1588 cm^{-1} was observed in FTIR, which can be ascribed to either nickel bounded with multiple malonamide ligands, or nickel bound with nitrate ions [45, 46]. By comparing the FTIR results of calcined TTPMA with calclined Ni-TTPMA, a clear shift in the carbonyl vibrations from 1628 cm^{-1} to 1604 cm^{-1} can be observed, indicating a modification in structure of TTPMA through the addition of nickel.

Further details on the FTIR results on TTPMA, Ce-TTPMA and Ni-TTPMA are given in [36].

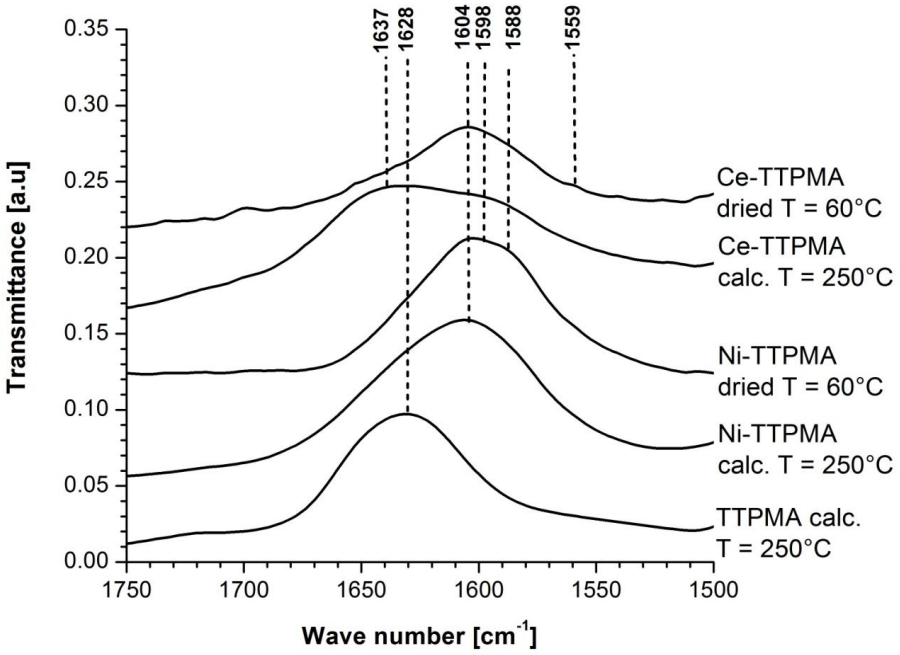

Figure 5.6: FTIR-ATR absorbance spectra of pure TTPMA, Ce-TTPMA and Ni-TTPMA.

5.3.2 Single Gas Permeation Performance

In order to obtain information on the applicability of Ce- and Ni- doped TTPMA membranes for separating small molecules (< 1nm), single gas permeances of individual gases (He, H_2, CO_2, N_2, CH_4 and SF_6) were performed at 200 °C. These

results are shown in figure 5.7. The permeation data are compared with membranes made from a BTESE (1,2-*bis* triethoxysilylethane) hybrid silica precursor. This BTESE membrane was calcined under identical atmosphere and heating rate, but at a higher temperature of 300 °C [39].

No permeation of hexafluoro-sulfide (SF_6) gas was observed through either Ce-TTPMA or Ni-TTPMA membranes, indicating that the largest pore size of these membrane is less than 0.55 nm, thus a defect-free pore microstructure is established and confirmed. With Ce-TTPMA membranes, despite the affinity of cerium towards CO_2, no remarkable improvement in CO_2/CH_4 permselectivity was observed as the permselectivity of 4.3 was lower than pure BTESE hybrid-silica precursor [39]; $[CO_2/CH_4)_{BTESE}$ = 5] but was considerably higher than its corresponding Knudsen diffusion value of 0.6.Adding to that, H_2/N_2 and H_2/CH_4 permselectivities are not only better than their corresponding Knudsen diffusion values of 3.9 and 2.8 respectively, but also higher than a membrane made from the BTESE hybrid-silica precursor [39]. BTESE membranes showed H_2/N_2 and H_2/CH_4 permselectivity of 14 and 20 respectively while Ce-TTPMA membranes have H_2/N_2 and H_2/CH_4 permselectivities of 20 and 26 respectively (Table 5.1). These results indicate that Ce-TTPMA membranes show a slightly better permselectivity for bigger gas molecules over hydrogen than BTESE membranes and that gas transport is based on a size exclusion transport mechanism. Furthermore, a minimal variation (*i.e.* less than 5%) was observed in hydrogen permeance at the start and at the end of the gas permeation analysis, indicating that Ce-TTPMA derived membranes possessed a sustainable pore microstructure. The Ce-TTPMA membrane has a selective layer thickness of about 35 nm, while the layer thickness for a BTESE membrane was about 260 nm, using in both cases an identical dip-sol concentration. From the comparable hydrogen permeance and the thinner (seven times thinner) selective layer it can be concluded that the Ce-TTPMA membranes develop a pore microstructure with a smaller pore-size than for BTESE membranes (by assuming that permeance resistance over α-alumina support and γ-alumina intermediate layer is identical for both membranes).

For Ni-TTPMA membranes, helium and hydrogen fluxes were one order of magnitude lower than pure hybrid silica (BTESE) membranes, with an almost identical separation layer thickness, forming a tight pore microstructure where the gas transport mechanism is dominated by molecular sieving. Nitrogen and methane

permeances were found below the detection limit of the gas permeation equipment (*i.e.* below 5 X 10^{-10} moles/m^2.s.Pa), from which it can be concluded that the Ni-TTPMA membranes are nitrogen and methane impermeable at 200 °C (figure 5.7). Furthermore, the identical hydrogen permeance values observed at the start and at the end of gas permeances analysis indicated no (irreversible) structural changes in the membrane during the measurements. In [47, 48] nickel has been incorporated into a pure silica matrix in order to obtain hydrothermally stable silica membranes. However, these membranes showed some nitrogen permeance. The results reported in our work are the first results for Ni-doped silica systems that formulated nitrogen impermeable membranes.

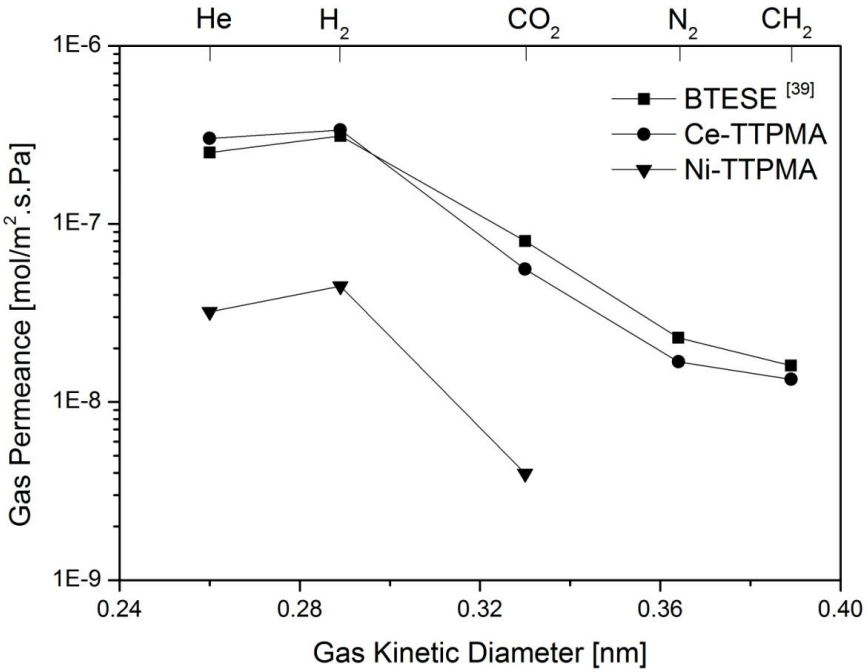

Figure 5.7: Single Gas permeation results as a function of gas kinetic diameter for Ce-TTPMA and Ni-TTPMA and BTESE hybrid silica membranes.

Table 5.1: Single Gas Permeation and selectivity results at 200 °C of Ce-TTPMA, Ni-TTPMA and BTESE hybrid silica membranes.

Gas Kinetic Diameter [nm]	Gas Permeance (10^{-7} mol/m^2.s.Pa)	Selectivity H_2/X	Gas Permeance (10^{-7} mol/m^2.s.Pa)	Selectivity H_2/X	Gas Permeance (10^{-7} mol/m^2.s.Pa)	Selectivity H_2/X
	Ce-TTPMA (This work) δ = 35 nm**		**Ni-TTPMA (This work) δ = 210 nm**		**BTESE [39] δ = 260 nm**	
He = 0.26	3.02	1.11	0.32	1.4	2.52	1.23
H_2 = 0.289	3.37	1	0.45	1	3.12	1
CO_2 = 0.33	0.56	6	0.04	11.3	0.8	3.9
N_2 = 0.364	0.17	19.8	*	∞	0.23	13.5
CH_4 = 0.369	0.13	25.9	*	∞	0.16	19.5
SF_6 = 0.55	*	∞	*	∞	*	∞

* Below detection limit of equipment i.e. below 5 X 10^{-10} mol/m^2.s.Pa.

** **δ**: thickness of the separation layer.

5.4 Conclusions

N,N,N',N'-tetrakis-(3-(triethoxysilyl)-propyl)-malonamide (TTPMA) was synthesized successfully through a reaction of *bis*-(3-(triethoxysilyl)-propyl)-amine with malonyl chloride. The malonamide ligand of TTPMA was found to coordinate with both Ce^{4+} and Ni^{2+} of cerium isopropoxide and nickel nitrate hexahydrate.

For Ce-TTPMA, a CeO_2 phase separated while calcining the hybrid film at T = 250 °C. Consequently, nanosized clusters (2-3 nm) of CeO_2 were formed. Single gas permeances on Ce-TTPMA membranes revealed a slightly larger H_2/N_2 permselectivity as compared to a previously reported BTESE hybrid membrane, which was substantially thicker (260 nm) than the Ce-TTPMA layer. For Ni-TTPMA gels, after calcination, nanosized (2-15 nm) nickel oxide particles or clusters of particles were observed by TEM. The 210 nm thick selective layer of a Ni-TTPMA membrane was approximately one order of magnitude more resistive towards permeance of H_2, He and CO_2 as compared to a hybrid BTESE layer of similar thickness. No N_2 permeance was observed within the experimental error for this Ni-TTPMA membrane, which makes this material a promising gas-selective material for CO_2/N_2 separation. As future outlook, Ni-TTPMA membranes with thinner selective layer can be developed that would result in improved permeance and it would be very worthwhile to study the gas permeation properties of these membranes under hydrothermal conditions.

References

[1] R.W. Baker, Future Directions of Membrane Gas Separation Technology, Industrial & Engineering Chemistry Research, 41 (2002) 1393-1411.

[2] W.J. Koros, R. Mahajan, Pushing the limits on possibilities for large scale gas separation: which strategies?, Journal of Membrane Science, 175 (2000) 181-196.

[3] W.J. Koros, G.K. Fleming, Membrane-based gas separation, Journal of Membrane Science, 83 (1993) 1-80.

[4] A.J. Burggraaf, L. Cot, Fundamentals of Inorganic Membrane Science and Technology (Series 4), Elsevier, 1996.

[5] C.S. Ke Liu, Velu Subramani, Hydrogen and Syngas Production and Purification Technologies, Wiley, AIChE.

[6] G.A. Olah, A. Goeppert, G.K.S. Prakash, Chemical Recycling of Carbon Dioxide to Methanol and Dimethyl Ether: From Greenhouse Gas to Renewable, Environmentally Carbon Neutral Fuels and Synthetic Hydrocarbons, The Journal of Organic Chemistry, 74 (2008) 487-498.

[7] J.-R. Li, Y. Ma, M.C. McCarthy, J. Sculley, J. Yu, H.-K. Jeong, P.B. Balbuena, H.-C. Zhou, Carbon dioxide capture-related gas adsorption and separation in metal-organic frameworks, Coordination Chemistry Reviews, 255 (2011) 1791-1823.

[8] P. Bernardo, E. Drioli, G. Golemme, Membrane Gas Separation: A Review/State of the Art, Industrial & Engineering Chemistry Research, 48 (2009) 26.

[9] A. Brunettia, F. Scuraa, G. Barbieria, E. Drioli, Membrane technologies for CO_2 separation, Journal of Membrane Science, 359 (2010) 11.

[10] R.M. de Vos, H. Verweij, Improved performance of silica membranes for gas separation, Journal of Membrane Science, 143 (1998) 37-51.

[11] M. Kanezashi, M. Asaeda, Hydrogen permeation characteristics and stability of Ni-doped silica membranes in steam at high temperature, Journal of Membrane Science, 271 (2006) 86-93.

[12] R. Igi, T. Yoshioka, Y.H. Ikuhara, Y. Iwamoto, T. Tsuru, Characterization of co-doped silica for improved hydrothermal stability and application to hydrogen separation membranes at high temperatures, Journal of the American Ceramic Society, 91 (2008) 2975-2981.

[13] E.J. Granite, T. O'Brien, Review of novel methods for carbon dioxide separation from flue and fuel gases, Fuel Processing Technology, 86 (2005) 1423-1434.

[14] R.E. Buxbaum, A.B. Kinney, Hydrogen transport through tubular membranes of palladium-coated tantalum and niobium, Industrial & Engineering Chemistry Research, 35 (1996) 530-537.

[15] A. Gaudon, A. Dauger, A. Lecomte, B. Soulestin, R. Guinebretière, Phase separation in sol-gel derived ZrO_2-SiO_2 nanostructured materials, Journal of the European Ceramic Society, 25 (2005) 283-286.

[16] V.G. Kessler, G.I. Spijksma, G.A. Seisenbaeva, S. Håkansson, D.H.A. Blank, H.J.M. Bouwmeester, New insight in the role of modifying ligands in the sol-gel processing of metal alkoxide precursors: A possibility to approach new classes of materials, J Sol-Gel Sci Technol, 40 (2006) 163-179.

[17] C.J.S. Brinker, G. W. , Sol Gel Science, The Physics and Chemistry of Sol-Gel Processing, Acedemic Press, San Diego, 1990.

[18] C. Sanchez, J. Livage, M. Henry, F. Babonneau, Chemical modification of alkoxide precursors, Journal of Non-Crystalline Solids, 100 (1988) 65-76.

[19] M. Sedlar, M. Sayer, Reactivity of titanium isopropoxide, zirconium propoxide and niobium ethoxide in the system of 2-methoxyethanol, 2,4-pentanedione and water, J Sol-Gel Sci Technol, 5 (1995) 27-40.

[20] M. Percy, J. Bartlett, J. Woolfrey, B. West, The influence of β-diketones on the induction times for hydrolysis of zirconium (IV) alkoxides, Journal of Materials Chemistry, 9 (1999) 499-505.

[21] G. Dubois, W. Volksen, T. Magbitang, R.D. Miller, D.M. Gage, R.H. Dauskardt, Molecular Network Reinforcement of Sol–Gel Glasses, Advanced Materials, 19 (2007) 3989-3994.

[22] G. Dubois, W. Volksen, T. Magbitang, M.H. Sherwood, R.D. Miller, D.M. Gage, R.H. Dauskardt, Superior mechanical properties of dense and porous organic/inorganic hybrid thin films, J Sol-Gel Sci Technol, 48 (2008) 187-193.

[23] M.S. Oliver, G. Dubois, M. Sherwood, D.M. Gage, R.H. Dauskardt, Molecular Origins of the Mechanical Behavior of Hybrid Glasses, Advanced Functional Materials, 20 (2010) 2884-2892.

[24] Q. Tian, M.A. Hughes, Synthesis and characterisation of diamide extractants for the extraction of neodymium, Hydrometallurgy, 36 (1994) 79-94.

[25] H. Kudo, F. Sanda, T. Endo, Efficient synthesis of macrocycles by oxidation of cysteine-based dithiols, Tetrahedron Letters, 42 (2001) 7847-7850.

[26] R.J. Ellis, M.R. Antonio, Coordination Structures and Supramolecular Architectures in a Cerium(III)–Malonamide Solvent Extraction System, Langmuir, 28 (2012) 5987-5998.

[27] R.J. Ellis, L. D'Amico, R. Chiarizia, M.R. Antonio, Solvent extraction of cerium (III) using an aliphatic malonamide: The role of acid in organic phase behaviors, Separation Science and Technology, 47 (2012) 2007-2014.

[28] B.W. Parks, R.D. Gilbertson, J.E. Hutchison, E.R. Healey, T.J.R. Weakley, B.M. Rapko, B.P. Hay, S.I. Sinkov, G.A. Broker, R.D. Rogers, Solution and Structural Investigations of Ligand Preorganization in Trivalent Lanthanide Complexes of Bicyclic Malonamides, Inorganic chemistry, 45 (2006) 1498-1507.

[29] G.J. Lumetta, B.K. McNamara, B.M. Rapko, R.L. Sell, R.D. Rogers, G. Broker, J.E. Hutchison, Synthesis and characterization of mono- and bis-

(tetraalkylmalonamide)uranium (VI) complexes, Inorganica Chimica Acta, 309 (2000) 103-108.

[30] G.Y. Chan, M.G. Drew, M.J. Hudson, P.B. Iveson, J.-O. Liljenzin, M. Skålberg, L. Spjuth, C. Madic, Solvent extraction of metal ions from nitric acid solution using N, N'-substituted malonamides. Experimental and crystallographic evidence for two mechanisms of extraction, metal complexation and ion-pair formation, Journal of the Chemical Society, Dalton Transactions, (1997) 649-660.

[31] M.G. Drew, M.J. Hudson, P.B. Iveson, C. Madic, Crystal structure of [Yb $(L(NO_3)_2(H_2O)_2](NO_3)$, L= bromo-N, N, N', N'-tetraethylmalonamide, Journal of Chemical Crystallography, 30 (2000) 455-458.

[32] A.M. Fedosseev, M.S. Grigoriev, I.A. Charushnikova, N.A. Budantseva, Z.A. Starikova, P. Moisy, Synthesis, crystal structure and some properties of new perrhenate and pertechnetate complexes of Nd^{3+} and Am^{3+} with 2,6-bis(tetramethylfurano)-1,2,4-triazin-3-yl)-pyridine, tris(2-pyridylmethyl) amine and N,N'-tetraethylmalonamide, Polyhedron, 27 (2008) 2007-2014.

[33] P.B. Iveson, M.G. Drew, M.J. Hudson, C. Madic, Structural studies of lanthanide complexes with new hydrophobic malonamide solvent extraction agents, Journal of the Chemical Society, Dalton Transactions, (1999) 3605-3610.

[34] Kyriaki Polychronopoulou, Christos M. Kalamaras, A.M. Efstathiou., Ceria-Based Materials for Hydrogen Production Via Hydrocarbon Steam Reforming and Water-Gas Shift Reactions, Recent Patents on Material Science 4(2011) 24.

[35] Jens R. Rostrup-Nielsen, Jens Sehested, J.K. Nørskov., Hydrogen and synthesis gas by steam- and CO_2 reforming, in: Advances in Catalysis, Academic Press, 2002, pp. 65-139.

[36] R. Besselink, Understanding microstructural evolution of mixed metal oxide silsesquioxane glasses through wet chemical synthesis, PhD thesis (Chapter 7). University of Twente, 2014.

[37] R.M. de Vos, H. Verweij, High-Selectivity, High-Flux Silica Membranes for Gas Separation, Science, 279 (1998) 1710-1711.

[38] G.Z. Cao, Meijerink, J., Brinkman H. W., Burggraaf, A. J., Permporometry study on the size distribution of active pores in porous ceramic membranes, Journal of Membrane Science, 83 (1993) 14.

[39] Hammad F. Qureshi, Arian Nijmeijer, L. Winnubst, Influence of sol-gel process parameters on the micro-structure and performance of hybrid silica membranes., Journal of Membrane Science, 446 (2013) 19-25.

[40] L. Bo, L.B. Bing, L.Q. Jun, L.Z. Peng, Y.M. Guang, L. Ran, Z. Xu, L. Hang, W. Wei, C. Wen, L.Z. Dong, L.D. Mei, Z. Bo, C. Tian, Z.G. Tian, High-pressure Raman study on CeO_2 nanospheres self-assembled by 5 nm Ce O2 nanoparticles, Physica Status Solidi, Sectio B: Basic Research, 248 (2011) 1154-1157.

[41] R.R.M. Silverstein, F.X. Webster, D.J. Kiemle, The Spectrometric Identification of Organic Compounds, John Wiley & Sons Australia, Limited, 2005.

[42] K.A. Fleeting, P. O'Brien, D.J. Otway, A.J.P. White, D.J. Williams, A.C. Jones, Studies on Mixed β-Diketonate/Isopropoxide Compounds of Zirconium and Hafnium, the X-ray Single-Crystal Structures of $[M_2(OPri)_6(tmhd)_2]$ (M = Zr, Hf): Some Chemistry Important in the MOCVD of Oxides, Inorganic Chemistry, 38 (1999) 1432-1437.

[43] C. Den Auwer, M.C. Charbonnel, M.G.B. Drew, M. Grigoriev, M.J. Hudson, P.B. Iveson, C. Madic, M. Nierlich, M.T. Presson, R. Revel, M.L. Russell, P. Thuéry, Crystallographic, X-ray Absorption, and IR Studies of Solid- and Solution-State Structures of Tris(nitrato) N,N,N‘,N‘-Tetraethylmalonamide Complexes of Lanthanides. Comparison with the Americium Complex, Inorganic Chemistry, 39 (2000) 1487-1495.

[44] Ross J. Ellis, Laura D'Amico, Renato Chiarizia, M.R. Antonio., Solvent Extraction of Cerium(III) Using an Aliphatic Malonamide: The Role of Acid in Organic Phase Behaviors, Separation Science and Technology, 47 (2012) 2007-2014.

[45] K. Nakamoto, Infra red and Raman spectra of inorganic and coordinaiton compounds, John Wiley & Sons New York, 1986.

[46] Wolfgang Brockner, Claus Ehrhardt, M. Gjikaj, Thermal decomposition of nickel nitrate hexahydrate, $Ni(NO_3)_2{\cdot}6H_2O$, in comparison to $Co(NO_3)_2{\cdot}6H_2O$ and $Ca(NO_3)_2{\cdot}4H_2O$, Thermochimica Acta, 456 (2007) 64-68.

[47] M. Asaeda, Ni-Silica mems for H_2 permeation and hydrothermal stability, Journal of Membrane Science, 271 (2006) 8.

[48] T. Tsuru, Development of Metal-doped Silica Membranes for Increased Hydrothermal Stability and Their Applications to Membrane Reactors for Steam Reforming of Methane, Journal of Japan Petroleum Institute, 54 (2011) 10.

Chapter 6

Mesoporous organosilica material as a substitute of γ-alumina for membrane applications

Abstract

1-2,*bis*(triethoxysilyl)octane (BTESO) was used as a precursor for the fabrication of graded ceramic membranes. Sol-gel processing showed a neat and monodispersed particle size distribution of BTESO sols with an average size of about 25 nm. N_2 adsorption/desorption revealed that the structure of BTESO has almost identical meso-porous properties as γ-Al_2O_3.. However, when the BTESO sol was deposited on an α-Al_2O_3 support excessive sol infiltration occurred that inhibited the formation of a BTESO mesoporous layer onto the α-Al_2O_3 support. When the BTESO sol was deposited on a γ-Al_2O_3 support, a thin, homogenous and a crack-free layer of a few hundred nanometers was formed that offered no resistance to gas permeation at 200 °C. Strategies such as multiple dipping with or without the aid of a viscosity modifier can be employed to avoid infiltration and to improve the stability of BTESO derived thin mesoporous layers.

6.1 Introduction

For the fabrication of multi-layered ceramic membranes via sol-gel processing, the quality of the support is of crucial importance for the integrity of the selective layer that is applied in subsequent preparation steps [1]. A uniform pore size and porosity of the membrane support is one of the requirements for uniform deposition of an intermediate or a selective layer [2]. If properly prepared, ceramic membranes are suitable candidates in many separation applications, because of their high thermal stability, high solvent resistance (*i.e.* extreme pH or aggressive organic solvents), and ease of cleaning and long term stability [3-5].

For ceramic membranes, α-Al_2O_3 is commonly used as a support material and γ-Al_2O_3 as a mesoporous intermediate layer [6-8]. Besides, ceramic materials like titania [9] and zirconia [10] are also used as membrane. A good starting support for making a micro porous membrane is a macroporous α-Al_2O_3 support with a pore size in the range 70-90 nm, and a porosity of 35 % or more [11]. On such a support a few micrometer thick mesoporous γ-Al_2O_3 layer is applied with a pore size in the range of 3-5 nm and a porosity of around 50% [12]. It has been reported that macroporous α-Al_2O_3 is chemically stable while mesoporous γ-Al_2O_3 shows poor chemical stability at low pH solutions *i.e.* pH below 3 [13, 14], which limits the use of γ-Al_2O_3 as an intermediate layer in harsh separation environments.

Microporous hybrid silica (*bis*-(triethoxysilyl)ethane [BTESE]) membranes have proven their hydrothermal and chemical stability in water removal from alcohols where these membranes are stable at a pH as low as 2 [15-17]. In this contribution, it is aimed to exploit the structural properties of another hybrid silica precursor (*bis*-(triethoxysilyl)octane [BTESO]) to assess its suitability as a substitute material of γ-Al_2O_3 as intermediate layer. BTESO possesses a flexible molecular structure with an octyl-hydrocarbon in the silica backbone and has been used in the past to develop microporous membranes for affinity based gas separation [18]. Here it is intended to develop a mesoporous structure of BTESO with the aim to fabricate an intermediate hybrid silica layer that can directly be applied on an α-Al_2O_3 support.

6.2 Experimental

A γ-Al_2O_3 system was prepared from a boehmite sol as described in [2, 8]. Disc-shaped γ-Al_2O_3 membranes were prepared by dip-coating a boehmite sol with a PVA binder on α-Al_2O_3 membrane supports (pore diameter 70-80 nm; thickness 2.05 ± 0.01 mm; Pervatech, the Netherlands) followed by subsequent drying and calcination at 650 °C as described in [2]. The boehmite-PVA dip-sol was twice coated on the α-Al_2O_3 supports to obtain smooth intermediate layers. Dip-coating was performed in a class 100 laminar flow cupboard, situated in a class 1000 cleanroom, to minimize defect formation due to dust particles. The pore size of the γ-Al_2O_3 intermediate layer is around 3-5 nm, as measured by permporometry [19].

For the production of the hybrid silica sol, 1,2-bis(triethoxysilyl) octane (referred as BTESO; purity 97%; ABCR Germany) was used as precursor. Water was deionized at 18.2 MΩ/cm using a Millipore purification system. A polymeric sol was fabricated by drop-wise adding 2.37 ml BTESO to a nitric acid (0.31 ml; 65%; Aldrich)-water-ethanol mixture (0.39 ml water in 21.93 ml ethanol) at room temperature. This mixture was refluxed for 2 hr at 60 °C under continuous stirring to produce a BTESO sol. The final molar ratio of BTESO sol is BTESO/EtOH /H_2O/HNO_3 of 1/70.62/0.084/0.152.

20 ml of this hybrid sol was diluted with 20 ml of ethanol to produce a BTESO dip-sol for membrane fabrication.

The particle size of freshly prepared sols was determined by dynamic light scattering (DLS) using a Malvern Zetasizer Nano ZS at 25 °C. Details of this method are described in previous chapters.

Unlike γ-Al_2O_3 layers, dip-coating of BTESO was only performed once on α-Al_2O_3 supports. After coating of the hybrid sol, the membrane was calcined at 250 °C for 3 hr under nitrogen flow (99.99% pure) applying a heating and cooling rate of 1 °C/min.

The structure of calcined γ-alumina and BTESO gels was evaluated by nitrogen sorption porosimetry at 77K (Tristar 3000, Micromeritics). Before the measurements, the gels were degassed at 200 °C under vacuum for 3 - 10 hrs.

Membrane characterization was performed on in-house designed single gas permeation (SGP) set-up in a dead-end mode, the details of which are also described before. The cross-sectional micrographs of developed membranes were captured by high-resolution scanning electron microscope HR-SEM (ZEISS 1550) at an accelerated voltage of 2.0 kV.

6.3 Results

The boehmite sol showed a broad particle size distribution ranging from about 4 to 500 nm. In contrast, the hybrid silica (BTESO) sol resulted into a neat and monodispersed size distribution ranging from about 5 nm to 100 nm with an average particle size of about 25 nm (figure 6.1).

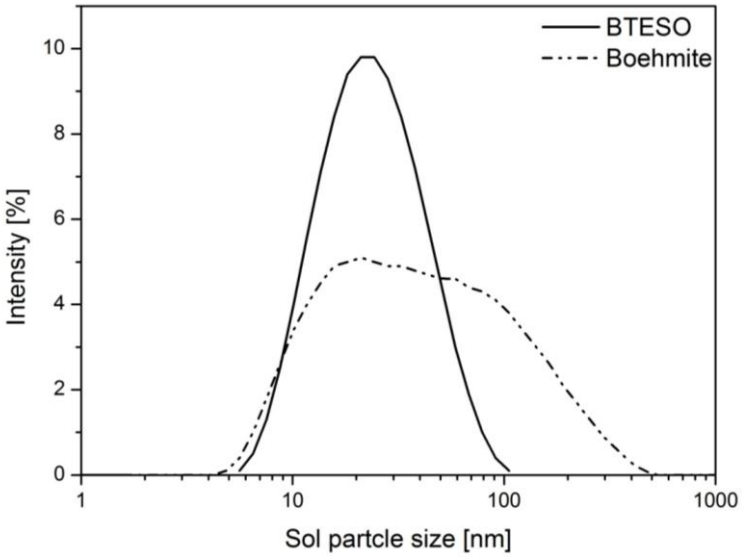

Figure 6.1: Comparison of sol particle size and distribution of freshly prepared boehmite sol and BTESO hybrid sol.

Figure 6.2 shows the nitrogen adsorption/desorption results of unsupported, calcined BTESO and γ-Al_2O_3 gels. For γ-Al_2O_3, the isotherm was a type IV-H2 hysteresis loop which was also observed previously by Uhlhorn et. al. [7]. For

BTESO, the isotherm is of type IV [20, 21] which can also be ascribed to mesoporous solids. This hysteresis can be regarded as of type IV-H4 which is associated with narrow-slit like pores [20]. The initial section (low relative pressure) of the BTESO adsorption/desorption curve is attributed to type I which is indicative for the presence of microporosity in the sample. At higher P/P_o the adsorption curve showed inclination indicative of multi-layer formation in the sample. The desorption line of the BTESO curve failed to reach zero relative pressures. During nitrogen desorption failure of the nitrogen meniscus inside the pore occurs at a relative pressure of around 0.4. If the system is not degassed properly, adsorbed nitrogen sticks to the pore walls at a relative pressure below 0.4. Therefore this part of the sorption curve does not contribute to any change in the analysis of sorption data [20, 22, 23]. In the case of BTESO, as described in this work, the desorption process did not occur completely. So, however the fact that the desorption part of hysteresis curve remained open at a partial pressure below 0.4, it is assumed that the part below 0.4 does not contribute to sorption data analysis.

The desorption part of the γ-Al_2O_3 hysteresis starts at a higher relative pressure (almost one order of magnitude higher) than the BTESO sample. The upper limit of the pore diameter of these γ-Al_2O_3 gels is about 5 nm [24] which was later confirmed on membranes as well [19]. For BTESO, the upper limit of the pore diameter is less than 5 nm. For γ-Al_2O_3, the relative pressure where the hysteresis loop closes is higher than for BTESO. It shows that BTESO has a lower-pore size limit than γ-Al_2O_3 (*i.e.* pore size of smallest meso pore in the sample). This could be due to presence of a large number of small mesopores or the presence of micropores. The BTESO isotherm also shows signs of microporosity at lower relative pressures.

The BET surface area of BTESO gels was calculated as 218 g/m^2 and for γ-Al_2O_3 as 240 g/m^2. The mean pore-diameter of the γ-Al_2O_3 sample was 4.5 nm, which was slightly higher than what was reported previously by Leenaars and Uhlhorn, (3.5 nm) [7, 24, 25], but slightly smaller than what was recently reported by Pinheiro [26]. For BTESO, the mean pore-diameter was measured to be 3 nm (as shown in Table 6.1).

Table 6.1: N_2-sorption measurements of unsupported γ-Al_2O_3 and BTESO calcined gels

	BET Surface area [m^2/g]	**Mean Pore diameter [nm]**
γ-Al_2O_3	240	4.5 nm
BTESO	218	3 nm

The size of the meso pores was calculated using the BJH method [20, 21]. It is reported by Uhlhorn that the pore diameter and pore structure of unsupported γ-Al_2O_3 membranes coincides with the pore size and structure of supported γ-Al_2O_3 membranes [7]. In this chapter it will now be examined, whether for BTESO it is also true that the pore morphology of calcined gels (i.e. unsupported membranes) matches with that of BTESO-supported α-Al_2O_3 membranes and that a mesoporous BTESO layer can be applied on α-Al_2O_3 supports by a single sol-dipping procedure, followed by a calcination step. The prepared membranes were analyzed by scanning electron microscopy and single-gas permeation tests.

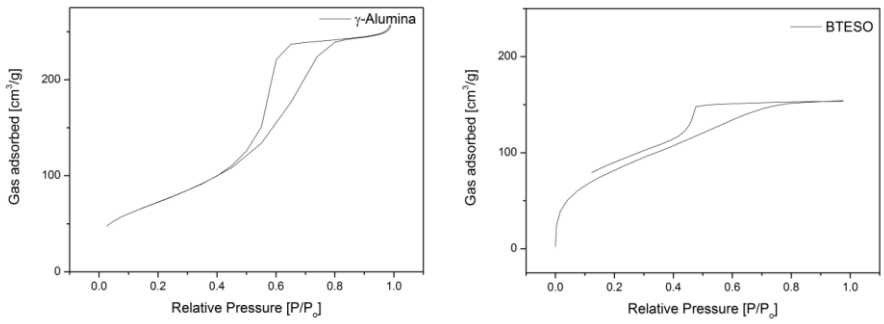

Figure 6.2: Nitrogen adsorption-desorption isotherms of calcined BTESO and γ-Al_2O_3 gels samples.

Figure 6.3 shows high resolution SEM-micrographs of γ-Al_2O_3 and BTESO layers deposited on α-Al_2O_3 supports. Figure 6.3(a) shows a cross-section of γ-Al_2O_3 deposited on an α-Al_2O_3 support. Figure 6.3(b) shows an α-Al_2O_3 support, which was dipped in a BTESO sol and subsequently calcined. In this case no separate top layer

can be observed on the α-Al_2O_3 support. At a few places (as encircled in the figure), some small particles are visible between the α-Al_2O_3 pores, which are expected to be BTESO particles. From this result it is concluded that the BTESO sol particles are infiltrated in the α-Al_2O_3 support without forming a rigid layer on it. The BTESO sol, having identical mesoporosity for dried/calcined gels as for γ-Al_2O_3, showed no indication of forming a rigid, thin layer on the α-Al_2O_3 support. The small average particle size of BTESO could be a reason for its infiltration. To study the BTESO sol infiltration in more detail, a BTESO dip-sol was coated on a γ-Al_2O_3 support. As shown in figure 6.3 (c), a uniform BTESO layer can be observed on the γ-Al_2O_3 support. Black highlighted circles on the α-Al_2O_3 pores indicate some BTESO sol infiltration through the γ-Al_2O_3 layer. It means that some particles of BTESO sol are even smaller than the pore size of the γ-Al_2O_3 layer. Nevertheless, the BTESO sol forms a rigid and uniform layer having thickness of about 400 nm when deposited on a γ-Al_2O_3 support by a single dipping procedure. No visible cracks on the BTESO surface are observed in the SEM-micrographs.

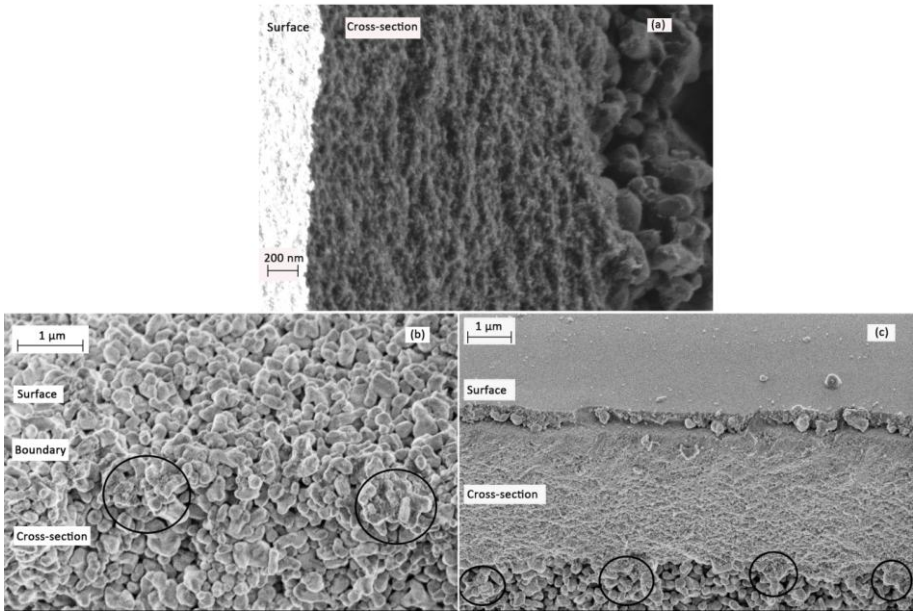

Figure 6.3: HR-SEM micrographs of supported membranes developed by using γ- Al_2O_3 and BTESO sols. **(a)** γ- Al_2O_3 deposited on an α-Al_2O_3 membrane support. **(b)** BTESO on an α-Al_2O_3 support. Black circles indicate BTESO sol infiltration. **(c)** BTESO on γ-Al_2O_3 / α-Al_2O_3.

The performance of the developed membranes was investigated by single gas permeation (figure 6.4 and table 6.2). Since it is assumed that all these membranes have pore sizes in the macro- or meso-porous range, meaning a pore diameter of 2 nm or more, gas transport will be through viscous flow or Knudsen diffusion flow [2, 3, 27, 28].

In macroporous membranes, at pore-sizes ranging 200 nm – 3000 nm, the gas transport is governed by viscous flow (often termed as Poiseuille flow) [28, 29]. In such systems, gas transport occurs under the influence of a pressure gradient across the membrane (*i.e.* pressure difference acts as a driving force) and the actual flow resistance is determined by gas viscosity (η), which is why this flow is termed as viscous flow. Here, the mean free path of the gas molecule (λ) is smaller than mean pore diameter, which ends up in a non-selective transport. The gas flux in such systems can be described by the Poiseuille equation which is modified by taking into account the structural geometry of the porous medium [2]:

$$N = -\frac{\varepsilon}{\tau}\frac{r^2}{8\eta}\frac{P}{RT}\frac{dP}{dz} \qquad (1)$$

Where N is molar flux [mole/m^2.s], ε is membrane porosity [-], τ is the pore tortuosity [-], r is the pore radius [m], P is pressure [Pa], R is gas constant [J/K.mol], T is absolute temperature [K].

Knudsen diffusion is typical for gas transport in systems where the pore diameter is in the range of 2 – 100 nm. Knudsen diffusion occurs when the mean free path length (λ) of the gas molecule is larger than the membrane pore size. Here, the interactions between the gas molecules with each other are negligible compared to the molecule-wall interactions. Knudsen diffusion leads to gas-selectivity based on the differences in gas molecular weights. For pure Knudsen permeance, the following equation can be used.

$$F = \frac{N}{\Delta P} = -\frac{\varepsilon}{\tau}\frac{2}{3}\frac{r}{L}\sqrt{\frac{8}{\pi MRT}} \qquad (2)$$

Where F is the permeance [mol/m^2.s.Pa], r is the pore radius [m], L is membrane thickness [m], and M is the molar mass of the gas molecule [g/mol].

For the membranes developed in this research, Knudsen diffusion transport is the dominant transport mechanism through the BTESO and γ-Al_2O_3 membranes, whereas viscous transport occurred in the α-Al_2O_3 membranes [2, 27]. However, all the membranes show a Knudsen type of selectivity for all gases at 200 °C.

Any significant influence of applying a BTESO layer on gas transport was not observed. When BTESO was directly applied on α-Al_2O_3, there was a small decrease in the gas permeances which can be due to particles infiltration (as seen in figure 6.3b). When BTESO was deposited on γ-Al_2O_3, a marginal increase in the gas permeances was observed. The variations in gas permeance were very small so there was no hard proof of BTESO influence. These small differences between the several membranes might also be due to experimental errors in the permeation measurements. So it seems that deposition of the thin BTESO on γ-Al_2O_3 has no influence on the resistance to gas flow.

Benes et. al. [29] showed on almost identical membranes that the resistance to gas flow was negligible over the relative thin (few μm thick) γ-Al_2O_3 layer and that the main resistance to permeation comes from the α-Al_2O_3 support which has a thickness of around 2 mm. The BTESO layer is almost 6-7 times thinner than the γ-Al_2O_3 and gas permeation results show that this layer also offers no extra resistance to permeance at 200 °C.

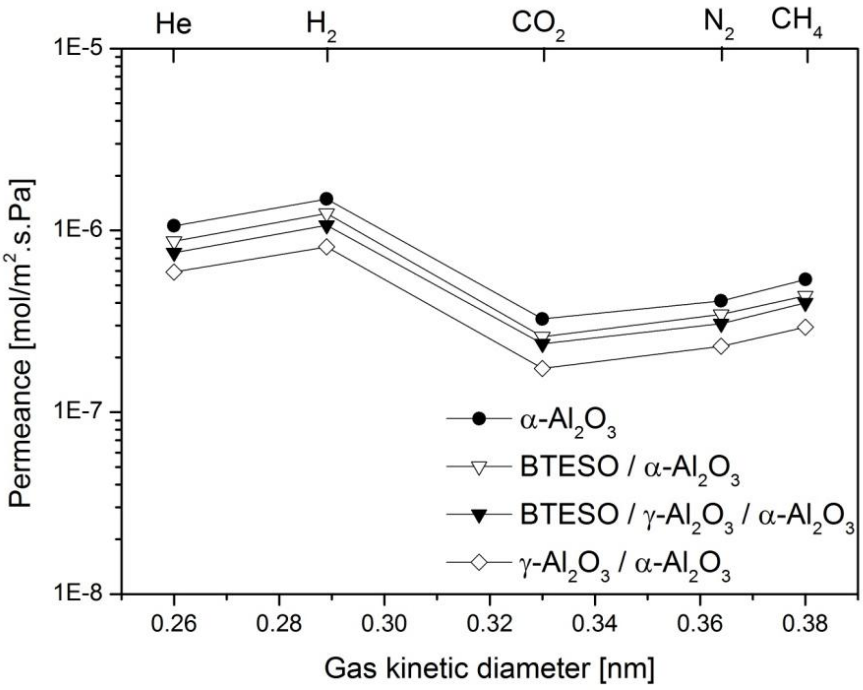

Figure 6.4: Single gas permeation (SGP) analysis of BTESO, γ-Al_2O_3 and α-Al_2O_3 membranes at 200 °C.

Table 6.2: Single gas permeation (SGP) analysis of BTESO, γ-Al_2O_3 and α-Al_2O_3 membranes at 200 °C. Knudsen selectivity is indicated in between brackets.

	Gas Permeances [mol/m^2.s.Pa]					Permselectivity			
	He	**H_2**	**CO_2**	**N_2**	**CH_4**	**H_2/He** **(1.4)**	**H_2/CO_2** (4.7)	**H_2/N_2** **(3.7)**	**H_2/CH_4** **(2.8)**
α-Al_2O_3	1.06E-6	1.49E-6	3.26E-7	4.1E-7	5.38E-7	1.4	4.5	3.6	2.8
γ- Al_2O_3	5.91E-7	8.12E-7	1.74E-7	2.31E-7	2.94E-7	1.4	4.6	3.5	2.7
BTESO/γ-/α-Al_2O_3	8.71E-7	1.24E-6	2.6E-07	3.45E-7	4.37E-7	1.4	4.7	3.6	2.8
BTESO / α-Al_2O_3	7.55E-7	1.07E-6	2.38E-7	3.07E-7	4E-7	1.4	4.5	3.5	2.6

Detection limit of equipment: 5 X 10^{-10} mol/m^2.s.Pa.

6.4 Discussion

The average particle size of the BTESO sol is 25 nm and that of the boehmite sol is about 45 nm, with high polydispersity. From figure 6.1, it is clear that the proportion of small sol particles (for example. < 30 nm) in the boehmite sol is considerably less compared to that of the BTESO sol. Due to this reason, the large amount of small BTESO particles can easily penetrate in the α-Al_2O_3 support during the dip-coating procedure, while for the boehmite sol a layer is formed by the relative large amount of particles which have a size equal or larger than the pore size of the α-Al_2O_3 support. So a bigger average particle size of BTESO is important for not penetrating in the α-Al_2O_3 support. The particle size of BTESO sols can be increased by either increasing its concentration during sol synthesis or by prolonging the synthesis time. However, care must be taken to avoid gelation during the condensation reaction, as concentrated sols tend to gelate quickly [30].

In order to avoid BTESO sol infiltration in the α-Al_2O_3 supports other strategies, than starting with bigger sol particles, can be applied as well. The use of a binder during sol-synthesis or in the dip-sol can be a suitable strategy. For example, Uhlhorn et al. [7] added a binder (PVA solution) to the boehmite dip-sol and performed multiple dipping (*i.e.* 2x) that resulted in the formation of a defect-free γ-Al_2O_3 layer on an α-Al_2O_3 support. Boffa et al. [32] used a surfactant (cetyl-trimethyl-ammonium bromide CTAB) during the synthesis of silica sols and used a rheological additive (BYK-420) in small proportions (2-6 vol %) in the dip-sol to avoid sol infiltration. BYK-420 is a modified urea solution that is used in aqueous coatings as anti-settling agent for pigments [33]. Besides, in the work of Boffa et al. the silica dip-sol was coated twice on the α-Al_2O_3 membrane supports.

It is shown that after calcination at 250 °C a mesoporous BTESO structure can be obtained by gelation of a 25 nm BTESO sol. A uniform BTESO layer was formed on an already established meso-porous γ-Al_2O_3 layer. It elucidates that particle size of BTESO sols was adequate to form a rigid mesoporous BTESO layer on a γ-Al_2O_3 support.

It must also be emphasized that layer formation is a distinct and separate phenomenon that is dependent on several structural properties of a material. The

surface area, porosity, and pore size, as measured on dried/calcined gels is not in all cases a direct proof that a rigid coating with the same microstructure will be formed after dipping the sol on a (macro) porous support and subsequent calcination. Thin layer deposition is an entire different phenomenon that involves complex kinetics like substrate wettability, contact time, drying, calcination, environment and duration of drying and calcination etc. as have been extensively discussed by Bonekamp [31].

As an outlook for further research, it is recommended to focus on increasing the particle size of BTESO hybrid sols. Multiple dipping with sol particle size of about 40-50 nm, and the use of viscosity modifiers like BYK-420 in the BTESO dip-sol would most likely result in the sustained deposition of a BTESO layer on an α-Al_2O_3 membrane support.

6.5 Conclusions

Hybrid silica (BTESO) sols were successfully synthesized with an average particle size of about 25 nm. When this sol was deposited on an α-Al_2O_3 macroporous support via dip-coating, it was not possible to form a smooth layer as was observed for γ-Al_2O_3. When the BTESO sol was deposited on a γ-Al_2O_3 support, a uniform layer was formed and showed no additional resistance to gas transport through the membrane. The membranes showed permselectivities in the Knudsen selectivity range. To develop a smooth BTESO layer on an α-Al_2O_3 support, it is recommended to increase the sol particle size of BTESO sols up to at least 40 nm and to use a sol viscosity modifier (for e.g. BKY-420) that would prevent sol infiltration and could lead to stable deposition of BTESO on α-Al_2O_3 membrane supports. Finally it is advised to use multiple dipping to have sustained deposition of BTESO on α-Al_2O_3.

References

[1] A.J. Burggraaf, L. Cot, Fundamentals of Inorganic Membrane Science and Technology (Series 4), Elsevier, 1996.

[2] R.d. Vos, High-Selectivity, High-Flux Silica Membranes for Gas Separation, PhD Thesis, University of Twente, 1998.

[3] M. Mulder, Basic Principles of Membrane Technology, 2nd Edition, Kluwer Academic Publishers, 1996.

[4] G. Saracco, G.F. Vesteeg, W.P.M. van Swaaij, Current hurdles to the success of high-temperature membrane reactors, Journal of Membrane Science, 95 (1994) 105-123.

[5] J. Zaman, A. Chakma, Inorganic membrane reactors, Journal of Membrane Science, 92 (1994) 1-28.

[6] A.F.M. Leenaars, K. Keizer, A.J. Burggraaf, Formation, structure and separation characteristics of ceramic alumina membranes, Abstracts of Papers of the American Chemical Society, 188 (1984) 5-INDE.

[7] R.J.R. Uhlhorn, M.H.B.J.H. Veld, K. Keizer, A.J. Burggraaf, Synthesis of ceramic membranes, J Mater Sci, 27 (1992) 527-537.

[8] R.S.A. de Lange, J.H.A. Hekkink, K. Keizer, A.J. Burggraaf, Formation and characterization of supported microporous ceramic membranes prepared by sol-gel modification techniques, Journal of Membrane Science, 99 (1995) 57-75.

[9] J. Luyten, T. Van Gestel, J. Cooymans, C. Smolders, Processing of multilayer ceramic nanofiltration membranes, Innovative Processing/Synthesis: Ceramics, Glasses, Composites IV, Ceramic Transactions, 115 (2000).

[10] R. Vacassy, C. Guizard, V. Thoraval, L. Cot, Synthesis and characterization of microporous zirconia powders: Application in nanofilters and nanofiltration characteristics, Journal of Membrane Science, 132 (1997) 109-118.

[11] A. Nijmeijer, Hydrogen-selective Silica Membranes for Use in Membrane Steam Reforming, PhD thesis, University of Twente, 1999.

[12] R.M.d. Vos, H. Verweij, High-Selectivity, High-Flux Silica Membranes for Gas Separation, Science, 279 (1998) 1710-1711.

[13] J. Schaep, C. Vandecasteele, B. Peeters, J. Luyten, C. Dotremont, D. Roels, Characteristics and retention properties of a mesoporous γ-Al_2O_3 membrane for nanofiltration, Journal of Membrane Science, 163 (1999) 229-237.

[14] Tim Van Gestel, Carlo Vandecasteele, Anita Buekenhoudt, Chris Dotremont, Jan Luyten, Roger Leysen, Bart Van der Bruggen, G. Maesc., Alumina and titania multilayer membranes for nanofiltration: preparation, characterization and chemical stability, Journal of Membrane Science, 207 (2002) 15.

[15] H.L. Castricum, R. Kreiter, H.M.v. Veen, D.H.A. Blank, J.F. Vente, J.E. ten Elshof, High-performance hybrid pervaporation membranes with superior hydrothermal and acid stability, Journal of Membrane Science, 324 (2008) 111-118.

[16] H.L. Castricum, A. Sah, J.A.J. Geenevasen, R. Kreiter, D.H.A. Blank, J.F. Vente, J.E. ten Elshof, Structure of hybrid organic–inorganic sols for the preparation of hydrothermally stable membranes, Journal of Sol-Gel Science and Technology, 48 (2008) 11-17.

[17] R. Kreiter, H.L. Castricum, J.F. Vente, J.E. ten Elshof, M.D. Anna, H.M. Veen, Hybrid silica membrane for water removal from lower alcohols and hydrogen separation, in, Google Patents, 2011.

[18] H.L. Castricum, G.G. Paradis, M.C. Mittelmeijer-Hazeleger, R. Kreiter, J.F. Vente, J.E. ten Elshof, Tailoring the Separation Behavior of Hybrid Organosilica Membranes by Adjusting the Structure of the Organic Bridging Group, Advanced Functional Materials, 21 (2011) 2319-2329.

[19] G.Z. Cao, J. Meijerink, H. W. Brinkman, A.J. Burggraaf, Permporometry study on the size distribution of active pores in porous ceramic membranes, Journal of Membrane Science, 83 (1993) 14.

[20] K. S. W. Sing, D. H. Everett, R. A. W. Haul, L. Moscou, R. A. Pierotti, J. Rouquerol, T. Siemieniewska, Reporting physisorption data for Gas/Solid systems with special reference to the determination of surface area and porosity (IUPAC Recommendations 1984), Pure and Applied Chemistry, 57 (1985) 17.

[21] E.P. Barrett, L.G. Joyner, P.P. Halenda, The Determination of Pore Volume and Area Distributions in Porous Substances. I. Computations from Nitrogen Isotherms, Journal of the American Chemical Society, 73 (1951) 373-380.

[22] P.A. Webb, C. Orr, Analytical Methods in Fine Particle Technology, Micromeritics Instrument Corporation, USA.

[23] Q.I. USA, Presentation: Physisorption Methods and Techniques in.

[24] A. F. M. Leenaars, K. Keizer, A.J. Burggraaf, The preparation and characterization of alumina membranes with ultra-fine pores, J Mater Sci, 19 (1984) 1077-1088.

[25] A.F.M. Leenaars, A.J. Burggraaf, The Preparation and Characterization of alumina membranes with Ultrafine Pores 2. The Formation of Supported Membranes, Journal of Colloid and Interface Science, 105 (1985) 14.

[26] A.F.d.M. Pinheiro, Development and Characterization of Polymeric-grafted Ceramic Membranes for Solvent Nanofiltration, PhD thesis, Chapter 4, University of Twente., 2013.

[27] R.W. Baker, Membrane Technology and Applications, Second Edition ed., John Wiley & Sons, Ltd, 2004.

[28] J.G.A. Bitter, Transport mechanism in membrane separation processes, Plenum Press, New York, 1991.

[29] N.E. Benes, Mass Transport in Thin Supported Silica Membranes, PhD thesis, University of Twente, 2000.

[30] A.C. Pierre, Introduction to Sol-Gel Processing, Kluwer Academic Publishers (1998).

[31] A.J. Burggraaf, Fundamentals of Inorganic Membrane Science and Technology. Chapter 6: "Preparation of asymmetric ceramic membrane supports by dip-coating". in: B.C. Bonekamp (Ed.), Elsevier Science, 1996.

[32] V. Boffa, J.E. ten Elshof, D.H.A. Blank, Preparation of templated mesoporous silica membranes on macroporous α-alumina supports via direct coating of thixotropic polymeric sols, Microporous and Mesoporous Materials, 100 (2007) 173-182.

[33] Materials Saferty Data Sheet BYK-420, BYK Additives & Instruments USA Inc. www.byk.com (2008).

Chapter 7

Conclusions and Recommendations

7.1 Conclusions and Evaluation

In this thesis the fabrication and viability of hybrid silica (*i.e.* BTESE) membranes for molecular separation is described. The focus is on gaining a better insight in the membrane fabrication process of these organosilica membranes and to further broaden their application range.

In the past decades, ceramic membranes prepared by sol-gel methods have been investigated for molecular separation applications. Especially silica membranes were studied in great depth [1-3]. These silica membranes have intrinsic limitations with regard to hydrothermal stability [4, 5]. This has paved the way for hybrid silica (BTESE) membranes which possess high hydrothermal stability, even under acid environments, and show good performances in pervaporation for dewatering of several alcohols [6, 7]. With regard to applications, the main objective of this work is to obtain a good performance in gas separation for these membranes as well. This is tried to be achieved via a better understanding of the pore formation mechanism during gelation while dip-coating and subsequent drying and calcining. In this way it might be possible to *orchestrate* the pore structure in a better and more controlled way.

In **Chapter 2**, a one-pot, facile and reproducible acid-catalyzed sol synthesis for the fabrication of hybrid silica membranes is described. The resulting membranes show a uniform membrane pore-microstructure with pore sizes < 1 nm and gas permselectivities based on molecular sieving. Several attempts are described in literature to prepare membranes by sol-gel processing from the same precursor (*i.e.* BTESE). In almost all these cases fabrication steps are found to be tedious (more reaction steps) and more time consuming (6-8 hrs processing) if compared with the method given in chapter 2. Besides, a less uniform pore size distribution with bigger pores is reported in literature [8, 9].

In this chapter reaction parameters (precursor concentration [Si], acid ratio [AR = H^+ : Si], hydrolysis ratio [HR = H_2O : OC_2H_5]) and processing conditions (temperature, time) are well described and their influences on sol, (dried and calcined) gel and membrane properties are explained. It is stressed that making the optimal hybrid silica sol for a membrane demands a defined precursor concentration, an optimized

hydrolysis and condensation reaction as well as a reaction time and temperature that results in stable, non-gelated and uniform sols with average particle sizes ranging from 7-10 nm. It was figured out that by tuning the precursor concentration ([Si] = 1.8 M), hydrolysis ratio (HR = 1), acid ratio (AR = 0.1) and reaction time and temperature (60 °C and 90 minutes), the sol synthesis resulted in a hybrid silica sol, applicable for membrane fabrication. After proper dilution of the sol it was possible to make thin selective layers on a porous support after coating of the "dip-sol" and subsequent calcining. A direct relation between dip-sol concentration, resulting selective layer thickness and gas permselectivities was observed. With an increase in dip-sol concentration the membranes showed a higher H_2/CH_4 selectivity. Dip-sol concentrations higher than 0.6 M resulted in cracked membranes with crack-lines visible by the naked-eye (as shown in figure 2.3). On the other hand, reduced dip-sol concentrations resulted in ultrathin selective layers with thicknesses less than 100 nm and increased permeances of larger molecules (N_2, CH_4) but still impermeable to SF_6. Based on gas transport theory and permeance data, a relatively concise estimation of the pore size range of the developed BTESE membranes is reported. It was shown that these hybrid silica membranes possess a pore size ranging from 0.3 to 0.54 nm. SF_6 impermeable BTESE membranes are made, which, to the best of our knowledge, has never been reported before. To summarize, it was shown that the pore-size of BTESE membranes can be adjusted to some extend by tuning he dip-sol concentration.

The knowledge, acquired in chapter 2, regarding the control of sol processing and membrane fabrication, is used for further research as described in **Chapter 3**. The aim was to induce changes in the sol fabrication process to modify the BTESE membrane microstructure in such a way that it can be targeted for the separation of small gas molecules (< 0.4 nm). In chapter 3 the effect of adapting the acid concentration during the sol synthesis on the BTESE membrane microstructure is discussed. Ten times less acid was used to prepare BTESE sols, while the sol polymerization time was reduced to 30 minutes. Microporous membranes, prepared in this way showed a more tight pore-microstructure than was found from the results as described in chapter 2.

It was observed in chapter 2 that hydrolysis ratios above 1 and acid-ratios above 0.1 (including all possible combinations) resulted in a gelated sol structure even after

reaction at ambient (room) temperature. In chapter 3, along with reducing the acid ratio from 0.1 to 0.01, the precursor concentration was increased from 1.8 M to 2.7 M to achieve a sufficient large sol particle size under these relative acid lean conditions. The higher pH of this sol system (compared to the pH applied in chapter 2) leads to a slower hydrolysis reaction which resulted in a more controlled and homogeneous growth of sol particles without fast gelation [10, 11]. In this way the non-gelation boundaries of hybrid silica sol processing were extended by combining a reduced acid ratio (AR = 0.01) with a high Si precursor concentration (2.7 M) and a hydrolysis ratio of 1. Here the best result in terms of membrane characteristics was obtained after reaction for 90 minutes at 60 °C. The reproducible results on sols and membranes showed that, with a high dip-sol concentration of 0.6 M, a uniform selective hybrid silica layer of 440 nm was formed that showed a H_2/N_2 permselectivity of at least 50. At some instances these membranes were also found nitrogen and methane impermeable.

Membranes developed from sols prepared in a water lean condition, meaning a hydrolysis ratio (HR) of 0.5, (acid ratio: 0.1) showed very high gas permeances and low H_2-permselectivities (H_2/N_2 = 5; H_2/CH_4 = 4; H_2/SF_6 = 300). This could be due to insufficient formation or presence of siloxane bonds in the selective layer after calcination. Sol growth under water lean conditions can result in non-gelated sols with particle sizes adequate to form membranes, but care must be taken to add sufficient water during sol synthesis for silanol (and siloxane) formation [11]. In the studied system, we can say that probably not all the BTESE was hydrolyzed under the HR of 0.5.

In literature it was concluded from experimental [12, 13] and molecular simulation research [14, 15] that the permselectivity for hybrid silica membranes can be tuned by tuning the length of the organic functional groups between the silica moieties. With these “spacer techniques”, *i.e.* adjusting the length of the hydrocarbon bridge, the membrane pore size can be altered. This also demands adaptations in the sol synthesis route for each precursor. In chapter 3 a new approach is presented, which shows that pore structure tuning of the hybrid silica matrix can also be performed by modifying the reaction parameters of a specific precursor during sol synthesis. Based on the ease-of-use in membrane development and the overall high

membrane performances, the strategy mentioned in this chapter clearly prevails over previous claims of structural tuning by spacer technology.

Chapter 4 presents a new approach to incorporate different elements in the BTESE matrix by acid catalyzed sol processing. After doping BTESE with other ions a well-defined sol particle size and particle size distribution as well as the tendency to gelate (and consolidate) without cracking during dip-coating and calcination is imperative in forming a uniform membrane microstructure. For example, Nb-doping in a silica matrix has resulted in improved hydrothermal stability of silica membranes [16], which was mainly due to the fact that the doped element was coherently dispersed in the silica structure and improved its stability without damaging the structure of the selective layer.

Boron, niobium, and tantalum were doped in the BTESE matrix with the aim to enhance the gas permselectivities. An in-situ FTIR analysis was conducted to ensure successful incorporation of these elements in the BTESE matrix. TGA and FTIR results on all dried and calcined doped-BTESE gels ensured that the ethylene bridge in doped-BTESE was retained in inert gas atmosphere until at least 500 °C. The developed membranes tend to form a relatively loose microstructure than undoped BTESE membranes as indicated by higher single gas permeances. High resolution scanning electron microscopy studies showed no visible defects or cracks in the membrane layers *i.e.* all doped-BTESE materials formed a smooth and uniform selective layer. As the dopant and dip-sol concentrations were identical for all doped membranes, any difference in the selective layer thickness must be ascribed to the effect of the presence of the specific doping element on the selective layer microstructure. The Ta-BTESE layer thickness (230 nm) was relatively close to the layer thickness of pure BTESE (260 nm), but a large decrease in H_2/N_2 and H_2/CH_4 permselectivities was observed. The B-BTESE (180 nm) layer thickness was found to be much thinner than that of undoped BTESE and an excessive permeance was observed for bigger gas molecules such as N_2, CH_4 and even SF_6, indicating the formation of a very open/loose pore network for these B-BTESE membranes. On the other hand, the Nb-BTESE selective layer was 360 nm thick which is almost 40% thicker than undoped BTESE, while nitrogen and methane permeances were found respectively 80% and 60% higher than undoped-BTESE membranes with reduced the H_2/N_2 and H_2/CH_4 permselectivities. The fabrication strategy presented in this

work resulted in doped-BTESE sols, adaptable for membrane coating, but the prepared membranes were found to have a lower permselectivity compared to undoped BTESE membranes. These results show that sol synthesis and membrane fabrication are two distinct and independent phenomena and a "*good*" hybrid sol does not necessarily guarantee a good a membrane. Furthermore, with Nb-BTESE, no clear affinitive effect towards CO_2 permeance was observed contrary to what was reported earlier by Qi et. al. [17].

In **Chapter 5** an approach to disperse metal-ions in a new type of hybrid silica precursor, named *N,N,N',N'*-tetrakis-(3-(triethoxysilyl)-propyl)-malonamide (TTPMA), is described. This precursor was synthesized by a base-catalyzed nucleophilic substitution of bis-(3-triethoxysilyl)-propyl)-amine on malonyl chloride. Ce and Ni ions were introduced in the malonamide ligand, and from the developed sols membranes were fabricated and characterized. TEM observations on calcined samples showed that nano-particles of cerium oxide (2-4 nm) and nickel oxide (2-15 nm) were present in the Ce-TTPMA and Ni-TTPMA membranes respectively. The sol particle size distribution was bimodal for Ce-TTPMA sols (figure 5.2), while a smooth and ultra-thin selective layer of 35 nm was formed that showed slightly better H_2/N_2 and H_2/CH_4 permselectivity than BTESE membranes. Ni-TTPMA formed well-defined sol particles that resulted in membranes with a selective layer thickness of 210 nm (*i.e.* 20% thinner than that of BTESE). The gas fluxes of smaller gases (*i.e.* He, H_2) through these membranes were one order of magnitude lower than BTESE membranes with no detectable permeation of nitrogen or methane, showing that the Ni-TTPMA pore network was too dense to allow any permeation of nitrogen or methane.

As a future outlook, it would be worthwhile to perform hydrothermal stability and chemical resistance tests on these membranes. Furthermore, doping of metals such as Nb, and Ta in a TTPMA membrane matrix should be conducted to enable direct comparison with Ta and Nb doped BTESE membranes.

In literature another way to reduce the pore size of silica membranes is described. This so-called "ageing" implies that after dipping the freshly prepared silica membranes were left in a controlled environment (temperature and humidity) for a certain period of time, prior to calcination [18]. BTESE membranes were developed as stated in chapter 2, and were aged at different time intervals to study the effect

of ageing on the BTESE pore microstructure. As can be seen in table 7.1 and figure 7.1, there was a marginal improvement in H_2/N_2 and H_2/CH_4 permselectivities when the BTESE membranes were aged for 1 hr after dip-coating prior to membrane calcination. Prolonged duration of membrane ageing (*i.e.* 1 week to 3 weeks) resulted in a drastic reduction of H_2-permselectivities which were found closer to Knudsen selectivities. So, in our work we did not observe any improvement in (perm) selectivity by "ageing" the dip-coated membranes prior to calcining. It could be that when left in air for long time intervals after dipping, the siloxane gel was infiltrated in the underneath support.

Table 7.1: Permselectivity data of BTESE membranes recorded at 200 °C, when aged for different intervals after dip-coating and before calcination.

Permselectivity	**BTESE (300)**				
(H_2/X)	**(No ageing)**	**(1 hr)**	**(1 day)**	**(1 week)**	**(3 weeks)**
H_2/He	1.2	1.3	1.2	1.3	1.4
H_2/CO_2	3.9	4.1	4.0	3.5	4.5
H_2/N_2	13.5	16	12	6	3.7
H_2/CH_4	19.5	22.2	22.3	4.1	4.1
H_2/SF_6	∞	∞	∞	875	850
CO_2/CH_4	5	5.5	5.5	1.1	1.1

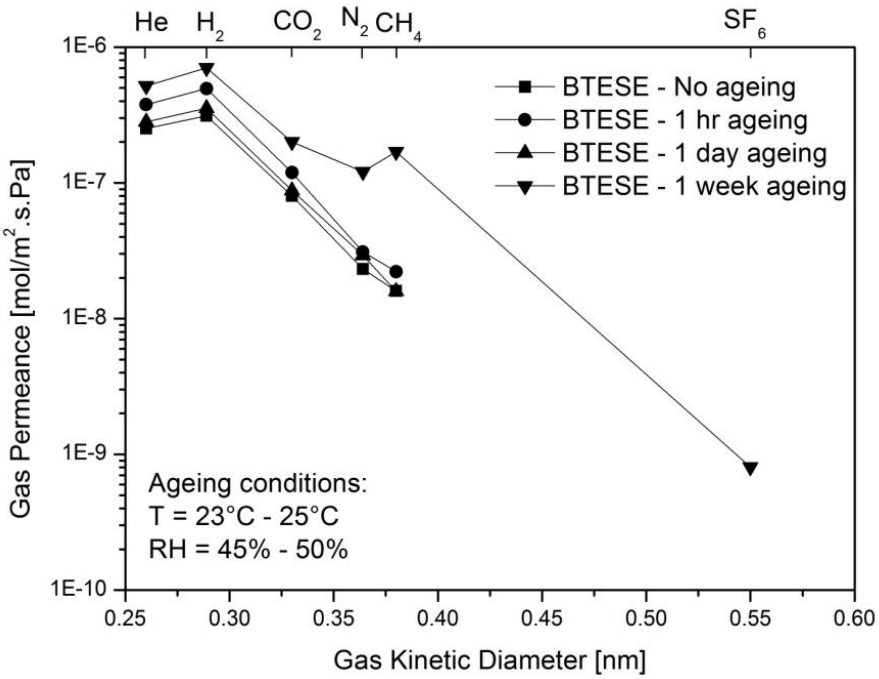

Figure 7.1: Single gas permeation analysis of BTESE membranes at 200 °C after ageing for different durations before subsequent calcination.

Chapter 6 describes the fabrication and characterization of another hybrid silica material 1,2-*bis*(triethoxysilyl) octane (BTESO) for its applicability as a substitute material for mesoporous γ-Al_2O_3 membrane layers. Hybrid silica mesoporous interlayers would extend the applications of membranes in processes where hydrothermal and chemical stabilities are of paramount importance. BTESO sol synthesis resulted in sols with average particle sizes of about 25 nm and a neat size distribution, whereas the dried and calcined gel formed into a mesoporous structure. However, when the sol was deposited on an α-Al_2O_3 support by dip-coating, the particles penetrated in the support without forming a rigid surface layer. This was probably due to the small average particle size of BTESO sols in relation to the pore size of the α-Al_2O_3 support (80 nm). It is assessed that an increase in the BTESO sol particle size up to at least 40 nm would reduce its infiltration effects considerably.

7.2 Recommendations

Figure 7.2 [19] shows the exploitation trends for various separation processes based on their fundamental understanding and commercial implementation. The x-axis of this figure represents the growth trend of an invention from an idea towards its maturity for entering in the market. The y-axis shows the growth trend of a process from initial results to its fully utilization.

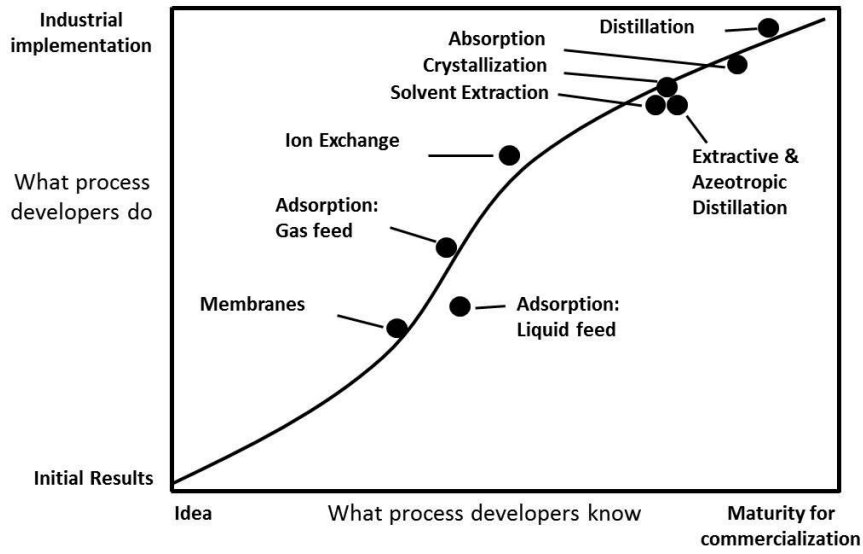

Figure 7.2: Technological and use maturities of separation processes [19].

As can be seen from this figure, a process such as distillation is fully understood and is commercially utilized for its benefits in purification and separation domains. On the other hand, membranes still have a lot to offer with regard to their fundamental understanding and commercial viability. Due to their ease-of fabrication and energy-efficient performance with no waste generation, membranes can be seen as one of the most viable separation tool to serve humanity in the future surrounding with scarce energy resources and less-clean environment. However, for sol-gel derived membranes a better understanding of precursor chemistry, a better control of reaction kinetics and microstructure development is still necessary for fully

translating these types of membranes into applications, ranging from microfiltration to molecular separation.

The hybrid silica membranes, as described in this thesis, certainly have a place in future separation processes. Orchestrating their pore microstructure, either by tuning the synthesis parameters or by addition of dopants, would certainly enhance their viability in applications ranging from gas separation (d_p < 0.4 nm) to nanofiltration (d_p > 1 nm). The membranes, described in chapter 3, showed excellent H_2/CH_4 and CO_2/CH_4 permselectivities. The next step could be to utilize their applicability in biogas purification / upgrading. The polymeric membranes (such as cellulose acetate) currently in use for this process show poor H_2S stability and they plasticize at high CO_2 partial pressure [20]. BTESE membranes are less prone to attack by H_2S and don't plasticize in CO_2 and therefore these membranes are promising to be applied in biogas upgrading.

In chapter 6, BTESO was synthesized and it formed a mesoporous structure. Orchestrating the fabrication strategy of BTESO to develop micro/meso porous membranes would result in membranes with bigger pores than BTESE and a more hydrophobic surface due to the presence of an increased number of hydrocarbon chains. The water contact angle of BTESE membranes developed in chapter 2 was 64°±2, with BTESO membranes it is expected to be above 85°. The larger pore size and the more hydrophobic character of BTESO-derived membranes could yield interesting nanofiltration membranes for energy effective recovery of solvents from waste chemical streams. Solvents such as alcohols, THF, acetonitrile could be recovered in an effective way either by using these membranes or by coupling the developed membranes with distillation columns, thus making a hybrid separation process. The increased hydrophobicity can also be utilized in dehydration of natural gas.

Tuning the reaction parameters of BTESO for obtaining bigger sol particles as achieved in chapter 6 would cease sol entrainment in the underneath α-Al_2O_3 support layer. In this way a graded BTESE / BTESO / α-Al_2O_3 membrane could be fabricated that can be used in separation processes at very low pH (< 2) where it was not used before due to decomposition of the γ-Al_2O_3 layer.

Tuning of the pore size of BTESE membranes can also be achieved by incorporating small organic monomers to its matrix during sol synthesis. A thermal treatment of the resulting "templated" membrane layer would end-up in burning-off the monomer from the BTESE matrix, resulting in creating cavities having the size of the burnt monomer. However, care must be taken in the choice of monomers that can burnt off completely below 200 °C in air or below 400 °C in inert atmosphere without leaving any residue.

Ni-TTPMA derived membranes showed a N_2-impermeable microstructure but the low permeances of helium and hydrogen indicated a very tight pore structure. Tuning of reaction parameters or reducing the dipping concentration of Ni-TTPMA sols could result in a thinner selective layer to obtain larger fluxes for small gases like He and H_2.

References

[1] C.J. Brinker, Structure Property Relationships in Thin Films and Membranes, Journal of Sol-Gel Science and Technology, 4 (1995) 117-133.

[2] R.M. de Vos, H. Verweij, High-Selectivity, High-Flux Silica Membranes for Gas Separation, Science, 279 (1998) 1710-1711.

[3] R.S.A. de Lange, J.H.A. Hekkink, K. Keizer, A.J. Burggraaf, Formation and characterization of supported microporous ceramic membranes prepared by sol-gel modification techniques, Journal of Membrane Science, 99 (1995) 57-75.

[4] H.M. van Veen, Y.C. van Delft, C.W.R. Engelen, P.P.A.C. Pex, Dewatering of organics by pervaporation with silica membranes, Separation and Purification Technology, 22–23 (2001) 361-366.

[5] R.d. Vos, High-Selectivity, High-Flux Silica Membranes for Gas Separation, PhD Thesis, University of Twente, 1998.

[6] H.L. Castricum, R. Kreiter, H.M. van Veen, D.H.A. Blank, J.F. Vente, J.E. ten Elshof, High-performance hybrid pervaporation membranes with superior hydrothermal and acid stability, Journal of Membrane Science, 324 (2008) 111-118.

[7] H.L. Castricum, A. Sah, R. Kreiter, D.H.A. Blank, J.F. Vente, J.E. ten Elshof, Hybrid ceramic nanosieves: stabilizing nanopores with organic links, Chemical Communications, (2008) 1103.

[8] M. Kanezashi, K. Yada, T. Yoshioka, T. Tsuru, Design of Silica Networks for Development of Highly Permeable Hydrogen Separation Membranes with Hydrothermal Stability, Journal of the American Chemical Society, 131 (2009) 414-415.

[9] M. Kanezashi, K. Yada, T. Yoshioka, T. Tsuru, Organic-inorganic hybrid silica membranes with controlled silica network size: Preparation and gas permeation characteristics, Journal of Membrane Science, 348 (2010) 310-318.

[10] R.K. Iler, The Chemistry of Silica, John Wiley and Sons, New York, 1979.

[11] A.C. Pierre, Introduction to Sol-Gel Processing, Kluwer Academic Publishers (1998).

[12] Gang Li, Masakoto Kanezashi, T. Tsuru, Preparation of organic–inorganic hybrid silica membranes using organoalkoxysilanes: The effect of pendant groups, Journal of Membrane Science, 379 (2011) 9.

[13] H.R. Lee, M. Kanezashi, Y. Shimomura, T. Yoshioka, T. Tsuru, Evaluation and fabrication of pore-size-tuned silica membranes with tetraethoxydimethyl disiloxane for gas separation, Aiche Journal, 57 (2011) 2755-2765.

[14] K.S. Chang, T. Yoshioka, M. Kanezashi, T. Tsuru, K.L. Tung, A molecular dynamics simulation of a homogeneous organic-inorganic hybrid silica membrane, Chemical Communications, 46 (2010) 9140-9142.

[15] K.-S. Chang, Tomohisa Yoshiokaa, Masakoto Kanezashia, Toshinori Tsurua, K.-L. Tungb, Molecular simulation of micro-structures and gas diffusion behavior of organic–inorganic hybrid amorphous silica membranes, Journal of Membrane Science, 381 (2011) 12.

[16] V. Boffa, J.E. ten Elshof, R. Garcia, D.H.A. Blank, Microporous niobia–silica membranes: Influence of sol composition and structure on gas transport properties, Microporous and Mesoporous Materials, 118 (2009) 202-209.

[17] H. Qi, H. Chen, L. Li, G. Zhu, N. Xu, Effect of Nb content on hydrothermal stability of a novel ethylene-bridged silsesquioxane molecular sieving membrane for H_2/CO_2 separation, Journal of Membrane Science, 421–422 (2012) 190-200.

[18] Rob S. A. de Lange, Klaas Keizer, A.J. Burggraaf, Aging and Stability of Microporous Sol-Gel-Modified Ceramic Membranes, Industrial & Engineering Chemistry Research, 34 (1995) 10.

[19] A.B.de Haan, H. Bosch, Fundamentals of Industrial Separations , 2nd Edition, 2007.

[20] Colin A. Scholes, Geoff W. Stevens, S.E. Kentish, Membrane gas separation applications in natural gas processing, Fuel, 96 (2012).

Summary

This thesis deals with the synthesis and applicability of sol-gel derived porous hybrid silica membranes and their feasibility in molecular separation applications. A special emphasis was given to process parameters, which are found responsible for *orchestrating* the pore structure of the microporous membranes.

Chapter 1 gives a brief overview of acid catalyzed sol-gel derived silica membranes which have been used for molecular separations. These membranes show an exceptional high selectivity under dry conditions but their performance under hydrothermal conditions was found to be low due to their insufficient inherent stability against steam. Two different strategies are reported in literature to deal with this issue; either by the addition of metal ions in the silica matrix, or by incorporating hydrocarbons (either as a bridge or at terminals) in the silica matrix. Both routes have resulted in the improved hydrothermal stability of silica system. The possibility of utilizing bridged-hydrocarbons in silica system *i.e.* hybrid silica, has not been studied in details for gas separation, which was one of the aims of this research.

Chapter 2 describes the fabrication of hybrid silica membranes that were reproducibly prepared from a single-step sol-gel synthesis route, using an ethoxy-bridged silane (1,2-bis(triethoxysilyl)ethane: BTESE) as precursor. The resulting membrane, obtained by a single dipping/calcining step, had a relative more open micropore structure than pure silica membranes. The sol process parameters such as precursor concentration, acid ratio and hydrolysis ratio were tuned to develop a mono-model particle size distribution. The H_2-permselectivity, obtained at 200 °C, and thickness of the selective hybrid layer was found to be dependent on the dip-sol concentration. The developed membrane microstructure was found defect-free and SF_6 impermeable whereas, the selective layer thickness ranging from 90 nm to 500 nm were obtained at dip-sol concentrations of 0.15 M and 0.6 M respectively.

Chapter 3 exploits the understanding of BTESE membranes fabrication as explained in chapter 2, to produce membranes that showed improved permselective properties. Here a more efficient and effective procedure was presented to synthesize a hybrid silica (BTESE) sols. By reducing the acid concentration with a factor 15, compared to the sol synthesis as described in chapter 2, BTESE sols were synthesized at a much faster rate *i.e.* at a condensation time of 30 minutes, resulting in homogenous hybrid sols that formed a more constricted pore

microstructure to what was observed in chapter 2. The developed membranes showed sufficient hydrogen permeance but were found almost nitrogen and methane impermeable at 200 °C (H_2/N_2 permselectivity more than 50 and for H_2/CH_4 90 or more). A defect-free microstructure was obtained with a selective layer thickness of about 440 nm at a dip-sol concentration of 0.6 M.

Chapter 4 reported the doping effect of elements in the BTESE membrane matrix. A new approach of doping boron, niobium or tantalum in BTESE by sol -gel processing was introduced and microporous membranes were fabricated by a single dipping procedure. TGA studies on dried samples and FT-IR analysis on calcined samples confirmed the presence of an ethylene-bridge between the Si atoms in all metal-doped BTESE samples and the material was found thermally stable until at least 500 °C in inert atmosphere. Although the single gas permeation results indicated a relatively open pore microstructure for all doped BTESE membranes when compared with undoped-BTESE membranes, the HR-SEM showed no defects or cracking in or in the selective microporous selective layer.

To facilitate the homogenous dispersion of metal-ions in a hybrid silica matrix, a new type of hybrid silica precursor named *N, N, N′, N′*–tetrakis-(3-ethoxysilyl)-propyl)-malonamide (TTPMA) is studied in **chapter 5**. TTPMA was synthesized under base-catalyzed conditions and Ce and Ni ions were introduced in the malonamide ligand to fabricate microporous membranes. TEM-results showed cerium oxide nanoparticles (2-4 nm) and nickel oxide nanoparticles (2-15 nm) in the calcined Ce-TTPMA and Ni-TTPMA samples. HR-SEM micrographs showed that both Ce-TTPMA and Ni-TTPMA membranes formed a defect-free microstructure. Ce-TTPMA membranes formed an ultra-thin selective layer of about 35 nm that showed slightly better H_2/N_2 and H_2/CH_4 permselectivity at 200 °C than BTESE membranes. Ni-TTPMA membranes formed a selective layer of about 210 nm and showed one order of magnitude lower gas flux of the smaller gases (*i.e.* He, H_2) if compared with BTESE membranes, while no detectable permeation of N_2 or CH_4 was observed, indicating a more dense pore network than BTESE membranes.

Chapter 6 presented the fabrication and characterization of the hybrid silica material 1,2-*bis*(triethoxysilyl) octane (BTESO) as a possible alternative material for mesoporous γ-Al_2O_3 membrane interlayers. γ-Al_2O_3 membranes have a limited stability under extreme pH and hydrothermal conditions. Replacement by BTESO

would extend application of these membranes in environments where chemical and hydrothermal stability is of paramount importance. BTESO sols with an average particle size of about 25 nm were synthesized by acid catalyzed sol processing and its calcined gels showed a mesoporous microstructure. When coated on α-Al_2O_3 supports, BTESO sol penetrated in the α-Al_2O_3 support without forming a smooth and rigid layer. The penetration of the BTESO sol particles was probably due to the small average particle size of BTESO sols compared to the average pore size of the α-Al_2O_3 support (about 80 nm). Increasing the average particle size of BTESO sols up to at least 40 nm would significantly reduce its penetration in α-Al_2O_3 support and therefore a smooth and homogenous mesoporous BTESO layer can be fabricated. The use of viscosity modifiers in the BTESO dip-sol can also be an option to form stable and uniform BTESO layer on α-Al_2O_3 support.

Chapter 7 compiles the overall conclusions drawn from the research with an outlook for future prospects. It was shown that apart from sol process parameters, pore tuning of hybrid silica membranes can also be accomplished by elemental doping or ageing of the freshly prepared membranes. Membranes fabrication, as described in chapter 3, can be utilized in biogas purification / upgrading. Successful hydrothermal and chemical stability tests of membranes presented in chapter 5 would lead to a new class of hybrid malonamide membranes that can withstand challenging industrial conditions without compromising on performances. Membrane pore orchestration can also be performed with strategies such as monomer templating, where small monomers can be incorporated in the BTESE matrix during synthesis followed by their removal during thermal treatments.

Samenvatting

In dit proefschrift worden de bereiding en eigenschappen beschreven van verschillende hybride silica membranen, gebaseerd op organisch gebrugde siloxaan verbindingen. De beschreven membranen kunnen toegepast worden in verschillende moleculaire scheidingsprocessen. Aandacht wordt besteed aan verschillende procesparameters, die een belangrijke rol spelen bij het vormen van de poriestructuur in deze microporeuze membranen.

In **hoofdstuk 1** wordt een overzicht gegeven van de fabricage van silica membranen uitgaande van een zuur gekatalyseerde solbereiding. Deze membranen vertonen een bijzonder hoge selectiviteit onder droge omstandigheden. Echter, in een vochtige, hydrothermale, omgeving neemt de selectiviteit snel af vanwege de inherente instabiliteit van deze silica systemen in stoom. Om deze instabiliteit tegen te gaan worden in de literatuur twee strategieën vermeld: (1) toevoegen van metaalionen aan de silica matrix of (2) door de toevoeging van koolwaterstoffen in de silica matrix als brug tussen de silicium atomen of als eindgroep. Beide manieren van aanpak resulteerden in een verbeterde hydrothermale stabiliteit. In dit proefschrift zal met name aandacht besteed worden aan de mogelijkheid om koolwaterstof gebrugde silica membranen te kunnen gebruiken voor gasscheiding.

In **hoofdstuk 2** wordt een reproduceerbare bereidingsmethode beschreven voor een eenstaps sol synthese, uitgaande van een ethoxy-gebrugde silaan (1,2-bis(triethoxysilyl)ethaan: BTESE). Uitgaande van deze sol is, door middel van één enkele dip en calcineer stap een membraan verkregen met een meer open poriestructuur dan pure silica membranen. De synthese parameters in de solbereiding, zoals concentratie van de uitgangsverbinding (precursor), de zuurverhouding en de water/precursor verhouding, zijn zodanig geoptimaliseerd, dat een uniforme sol deeltjesgrootte is verkregen waarmee een defect-vrij membraan gemaakt kan worden, dat een goede H_2 permselectiviteit t.o.v. CO_2, N_2 en CH_4 vertoond, terwijl deze membranen geen SF_6-permeatie vertonen . Door de concentratie van de dipsol te variëren tussen 0.15 M en 0.6 M werden membraanlagen verkregen variërend van 90 tot 500 nm in dikte.

Met de kennis, verkregen uit het onderzoek zoals omschreven in hoofdstuk 2, is in **hoofdstuk 3** een methode beschreven voor de fabricage van een hybride silica (BTESE) membraan met verbeterde permselectiviteit. De bereiding van een BTESE sol gaat veel sneller (in 30 in plaats van 90 minuten) in vergelijking met de methode

zoals beschreven in hoofdstuk 2, door de zuur concentratie tijdens de sol synthese met een factor 15 te verlagen. Deze aangepaste synthesemethode geeft membranen met een kleinere poriegrootte en resulteert in membranen die voldoende waterstof en vrijwel geen stikstof of methaan doorlaten bij 200 °C (H_2/N_2 en H_2/CH_4 permspelactiviteiten van respectievelijk meer dan 50 en 90). Een defectvrije membraan microstructuur met een dikte van 400 nm kan worden verkregen door uit te gaan van een dip-sol concentratie van 0.6 M.

Hoofdstuk 4 rapporteert het effect van het doteren van verschillend elementen in het BTESE op de membraan eigenschappen. Nieuwe sol-gel methodes zijn ontwikkeld voor het doteren van boor, niobium of tantaal in het BTESE. Microporeuze membranen zijn hieruit gemaakt door middel van een eenstaps dipproces. TGA-studies aan gedroogde gels en FT-IR-analyses aan gecalcineerde gels tonen aan dat er ethyleenbruggen zijn tussen de siliciumatomen in de metaal gedoteerde BTESE materialen en dat deze systemen thermisch stabiel blijven tot een temperatuur van tenminste 500 °C in een inerte gas atmosfeer. Gaspermeatie experimenten tonen aan dat deze gedoteerde BTESE systemen een meer open porie structuur hebben dan de ongedoteerde BTESE membranen. Aan de hand van hoge resolutie SEM-opnames is aangetoond dat geen (micro)scheurtjes in het membraanoppervlak aanwezig zijn.

Om een nog betere verdeling van metaalionen in een hybride silica matrix te verkrijgen is een nieuw type hybride-silica precursor ontwikkeld, namelijk N,N,N',N'–tetrakis-(3-ethoxysilyl)-propyl)-malonamide (TTPMA) en beschreven in **hoofdstuk 5**. TTPMA werd gesynthetiseerd onder base-gekatalyseerde condities en cerium of nikkel ionen werden gebonden aan het malonamide ligand. TEM-analyse van gecalcineerde (*T* = 250 °C) Ce-TTPMA en Ni-TTPMA gels toonden respectievelijk ceriumoxide nanodeeltjes (2-4 nm) en nikkeloxide nanodeeltjes (2-15 nm) aan. HR-SEM opnames van gecalcineerde membraanoppervlakken toonden aan dat beide type membranen defectvrij waren. De Ce-TTPMA membranen hadden een laagdikte van slechts 35 nm en een iets betere H_2/N_2 en H_2/CH_4 permselectiviteit bij 200 °C dan BTESE membranen. Ni-TTPMA membranen vormden een selectieve laag met een dikte van ongeveer 210 nm en hadden een gaspermeatie die een ordegrote lager was voor de kleine gas moleculen (d.w.z. He, H_2) in vergelijking met BTESE

membranen, terwijl er geen aantoonbare permeatie van N_2 of CH_4 werd gevonden. Dit geeft aan dat Ni-TTPMA een dichter porienetwerk heeft dan BTESE membranen.

Hoofdstuk 6 geeft de synthese en karakterisering weer van het hybride silica materiaal 1,2-*bis*(triethoxysilyl) octaan (BTESO) als een mogelijk alternatief voor de mesoporeuze γ-Al_2O_3 membraantussenlagen. γ-Al_2O_3 membranen hebben een beperkte stabiliteit onder extreme pH en hydrothermale omstandigheden. Vervanging van γ-Al_2O_3 door BTESO zou het mogelijk moeten maken om membranen toe te kunnen passen onder omstandigheden waar chemische en hydrothermale stabiliteit van groot belang zijn. BTESO solen met een gemiddelde deeltjesgrootte van 25 nm werden gemaakt d.m.v. een zuur gekatalyseerde sol synthese. Gecalcineerde BTESO gels lieten een mesoporeuze structuur zien. Echter, de BTESO sol infiltreerde in het α-Al_2O_3 drager materiaal tijdens de dipcoating procedure zonder dat er een laag op de drager werd gevormd. Dit werd waarschijnlijk veroorzaakt door de relatief kleine deeltjesgrootte van de BTESO sol in vergelijking met de poriegrootte van de α-Al_2O_3 drager (80 nm). Om een BTESO laag op een dergelijke drager aan te kunnen brengen is waarschijnlijk een gemiddelde sol deeltjesgrootte noodzakelijk van ten minste 40 nm. Het gebruik van viscositeitsregulatoren in de BTESO dip-sol kan ook een optie zijn om een stabiele en uniforme BTESO laag op de α-Al_2O_3 drager te vormen.

Hoofdstuk 7 tenslotte geeft een overzicht van de belangrijkste conclusies en geeft aanbevelingen voor verder onderzoek. Er is aangetoond, dat naast het aanpassen van de sol bereidingsparameters, de poriegrootte van hybride BTESE silica membranen ook aangepast kan worden door andere elementen aan het BTESE toe te voegen of het membraan te “verouderen” voordat het gecalcineerd wordt. De membranen, zoals beschreven in hoofdstuk 3, kunnen bijvoorbeeld toegepast worden in het zuiveren/verbeteren van biogas. Als ook aangetoond kan worden dat de van TTPMA afgeleide membranen een goede hydrothermale en chemische stabiliteit vertonen, dan kan deze nieuwe klasse van membranen een interessant alternatief zijn. Het arrangeren van de poriegrootte van de deze membranen kan ook uitgevoerd met strategieën zoals monomeer “templating”, waar kleine monomeren in de BTESE matrix worden opgenomen tijdens de synthese gevolgd door het verwijderen van de template door thermische behandelingen.

Acknowledgments

Finally I am about to write the last, and most probably the most readable, chapter of my thesis. There might be possibilities that it will get more attention than any of my other research contributions.

I would like to start this chapter by thanking my promotor and mentor Prof. Dr. Arian Nijmeijer. *Arian*, thank you very much for showing your trust in me and giving me the opportunity to do my PhD research at the Inorganic Membranes group (IM-group), which formally was a part of Membrane Technology Group (MTG). I still remember our first meeting on March 25th 2009, at around 11 am in ME 346. Until that time, I was very proud of my height and physique but when I saw a 7 feet man with a healthy built, I got a bit frightened. But you made me feel very relaxed with your typical way of communication.

During my research time, you have always been very supportive, encouraging and kind of a role-model for me. It will be hard to forget the way you supported my decision of working on Boron, at the STW annual meeting. I felt honored and it encouraged me to take independent decisions in my research. During my PhD, there were many times when I just smiled after receiving your comments and suggestions due to their extreme clarity and with your ease of communicating them. While reading your remarks during my dissertation writing, I (with Wei) started to use some of your phrases even in our conversations; phrases like "*that's a rather bold statement*" or "*I wouldn't jump into conclusions that fast*" or "*you might need a bridging sentence here*" and many more were a common tweet for us during coffee breaks. But that all was to help me in improving my work upon which I am very proud today. My apologies in case my dissertation reviewing caused any headache to you ☺. Once you approved my thesis, you literally took all the responsibility to finalize the related administrative issues and made things done very fast. Many thanks for that!

Even in your absence at the IM-office, you are always available and well-informed about proceedings within the IM-group. Irrespective to your global locations, you always replied in approx. 6 hours to all my queries and it has made me so overwhelmed that once I asked you how much time you work in a day. In my opinion, you must need to increase your rest and relaxation time as it seems you are working 24/7.

I would like to extent my gratitude to my daily supervisor and co-mentor Louis Winnubst who also got promoted as a professor in USTC China during my PhD research. *Louis*, I couldn't have found a better supervisor than you. I have found you a very sincere, dedicated and an experienced mentor; the one who was always there for not only constructive professional discussions but also advising students on their personal matters. There were times when my research roller-coaster drive was hitting rock bottom, but you were very supportive and I never found you devoid of encouraging tips. You took extra care of me in my last months of writing thesis; many times when we had meetings on Sunday afternoons at your office. It made me feel very special when you came to my home for the condolence of my father's death and told me that I must not feel alone in NL as long as you are around. Also, once you told me randomly that on the evening of Christmas 2013 you were constantly thinking about me and my post-PhD endeavors, rather than enjoying the occasion. These are only two of many instances where I have found myself very protected, attached and comfortable under your mentoring umbrella. I have always found you very open and available, never found your office / home door (and heart!) closed. Your extensive experience, sincerity and positive attitude imparted great values on me as a researcher and as a person. It has been an honor to work with you. I hope we will continue to strengthen our relation and co-operation in the future. Best wishes for your efforts in *grafting* your ways through *porous* and *dense* media. And good luck with your Chinese learning skills; At this moment my Dutch is far better than your Chinese ☺.

I would also like to thank my promotion committee for reading my thesis and allowing me to defend it. Prof. Dr. J. L. Lefferts, Prof. Dr. R.G.H. Lammertink, Prof. Dr. J.E. ten Elshof, thank you for accepting the invitation to take part in my committee. Special thanks to the members from abroad, Prof. Dr. J. Caro (Germany) and Asstt. Prof. V. Boffa (Denmark).

Furthermore, I would like to thank my project contributor STW for their valuable financial and intellectual support. Industrial partners such as Shell, AkzoNobil, Pervatech (*Han* Heuver, *Franz* Veltrop), ECN (*Rob* Kreiter, *Jaap* Vente, Marielle Rietkerk (*M.*), and Wim Haije) and academic partners, University of Twente – IMS (Prof. dr. André ten Elshof, Rogier Besselink), University of Amsterdam (Hessel Castricum). It was great to do collaborative work with you and I learnt a lot in that

process in terms of team-work and product development. *Hessel*, thank you very much for your guidance and cooperation with utmost politeness and clearity. *Rogier*, many thanks for patiently answering all my queries regarding materials chemistry. I wish you all the best for your bright future.

My special thanks go to my new boss Peter Kusters. Thank you for your encouragement and facilitations during the final months, and to my (new) office mates Hykle Sijbesma, Maarten Roks and Rob van Uden. *Hylke*, I hope these first months of working together are a good indication of nice things to come. Many thanks for facilitating me in my early days at Parker.

I would like to extend my gratitude to the IM-staff. *Henny* (Plofessor Henny!), I always found you very concise and to-the-point. My monthly meetings with you were very productive for me, during which there were also instances when I really enjoyed conversations between you and Louis ☺. *Nieck*, I found you very active and polite. I didn't get the opportunity to work with you directly, so I would be excited in case any such possibility would arise in future. *Mieke*, officially you are the first female PhD graduate of IM-group, now since you are also dealing the AMC and product volarization matters for the group so good luck to your new assignments and responsibilities. *Cindy*, I enjoyed travelling with you in China, especially when you were in your tights and young locals used to stare at you for some unknown reasons ☺. *Frank*, now you have got your own working place in the IM-group. Very good luck with your post-HBO endeavors in becoming a ceramic expert. *Susanne*, many thanks for your help in form fillings, arranging my schedules and guiding me to channels that could serve me best in resolving my administrative issues inside or outside the IM-group.

My panegyric words wouldn't be worthy if I cannot thank to my friends, colleagues and students within the Twente Membrane Alliance. My long tunnel of research was enlightened by the presence of colleagues such as Martin, Ana, Giri, Saim, Bas, Emiel, Marcel, Tan, Patrick, Michiel, Roland, Cheryl and my dear friend Wei Chen. *Martin*, I love your daughters especially charlotte; she is one of the few babies who didn't cry while sitting in my lap; good luck with the aspects regarding your PhD defense. *Ana*, it was great working and listening to you. You are one of the few researchers I found extremely dedicated and devoting. By the way, thanks for teaching me how to praise a 'beautiful lady' ☺. I wish you very best for your future.

Giri, many thanks for sharing lonely weekends with me in the labs. *Saim*, thanks a ton for the coffees in the Horst-Carré tunnel where we used to discuss everything about our current and future perspectives. *Tan*, not many people might have seen the funny side of yours; thanks for sharing your silly and meaningless jokes. *Chung-Yul, Chunlin, Weihua, Sergey, Cheryl* and *Shumin*, many thanks for being around and sharing your tips and experiences with me. It was great to listen to your ideologies and approaches towards life. *Bas*, it would be hard to forget your joke on HIM (Hybrid and Inorganic Membranes) research group where you threw Arian out of the IM-Headship and awarded it to Nieck ☺. By the way, it was always hard to argue with you as we know that you a martial-art expert with a bus-driver mindset (a super-deadly combination!), so we had no choice but to enjoy your 'intelligent' jokes, even if we don't want to! *Roland*, it was great to have your company in some cold winter nights at the office. *Marcel*, best of luck with your dopants and I am looking forward to your PhD defense. *Patrick*, good luck with your under water fact-finding missions ☺. *Wojtek*, it was nice to work with you in arranging the study-tour 2011. Now you are in the IM, so good luck for your post-doc research. *Michiel*, it was fun to arrange IM-annual meeting with you. Many thanks for your cordial and cooperative attitude. *Emiel*, it was great to have you in the group. We all know that you truly are a multi-talented person. I remember once we were talking at your desk and you were looking at me with extreme focus in your eyes, yet typing super-fast on your keyboard at the same time. Many thanks for being my paranymph; I'd make sure you don't have to work hard during my defense. And last but not the least, my dearest and best friend Dr. *Wei Chen*; I have shared the same desk for 4 years with you sitting next to me. I am happy that during my defense you will also be sitting next to me. Thanks to you that I have learnt some Chinese words and sentences. I hope you would also remember Urdu words and phrases in return. It was really great to have you around, having coffee with you that helped me a lot in releasing my stressful mindset, especially during my last month of writings. You are the first person with whom I shared my job confirmation news at Parker ☺. Many thanks for your photo clicks which I used to upload at social networking sites to increase my fan-club ☺. I greatly admire the way you helped me in finalizing my thesis. I wish very best of luck to you and your family for future. We will surely stay in contact in future.

Special thanks to my students, *Toni*, *Eduardo*, and *Yuan*. Thank you very much for your contributions.

Extended thanks to colleagues from SFI and MST: (In no particular order) Can, Elif, Vik, Damon, Yali, Katya, Mayur, Olga, Sander, Jiger, Sinem, Jeroen, Enver, Krzysztof, Salman, Beata, Shazia, Yusuf, Alhadidi, Karina, and many more. *Greet*, I don't think words can fully express my gratitude towards you. It was super easy to have you around. Many thanks for facilitating me especially in arranging matters related to my housing. I don't think life would be that easy for me if you were not there to help me resolving my house issues at the campus.

Cecile, many thanks for your help and assistance regarding the IND matters. You took special care for me even after I joined Parker and for that I am very much thankful to you. As I always have said to you, my office times were most effective because I knew you were taking care of my IND-related matters.

My time wouldn't be that enjoyable and memorable without the support of Pakistani community at Twente. I got the honor of presiding the Pakistani Student Association (PSA) for a year which taught me noticeable and life-long lessons about work-ethics, event management and decision making. The events and get-togethers under the PSA umbrella served as a home-away-from-home for me. My special thanks to all Pakistani students and colleagues of Twente. Friends like *Rahim, Danish, Tamoor, Sohail, Akram* etc. made my evenings and weekends very refreshing, thanks to their ethical behavior and cordial attitude that made me feel very comfortable in their company. We will surely remain in contact with each other.

Unlike popular global believes, my interaction with Indian community was super awesome. Friends like *Shushil*, *Prasad, Abhi* (and his wife *Shruti* whose warmth in maintaining friendships can be felt even in space), *Nishant, Omkar, Kartikya* and all. It was great to enjoy conversations and sports with you guys. Playing lawn-tennis would always be memorable thanks to the "expert skills" of *Ankit, Shushil, Abhi* and *Nishant*. "*Yeh point apna hai partner*" (partner, that next point would surely be ours!) always seemed to inject adrenaline during tense games ☺. My cricket skills wouldn't get better if there weren't as good competitors as *Rahim, Waqar, Khurram, Adeel, Shushil* (with a *smooth* bowling action!), *Prasad,* and *CP*.

Friends like you guys are hard to find and replace. I would surely miss you all. Thank you very much to you all!

Significant thanks to the *UT-Muslims Association*. Guys, you doing a phenomenal job, please keep it up and best of luck!

I would like to dedicate my thesis to *my parents*; my father (late) and my loving and caring mother for giving me their unconditional love and support. Daddy, it's still hard to believe that you are no more amongst us, I had a special bond with you especially as being the youngest in our family. You were one of the very few who stood-by me in my decision of going to Germany for my master studies in 2006. May your soul rest in peace and may the Almighty shower His blessings of forgiveness and fruitfulness on you. I miss you terribly in my life (*really!*). *Ammi* (mother), yes finally *its* over ☺ !! Like every mother, you are also filled with the nectar of motherly love and devotion, and it took me quite some time to convince you for giving me permission to go to Germany. I still remember your long 'Do's and Don'ts' list while leaving Pakistan. You have that surprising instinct to recognize just from my voice that either I am in trouble or I am facing difficult circumstances. I love you dear *Ammi* (mother) and daddy, you are the best parents in the world. *Ammi*, it's a pity that you are unable to come to my defense but I am excited to welcome you here later this summer.

My special (five star) compliments goes to my sister *baji* and brother *Muneeb*. *Baji*, many thanks for giving me your time, talking with me for hours and updating me with proceedings from Pakistan. It's always a pleasure to have your company. You have that amazing skill of spicing up tasteless issues and making them super juicy to hear ☺. *Muneeb*, it's great to have you as a brother; your daughter *Soha* is the light and life of our family. I was overwhelmed with joy when she started calling me *chacha* (uncle) in her own twisted way when last time you visited me here in NL. I wish you very best of luck in your personal and professional life.

My friends from Pakistan, *Shahid*, *Umair*, *Wajid*, Dr. *Munazza Bhabi* and all, thanks for being there for me in times where I was feeling lonely and sometimes sad. *Shahid*, it's a blessing to have a friend like you in my life; we might have got married if you were a female ☺. Best wishes to you in your personal and professional life. *Umair*, it's always enjoyable to make fun of your military ethics. But we know that

you also feel happy when you see us happy. *Munazza Bhabi*, I never knew that your short visit to SLO Enschede would lead to that strong and long lasting interaction between us. I am blessed to have you as an elderly sister who always remembers me, cares for me and snubs me whenever I am failed to interact with you in regular terms. Best wishes to you and Mahmood Bhai in your personal and professional lives respectively.

To everyone, who contributed and has been a part and parcel of my life. My sincere apologies if I missed to mention you. You mean no less to me, and I appreciate you all.

Hammad F. Qureshi

JUNE 1ST, 2014.